

Ihan Martoyo

# ■ **Frequency Domain Equalization in CDMA Detection**

Forschungsberichte aus dem  
Institut für Nachrichtentechnik  
der Universität Karlsruhe (TH)

---

Herausgeber: Prof. Dr. rer. nat. Friedrich Jondral

- Band 1 Marcel Kohl  
**Simulationsmodelle für die Bewertung von  
Satellitenübertragungsstrecken im 20/30 GHz  
Bereich**
- Band 2 Christoph Delfs  
**Zeit-Frequenz-Signalanalyse: Lineare und  
quadratische Verfahren sowie vergleichende  
Untersuchungen zur Klassifikation von  
Klaviertönen**
- Band 3 Gunnar Wetzker  
**Maximum-Likelihood Akquisition von Direct  
Sequence Spread-Spectrum Signalen**
- Band 4 Anne Wiesler  
**Parametergesteuertes Software Radio für Mo-  
bilfunksysteme**
- Band 5 Karl Lütjen  
**Systeme und Verfahren für strukturelle  
Musteranalysen mit Produktionsnetzen**
- Band 6 Ralf Machauer  
**Multicode-Detektion im UMTS**

Forschungsberichte aus dem  
Institut für Nachrichtentechnik  
der Universität Karlsruhe (TH)

---

Herausgeber: Prof. Dr. rer. nat. Friedrich Jondral

- Band 7    Gunther M. A. Sessler  
**Schnell konvergierender Polynomial Expansion Multiuser Detektor mit niedriger Komplexität**
- Band 8    Henrik Schober  
**Breitbandige OFDM Funkübertragung bei hohen Teilnehmergegeschwindigkeiten**
- Band 9    Arnd-Ragnar Rhiemeier  
**Modulares Software Defined Radio**
- Band 10    Mustafa Mengüç Öner  
**Air Interface Identification for Software Radio Systems**
- Band 11    Fatih Çapar  
**Dynamische Spektrumverwaltung und elektronische Echtzeitvermarktung von Funkspektren in Hotspotnetzen**
- Band 12    Ihan Martoyo  
**Frequency Domain Equalization in CDMA Detection**



# Vorwort des Herausgebers

Die Mobilkommunikation wird noch über längere Zeit ein ausgesprochen fruchtbares Forschungsgebiet bleiben. Die Nutzer von Übertragungstechniken lernen zunehmend, die Vorteile drahtloser Verbindungen zu schätzen. Physikalische Funkkanäle sind komplexe Systeme, deren Einflüsse auf die Übertragungsqualität durch geeignete Signalverarbeitungsverfahren in Sender oder Empfänger auf ein Minimum begrenzt werden müssen. Mit der Einführung der dritten Mobilfunkgeneration erleben wir zurzeit erstmalig den großflächigen Einsatz der Code Division Multiple Access (CDMA) Technik in Systemen, die sowohl Daten- als auch Sprachübertragung unterstützen.

Eine ganze Zeit lang wurde CDMA als höchst effizientes Zugriffsverfahren auf die knappe Übertragungsressource angesehen. Aufgrund des breitbandigen Übertragungsverfahrens erübrigt sich der in TDMA Systemen oft notwendige Einsatz aufwendiger Kanalentzerrer. Inzwischen hat sich jedoch gezeigt, dass auch CDMA mit gewissen Tücken zu kämpfen hat. Insbesondere die Multiple Access Interference (MAI) genannten Störungen, die durch dem gewünschten Signal am Empfänger überlagerte Signale anderer Teilnehmer entstehen, bereiten den Systementwicklern Kopfzerbrechen. Der traditionell zum Empfang von Direct Sequence Spread Spectrum (DSSS) Signalen eingesetzte RAKE arbeitet zwar als Maximum Ratio Combiner, trägt aber nicht zur Verminderung der MAI bei. Andererseits können Multi User Detektoren (MUDs) die MAI wirksam unterdrücken. Allerdings sind aufgrund ihrer numerischen Komplexität und dem damit verbun-

denen Verbrauch elektrischer Leistung ideale MUDs überhaupt nicht und vereinfachte, lineare MUDs nur in Basisstationen einsetzbar. In mobilen Endgeräten kommt nach wie vor das RAKE Prinzip zum Einsatz. Die vorliegende Arbeit widmet sich der Untersuchung einer bislang häufig übersehenen Alternative, die numerisch mit geringem Aufwand realisierbar ist, dem Frequency Domain Equalizer (FDE).

Die wissenschaftlichen Beiträge der Dissertation von Ihan Martoyo liegen

- in der systematischen Untersuchung des FDE für seinen Einsatz in CDMA Downlinks, einschließlich des Einsatzes der Overlap-Cut Methode zur Vermeidung von Änderungen in Übertragungsstandards
- in der gekonnten Gegenüberstellung von UMTS und OFDM, aus der folgt, dass die FFT mit Erfolg auch in CDMA Systemen eingesetzt werden kann
- im analytischen Nachweis der engen Approximation der linearen MUDs durch die entsprechenden FDEs bei orthogonalen CDMA Systemen
- in den Vorschlägen zum Einsatz von FDE-RAKE, Pre-FDE im CDMA Uplink und von FFT/IFFT Strukturen in SDRs

Das Potential, das der FDE für die Funkkommunikation bietet, ist bei weitem noch nicht ausgeschöpft. Daher bleibt zu hoffen, dass die vorliegende Arbeit zu weiteren Untersuchungen auf diesem Gebiet anregen wird.

Karlsruhe, im Dezember 2004

Friedrich Jondral



Copyright: Institut für Nachrichtentechnik  
Universität Karlsruhe (TH), 2005

Druck: Druckerei Peter Rohrhirsch, Kaiserstr. 61  
76131 Karlsruhe, Tel. 0721/373596

ISSN: 1433-3821



# Frequency Domain Equalization in CDMA Detection

Zur Erlangung des akademischen Grades eines

DOKTOR-INGENIEURS

von der Fakultät für  
Elektrotechnik und Informationstechnik  
der Universität Fridericiana Karlsruhe

genehmigte

DISSERTATION

von

Ihan Martoyo M.Sc.

aus

Jakarta, Indonesien

Tag der mündlichen Prüfung: 09.12.2004  
Hauptreferent: Prof. Dr. rer. nat. Friedrich Jondral  
Korreferent: Prof. Dr.-Ing. Andreas Czylik



# Acknowledgment

*Eine Dissertation ist ein Schriftstück von ca. 100 Seiten, das mit größter Sorgfalt verfasst und nach der Verteidigung kaum wieder gelesen wird. (Dieter Bochmann, "Vom Handwerk des Promovierens" Automatisierungstechnik 50 (2002) 4, Oldenbourg Verlag)*

*A dissertation is a document of about 100 pages, which is highly carefully composed and after its defense hardly be read anymore.*

However, if we consider the dissertation not as an end-product but as a journey, then it is a very exciting journey full of colorful people who left unforgettable impacts along the way. First of all, I would like to thank Professor Dr. rer. nat. Friedrich Jondral, who took me under his wings and made this work at all possible. Without his careful critiques on my *Knödeltapete* (dumplings-wallpaper)<sup>1</sup>, my work would not be as it is.

Professor Dr.-Ing. Andreas Czylwik, the head of the Communication Systems Lab (*Nachrichtentechnische Systeme*) at the Universität Duisburg-Essen kindly took the position of the second examiner. For his thorough reading of the work I am utterly grateful.

---

<sup>1</sup>Prof. Jondral used the term *Knödeltapete* to refer to the mind-map diagram of this work.

A number of students contributed their time on this work, sometimes even late into the night. Thanks to David Vicente Perez Garcia, Jaroslaw Luber, Zoltan Bartha, Nikolaus Bissias, Diego Garcia Gallen, Pureza Galindo Latorre, Liu Zhenhua, Yin Wenxuan, Sun Bo and Ignacio Izquierdo.

I was also blessed with colleagues who taught me, how fun it can be, to play and tinker around with technical problems. I would like to thank Dr.-Ing. Gunther Sessler who not only showed me how to guess around a mathematical riddle, but also let me win gracefully on several chess games. Thanks also to Dr.-Ing. Henrik Schober who provided a listening ear, however dumb my question was. Dr.-Ing. Ralf Machauer fascinated me with his technical understanding and humble manner. Dr.-Ing. Arnd-Ragnar Rhiemeier, Dr.-Ing. Timo Weiß and Dr.-Ing. Fatih Çapar were great companions to spend time on conferences.

This work would also be impossible without the contribution of Dipl.-Ing.(FH) Reiner Linnenkohl, who faithfully keeps all the computers in the lab humming and running. Thanks also to Fr. Kuntermann, Fr. Mast, and Fr. Olbrich, without whom the conference trips would not be so smooth.

I would also like to thank my parents, who were the source of constant encouragement during my studies in Germany. There were also a lot of friends who silently prayed and offered their support during the writing of this work, to whom I am very grateful. My special gratitude goes to my wife Lindawati SH. MDiv., who patiently accompanied me through the journey, and kept reminding me of the important things in life. My utmost gratitude is to my Lord Jesus Christ who gives meaning and hope to life.

Die in dieser Dissertation dokumentierten Arbeiten wurden zum Teil innerhalb des Teilvorhabens *Transceiverarchitekturen bei Spectrum Pooling* im Förderschwerpunkt *hyperNET HyEff (Universelle Nutzung von Kommunikationsnetzen für zukünftige Mobilfunkgenerationen)* durch das Bundesministerium für Bildung und Forschung unterstützt. Projektträger war das DLR in Köln-Porz.

**Förderkennzeichen: 01BU152**

The work presented in this dissertation was partially supported by the German Federal Ministry of Research and Technology within the project *Transceiver Architectures for Spectrum Pooling (TASP)*. TASP was part of the research focus *hyperNET Hyeff (Universal Use of Communications Networks for Future Mobile Radio Generations)*. The project was coordinated by the DLR in Köln-Porz.

**Grant number: 01BU152**



# Zusammenfassung

*Unterwegs VideoClips anschauen, zum Beispiel aktuelle Nachrichten oder Fußball-Ereignisse. Oder selber kurze Videos filmen und direkt verschicken. Per Vodafone-MMS an Video-Handys oder E-Mail-Adressen, Daten mit HighSpeed via UMTS und GPRS versenden, E-Mailen per Handy, Musik hören und vieles mehr - mit diesem Power-Tool haben Sie unglaublich viele Möglichkeiten. (Vodafone Werbeblatt vom Juli 2004)*

So trommelt die Firma die Werbepauke für ihre neueste Technik. Universal Mobile Telecommunication System (UMTS) - das europäische Mobilfunksystem der dritten Generation - verspricht eine grenzenlose mobile Datenkommunikation. Aber grenzenlos ist die Technik eigentlich nicht. Seit langem weiß man, dass das CDMA-System, worauf UMTS basiert, von Interferenzen begrenzt ist. Der RAKE Empfänger, der bis heute noch als der gängigste CDMA-Empfänger gilt, leidet unter Multiple Access Interference (MAI). Je mehr Nutzer auf das System zugreifen, desto schlimmer wird die MAI. Ein viel untersuchter Lösungsansatz dafür ist der Multiuser Detector (MUD). Dennoch ist der MUD so rechenintensiv, dass es bei den meisten Forschungsaktivitäten darum geht, suboptimale MUDs zu finden, die noch implementiert werden können.

Die vorliegende Arbeit schlägt eine oft übersehene Lösung vor, nämlich die Frequenzbereichsentzerrung (englisch: Frequency Domain Equalization (FDE)). Es wird gezeigt, dass die FDE die MAI im CDMA-Downlink sehr effektiv unterdrücken kann; dafür

aber mit einer sehr niedrigen Komplexität. Das heißt, die FDE ist zugleich besser als der RAKE-Empfänger im Sinne der MAI-Unterdrückung, aber auch viel einfacher als der MUD. Es kann sogar gezeigt werden, dass die Leistungsfähigkeit der FDE bei einer voll belasteten CDMA-Zelle genau so gut wie die des linearen MUD ist (orthogonale Spreizcodes angenommen). Der Vorteil der FDE für CDMA geht jedoch weiter. Die FDE ermöglicht auch eine gemeinsame Struktur zur Basisbandverarbeitung (Software Defined Radio Ansatz) für verschiedene Mobilfunksysteme, einschließlich TDMA, CDMA, OFDM und MC-CDMA Systeme.



# Abstract

*Watching video clips on the way, for example actual news or football events. Or film a short video on your own and send it right away. Via vodafone-MMS to video-cellphone or e-mail address, send data with high speed via UMTS and GPRS, e-mail through cellphone, listen to music and a lot more - with this power tool you have unbelievable many possibilities.*

*(Vodafone's promotional sheet, July 2004)*

That is how the company beats the promotion drum for its newest technology. Universal Mobile Telecommunication System (UMTS) - the European 3rd generation mobile communication system - promises a limitless mobile data communication. But actually, the technology is not limitless at all. It has been known for quite some time, that the CDMA system, on which UMTS is based, is interference limited. The RAKE receiver, which is still the most common receiver for CDMA, suffers from multiple access interference (MAI). The more users in the system, the worse the MAI gets. A frequently investigated approach to solve the MAI problem is the multiuser detector (MUD). However, the MUD is computationally very expensive, so that most research activities are conducted to find sub-optimal MUDs, which can still be implemented.

The present work proposes an often overlooked solution, namely the frequency domain equalization (FDE). It will be shown, that the FDE can suppress the MAI in CDMA downlink effectively, however with a very low complexity. It means, that the FDE is at

the same time better than the RAKE receiver in terms of MAI suppression, yet much simpler than the MUD. It can even be shown, that the performance of the FDE is equal to the MUD in a fully loaded CDMA cell (orthogonal codes assumed). But the advantage of the FDE does not stop there. The FDE also enables a common baseband processing structure (software defined radio approach) for different mobile communication systems, including TDMA, CDMA, OFDM and MC-CDMA systems.

# Table of Contents

<b>1</b>	<b>Introduction</b>	<b>1</b>
1.1	Why CDMA? . . . . .	4
<b>2</b>	<b>CDMA System Model and Detectors</b>	<b>9</b>
2.1	CDMA System Model . . . . .	10
2.2	CDMA Detectors . . . . .	13
2.2.1	RAKE . . . . .	13
2.2.2	Multiuser Detector . . . . .	17
2.2.3	Equalization . . . . .	18
<b>3</b>	<b>CDMA Versus OFDM</b>	<b>21</b>
3.1	Comparison Overview . . . . .	22
3.2	Simple CDMA versus OFDM . . . . .	24
3.3	DVB-T versus UTRA-FDD . . . . .	31
3.4	Is OFDM better than CDMA? . . . . .	35
<b>4</b>	<b>Frequency Domain Equalization for CDMA Downlink</b>	<b>39</b>
4.1	The FDE . . . . .	40
4.2	FDE for CDMA Downlink . . . . .	42
4.3	Cyclic Prefix, Zero-Padding, Overlap-Cut . . . . .	43
4.4	Performance of the FDE for CDMA Downlink . . . . .	49
4.5	Complexity Considerations . . . . .	53
<b>5</b>	<b>Equalizers Versus Multiuser Detectors</b>	<b>57</b>

5.1	Simulation Results . . . . .	58
5.2	FDE versus MUD . . . . .	60
5.3	TDE versus MUD . . . . .	68
5.4	Why MUD When an Equalizer is Good Enough?	70
<b>6</b>	<b>Ideas Derived From FDE</b>	<b>75</b>
6.1	FDE-RAKE . . . . .	76
6.1.1	Simulation Results . . . . .	78
6.1.2	Complexity Consideration . . . . .	82
6.1.3	Comparison with Conventional PIC . . . . .	83
6.2	Pre-FDE for CDMA Uplink . . . . .	87
6.2.1	Power Scaling and Zero Padding . . . . .	90
6.2.2	Simulation Results . . . . .	93
6.2.3	Implementation Considerations . . . . .	94
6.3	Software-Defined Radio . . . . .	96
6.3.1	SDR Based on FDE . . . . .	97
6.3.2	SDR for UTRA and WLAN . . . . .	100
6.3.3	Advance Spectrum Allocation with SDR . . . . .	104
<b>7</b>	<b>Conclusions &amp; The Continuing Work</b>	<b>109</b>
7.1	Why CDMA? (revisited) . . . . .	111
7.2	Further Research . . . . .	114
<b>A</b>	<b>UTRA</b>	<b>115</b>
A.1	UTRA-TDD . . . . .	117
<b>B</b>	<b>Channel Models</b>	<b>119</b>
	<b>Acronyms, Notation and Symbols</b>	<b>121</b>
	<b>References</b>	<b>125</b>

<b>Theses</b>	<b>135</b>
<b>Index</b>	<b>137</b>
<b>Curriculum Vitae</b>	<b>139</b>



# 1

## Introduction

*...it seemed like a very democratic way to use up the coordinates that you have, and to distribute the 'cost of living', the noise, evenly among everyone. (C. Shannon, a comment about CDMA [1])*

JOHN is on his way home after a hard day's work. He wants to reward himself with a nice meal in a local restaurant and maybe a movie. But he is new in town, he just started working here about two weeks ago. "That shouldn't be a problem," he says to himself, as he draws out his cellphone and dials some numbers. In a split second he sees the address and location of his favorite restaurants nearby and does a quick review on the latest movie clips. Thanks to the mobile communications technology.

This engineering dream might not be too far-fetched. The third generation (3G) mobile communication system was developed exactly to realize this dream. It is marked with the shift from (only) audio communication of the second generation system to the multimedia mobile communications that includes graphics and moving pictures. The enabling air interface technology behind the 3G standards is a technique called CDMA<sup>1</sup> (Code Division Multiple Access).

At the time of this writing, CDMA has been established as the chosen technique for the 3G systems. All kinds of 3G systems use one or another variant of CDMA. In Europe, two flavors of CDMA system were proposed within the UMTS (Universal Mobile Telecommunications System) standard. The UTRA-FDD is a wideband CDMA system, and a CDMA/TDMA system is represented under the name of UTRA-TDD. The cdma2000 standard in the U.S. includes cdma2000 1x and 3x options, in order to maintain the compatibility with the 2G CDMA system IS-95. cdma2000 1x has the same bandwidth as IS-95 (i.e. 1.25 MHz), whereas cdma2000 3x is a multicarrier CDMA system that has three times the bandwidth of IS-95. In Japan, the wideband CDMA system is adopted, and China pushes forward its own TD-SCDMA system (a synchronous CDMA system similar to UTRA-TDD [2]). All these 3G standards are known in the In-

---

<sup>1</sup>In this work, the term CDMA refers to the DS-CDMA (Direct Sequence CDMA) system



ternational Telecommunications Union (ITU) as the members of IMT-2000 [3].

Although the standardization process for the 3G systems has been settled, the search for a good CDMA detector still triggers lively and engaging research activities. The RAKE receiver, that has been around for almost five decades, is still considered as the most common detector for a CDMA system. This anti-multipath RAKE receiver was patented by Price and Green in 1956 [4], and it was for some time widely believed as, if not an optimal, an almost optimal receiver for channels with a large number of equal power users [5]. Now, it has been recognized that the RAKE receiver suffers from multiple access interference (MAI), a term that refers to the interference between CDMA users within the same cell.

The widely known solution to the MAI problem in CDMA systems is the multiuser detector. The multiuser detector includes the knowledge of the other users' signal into its detection strategy. By using this information of other users' signal jointly, the multiuser detector can cancel out interference from other CDMA users, and thus better detect each individual user. Unfortunately, the multiuser detector is still considered much too complex for practical CDMA systems [6]. Therefore, most of the research over multiuser detector has been directed to find suboptimal multiuser detection solutions which are more feasible to implement.

The present work breaks away from the common approach of taking multiuser detector as the solution for the MAI problem in CDMA systems. Here, a singleuser detection strategy is proposed, namely the equalization approach. Although an equalizer does not require the knowledge of other users' signal, it will be shown that an equalizer can effectively suppress MAI.

A specific implementation of the equalizer which operates in the frequency domain is proposed in this work. This frequency domain equalization (FDE) offers the important advantage that

it can be implemented efficiently with the FFT operation, thus it reduces the overall complexity of the CDMA detector significantly. Hence, the FDE detector avoids the MAI problem of the RAKE receiver and the huge computational cost of the multiuser detector. The FDE provides a very simple receiver structure, yet very effective in handling the MAI in CDMA systems.

Another important benefit from FDE is its potential for a multimode receiver structure that can handle several radio interfaces at the same time. This interesting feature comes from the fact that FDE shows a very similar structure to the multicarrier systems (e.g. OFDM or MC-CDMA). This similarity enables the use of the same receiver components in detecting signals from different air interfaces.

The next section will review the CDMA system shortly and take a look at the reasons that lead to the commercialization of this technique.

## 1.1 Why CDMA?

The CDMA technique enables several users to access the spectrum at the same time using the same frequency (c.f. Figure 1.1). This is accomplished by assigning a user specific signature to each user's signal. The signature codes will then allow the receiver to distinguish the signal of each user. Hence in CDMA systems, the multiple access is made possible neither by dividing the spectrum resource into frequency bands (FDMA) nor by dividing the resource into time slots (TDMA), but rather by differentiating the user's signal through the signature codes.

The term *spreading* comes from the fact that the signature sequences which are assigned to the user's signal have a much higher bandwidth than the information signal itself. The spreading process is simply done by multiplying the information signal

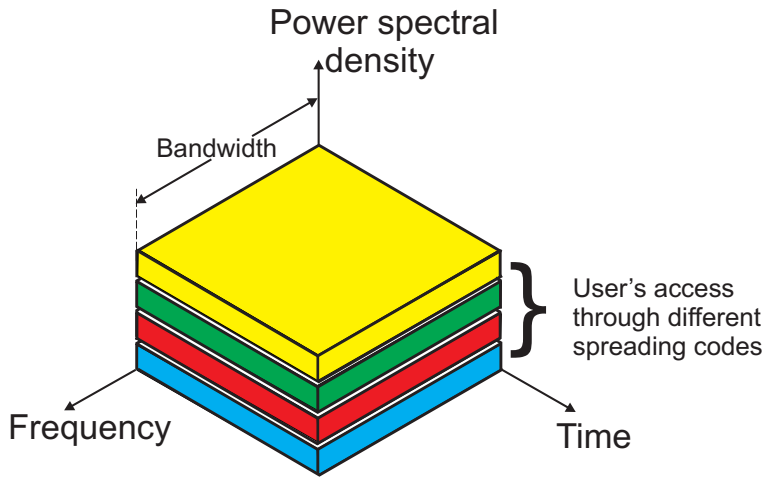


**Figure 1.1** DS-CDMA System

and the spreading sequence in chip rate. This is displayed in Figure 1.2.  $T_c$  is the chip duration of the spreading code, and  $T_b$  is the symbol duration of the information signal. The information signal can be retrieved by despreading, i.e. by multiplying the CDMA signal with the same sequence used in spreading. The despreading process without noise is illustrated in Figure 1.3<sup>2</sup>.

Spread spectrum systems were used almost exclusively in the military communications until the early 1980s. Its anti-jamming and low probability of intercept characteristics had caused the spread spectrum technique to flourish in the military field. As the attention moved to the commercial applications, other features became more important. The anti-jamming property implies a robustness against narrowband interferers, which is important for commercial applications. Furthermore, if the spreading codes are chosen such that they show a good autocorrelation property, the resulting spread spectrum system will be insensitive to multipath

---

<sup>2</sup>In the case of complex signals, the despreading process is done by multiplying with the complex conjugated version of the spreading code.

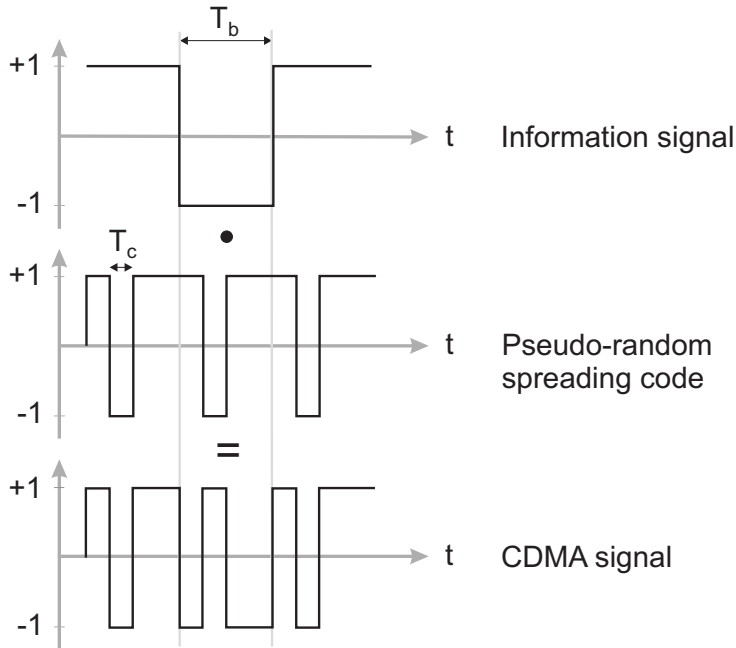


**Figure 1.2** Spreading process

distortions. A good crosscorrelation property of the spreading codes, on the other hand, ensures a good multiple access capability.

Beside the main advantages mentioned above, a CDMA system also displays these desirable properties: frequency reuse factor of one, graceful degradation and the possibility for soft handover [7]. Along with the hope that CDMA overlay will solve the problem of spectrum congestion, these properties motivated the introduction of the CDMA system [8].

The RAKE receiver is still the most common receiver for CDMA systems. It has been proposed since the introduction of CDMA systems [9]. The RAKE receiver exploits the time

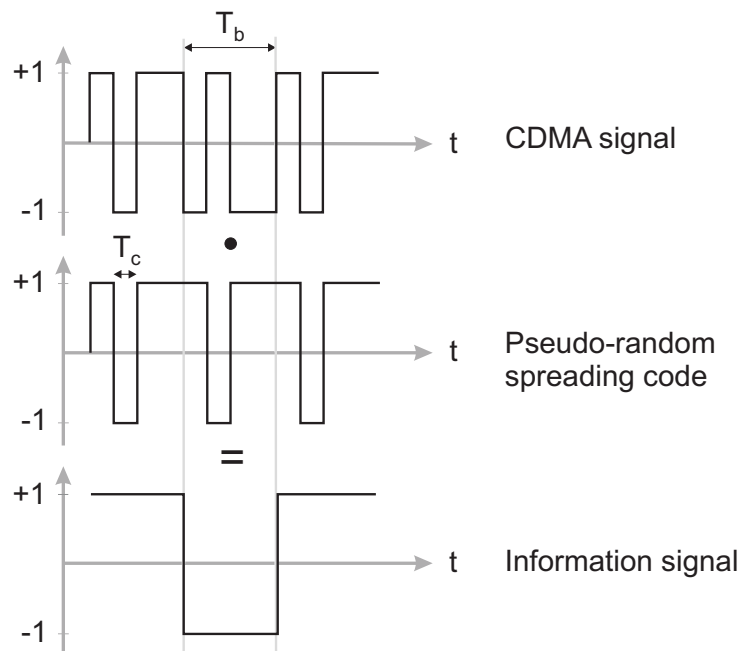


**Figure 1.3** Despreading process

diversity by delaying the signals received via different paths by appropriate amounts of delay time and then combines them. Despite its simplicity, the RAKE receiver suffers from MAI.

The multiuser detector can alleviate the MAI problem in CDMA systems, but it entails an intense computational effort. This work focuses on an often overlooked solution, namely the equalization approach. It is so often overlooked, because one of the initial thoughts motivating the introduction of CDMA is, that the use of complicated equalizers can be avoided with CDMA systems [7].

However, compared to the complex multiuser detector, the equalizer offers a simple, yet a very good detector in terms of

MAI suppression. This work will elaborate the idea of the frequency domain equalization (FDE), which not only solves the MAI problem in CDMA systems, but also opens up the possibility for a multimode baseband data processing.

# 2

## CDMA System Model and Detectors

*We thought multiplying a signal with a pseudo noise before transmitting was a great idea. We even bragged about the capacity gain. Now we have to take all users into account even if we just want to receive one. (The author's thought, May 2001)*

CDMA was introduced with a high optimism. Resistance to multipath fading and the possibility to exploit multipath diversity with the RAKE receiver often give an oversimplified impression on the complexity involved in the detection of CDMA signals [7],[9]. However, following Verdu's seminal work in 1986 [10], a more sober perception came into the picture. It was realized that the CDMA system is interference limited. The RAKE receiver which can work very well with a handful of users, becomes severely disturbed by MAI as the number of users increases. So, the pendulum of research swings to the other side, to the search of highly complicated receivers that can solve the MAI problem, the multiuser detectors.

Unfortunately, the kind of optimal non-linear (MLSE) multiuser detector implied by Verdu in [10] is too complicated. Hence, most of the research in this area has focused on finding multiuser detectors with low complexity [6]. The irony is that, there is a considerably simple solution for the MAI problem, which is almost forgotten in the heyday of CDMA early optimism, namely the equalizer. But before we move on to discuss how the equalizer solves the CDMA detection problem, we need a system model to begin with, which is the focus of the next section. It will be then followed by an overview of CDMA detectors.

## 2.1 CDMA System Model

CDMA baseband signals can be described and analyzed conveniently with a matrix-vector notation such as introduced in [11], [12]. With this notation, the received discrete vector  $\mathbf{r}$  of a CDMA system can be expressed as follows:

$$\mathbf{r} = \mathbf{A}\mathbf{d} + \mathbf{n}, \quad (2.1)$$

where  $\mathbf{d}$  represents the complex baseband data vector  $\mathbf{d}^T = [\mathbf{d}^{(1)T}, \mathbf{d}^{(2)T}, \dots, \mathbf{d}^{(k)T}, \dots, \mathbf{d}^{(K)T}]$  of the  $K$  users. The index  $k$



represents the data from user  $k$ , where  $k$  takes the values  $1, \dots, K$ . Each vector  $\mathbf{d}^{(k)}$  consists of  $N$  consecutive data symbols  $\mathbf{d}^{(k)} = [d_1^{(k)}, d_2^{(k)}, \dots, d_N^{(k)}]^T$ . The vector  $\mathbf{n}$  in (2.1) denotes the additive noise, and  $(\cdot)^T$  is the transpose of a matrix.

The matrix  $\mathbf{A}$  comprises the effects of spreading and transmission over the multipath channel <sup>1</sup>. It consists of  $(NQ + L - 1) \times (NK)$  complex-valued elements, i.e.  $\mathbf{A} \in \mathbb{C}^{(NQ+L-1) \times (NK)}$ , and it can be broken down and expressed as:

$$\mathbf{A} = [\mathbf{A}^{(1)} | \mathbf{A}^{(2)} | \dots | \mathbf{A}^{(k)} | \dots | \mathbf{A}^{(K)}]. \quad (2.2)$$

Each column of the submatrix  $\mathbf{A}^{(k)} \in \mathbb{C}^{(NQ+L-1) \times (N)}$  is obtained by:  $\mathbf{A}^{(k)} = \mathbf{c}^{(k)} * \mathbf{h}^{(k)}$ , which is the convolution between the spreading code  $\mathbf{c}^{(k)} = [c_1^{(k)}, c_2^{(k)}, \dots, c_Q^{(k)}]^T$  of length  $Q$  and the channel impulse response  $\mathbf{h}^{(k)} = [h_0^{(k)}, h_1^{(k)}, \dots, h_{L-1}^{(k)}]^T$  of length  $L$ . An example of the  $\mathbf{A}$  matrix with  $K = 3$ ,  $Q = 4$ ,  $N = 2$  and  $L = 3$  is displayed in (2.3).

$$\mathbf{A} = \begin{bmatrix} A_0^{(1)} & 0 & A_0^{(2)} & 0 & A_0^{(3)} & 0 \\ A_1^{(1)} & 0 & A_1^{(2)} & 0 & A_1^{(3)} & 0 \\ A_2^{(1)} & 0 & A_2^{(2)} & 0 & A_2^{(3)} & 0 \\ A_3^{(1)} & 0 & A_3^{(2)} & 0 & A_3^{(3)} & 0 \\ A_4^{(1)} & A_0^{(1)} & A_4^{(2)} & A_0^{(2)} & A_4^{(3)} & A_0^{(3)} \\ A_5^{(1)} & A_1^{(1)} & A_5^{(2)} & A_1^{(2)} & A_5^{(3)} & A_1^{(3)} \\ 0 & A_2^{(1)} & 0 & A_2^{(2)} & 0 & A_2^{(3)} \\ 0 & A_3^{(1)} & 0 & A_3^{(2)} & 0 & A_3^{(3)} \\ 0 & A_4^{(1)} & 0 & A_4^{(2)} & 0 & A_4^{(3)} \\ 0 & A_5^{(1)} & 0 & A_5^{(2)} & 0 & A_5^{(3)} \end{bmatrix} \quad (2.3)$$

The downlink of a CDMA system presents a special case of (2.1) in which the data of all users arrive through the same chan-

---

<sup>1</sup>All users are assumed to be received with the same power. This assumption can be fairly attained with a good power control mechanism.

nel. In this case, the  $\mathbf{A}$  matrix can be expressed as a multiplication of the channel matrix  $\mathbf{H}$  and the spreading matrix  $\mathbf{C}$ . The received discrete vector  $\mathbf{r}$  can then be expressed as:

$$\mathbf{r} = \mathbf{H}\mathbf{C}\mathbf{d} + \mathbf{n}. \quad (2.4)$$

$\mathbf{H} \in \mathbb{C}^{(NQ+L-1) \times (NQ)}$  and  $\mathbf{C} \in \mathbb{C}^{(NQ) \times (NK)}$  as can be seen in (2.5) and (2.6) represent the channel matrix and the spreading matrix with the spreading factor  $Q$ , respectively. Because the data of all users experience the same channel, the index  $k$  for the channel vector elements  $\mathbf{h}^{(k)}$  can be dropped.

$$\mathbf{H} = \begin{bmatrix} h_0 & 0 & \cdots & 0 \\ h_1 & h_0 & \cdots & 0 \\ h_2 & h_1 & \cdots & 0 \\ \vdots & \vdots & \ddots & \vdots \\ h_{L-1} & h_{L-2} & \cdots & 0 \\ 0 & h_{L-1} & \cdots & \vdots \\ \vdots & \vdots & \cdots & h_{L-2} \\ 0 & 0 & \cdots & h_{L-1} \end{bmatrix} \quad (2.5)$$

$$\mathbf{C} = \begin{bmatrix} c_1^{(1)} & 0 & 0 & \left| \right. & c_1^{(2)} & 0 & 0 & \left| \right. & \cdots & 0 \\ c_2^{(1)} & 0 & 0 & \left| \right. & c_2^{(2)} & 0 & 0 & \left| \right. & \cdots & 0 \\ \vdots & \vdots & \vdots & \left| \right. & \vdots & \vdots & \vdots & \left| \right. & \ddots & \vdots \\ c_Q^{(1)} & 0 & 0 & \left| \right. & c_Q^{(2)} & 0 & 0 & \left| \right. & \cdots & 0 \\ 0 & c_1^{(1)} & 0 & \left| \right. & 0 & c_1^{(2)} & 0 & \left| \right. & \cdots & \vdots \\ 0 & c_2^{(1)} & 0 & \left| \right. & 0 & c_2^{(2)} & 0 & \left| \right. & \cdots & 0 \\ \vdots & \vdots & \vdots & \left| \right. & \vdots & \vdots & \vdots & \left| \right. & \cdots & \vdots \\ 0 & 0 & c_{Q-1}^{(1)} & \left| \right. & 0 & 0 & c_{Q-1}^{(2)} & \left| \right. & \cdots & c_{Q-1}^{(K)} \\ 0 & 0 & c_Q^{(1)} & \left| \right. & 0 & 0 & c_Q^{(2)} & \left| \right. & \cdots & c_Q^{(K)} \end{bmatrix} \quad (2.6)$$

For the analysis in this work, the European UMTS standard is assumed. UMTS utilizes the orthogonal variable spreading factor (OVSF) codes, which as the name implies, are orthogonal codes<sup>2</sup>. The chiprate of UMTS is 3.84 Mchip/s, and the carrier frequency is located around 2 GHz. More details on the UMTS standard can be found in Appendix A.

## 2.2 CDMA Detectors

### 2.2.1 RAKE

The RAKE receiver is still considered as the most common detector for CDMA. By performing maximum ratio combining, the RAKE receiver exploits the multipath diversity in the received signal. Figure 2.1 displays the structure of the RAKE receiver.

The idea of the maximum ratio combining is to delay each signal arriving through the multipath with an appropriate delay time, so that all parts of the signal are delayed to an identical point and can be summed up together after being multiplied with the appropriate weight. This is shown in Figure 2.2. The signal arrived through the first path  $h_0$  will be delayed the most by  $(L - 1)T_c$ , and the largest signal will receive the largest weight because the weight is derived from the channel coefficients (c.f. Figure 2.1).

According to the matrix-vector notation, the signal received by the RAKE receiver can be written as:

$$\hat{\mathbf{d}}_{\text{RAKE}} = \mathbf{A}^H \mathbf{r} = \mathbf{A}^H \mathbf{A} \mathbf{d} + \mathbf{A}^H \mathbf{n}, \quad (2.7)$$

while  $(.)^H$  denotes the transpose conjugate of a matrix.

---

<sup>2</sup>For convenience sake, the scrambling codes are dropped from equation (2.1) and (2.4). However all simulations are performed with the scrambling codes according to the standard.

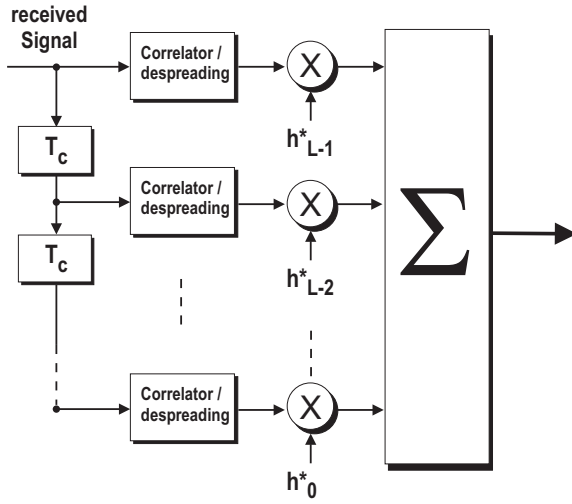


Figure 2.1 RAKE receiver

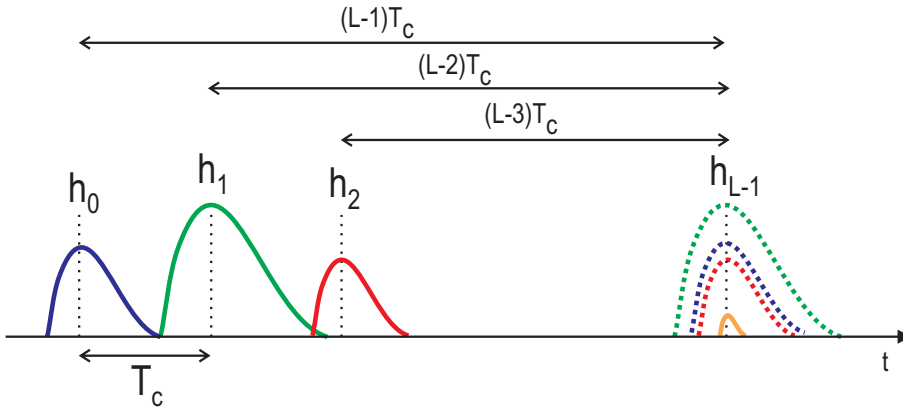
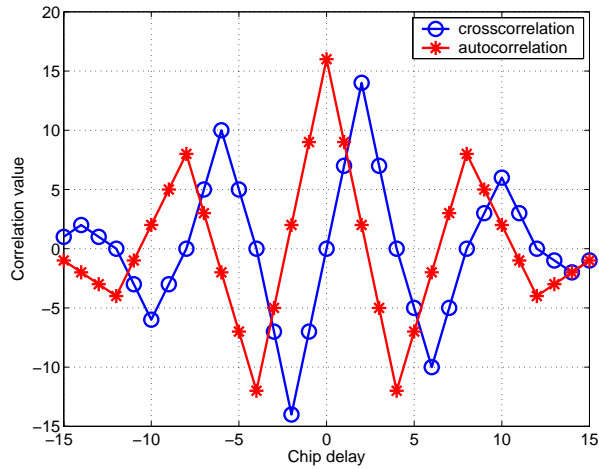


Figure 2.2 The maximum ratio combining on the signals arriving through the multipath  $\mathbf{h} = (h_0, h_1, h_2, \dots, h_{L-1})$

The phenomena of MAI can be readily observed in (2.7). If no multipath distortion is assumed, than the expression  $\mathbf{A}^H \mathbf{A}$

reduces into  $\mathbf{C}^H\mathbf{C}$  which gives us the identity matrix, since the spreading codes are orthogonal<sup>3</sup>. However, as soon as multipath distortion comes into play, the spreading codes are not orthogonal to each other anymore, and  $\mathbf{A}^H\mathbf{A}$  is not equal to an identity matrix.



**Figure 2.3** Examples of the autocorrelation and the crosscorrelation function of the OVSF codes

The intersymbol interference (ISI) and the MAI effect can be illustrated by using the autocorrelation and the crosscorrelation function of the spreading codes. An ideal set of spreading codes will have an autocorrelation function of a perfect delta impulse, and will always take the value zero in the crosscorrelation function. However, there are no known ideal spreading codes, so the autocorrelation and the crosscorrelation function will look like those shown in Figure 2.3. This figure shows an example of the crosscorrelation and the autocorrelation of the OVSF codes. The autocorrelation is from the third code of the OVSF code-family

<sup>3</sup>This work concentrates on the UMTS with orthogonal codes. In systems with non-orthogonal codes, MAI exists even without multipath.

with the spreading factor 16 as is used in the UTRA-TDD system. The crosscorrelation shown, is between the third and the seventh code of the same code-family.

The OVSF codes are orthogonal codes, therefore the cross-correlation value at the delay-time zero is zero. However, the multipath effect destroys this orthogonality which in turn distorts the received signal. This is illustrated in Figure 2.4. At point A and B, the RAKE receiver experiences the side-lobes of the autocorrelation and the crosscorrelation several chips away. The side-lobe of the autocorrelation function depicts the ISI and the side-lobe of the crosscorrelation function implies MAI.

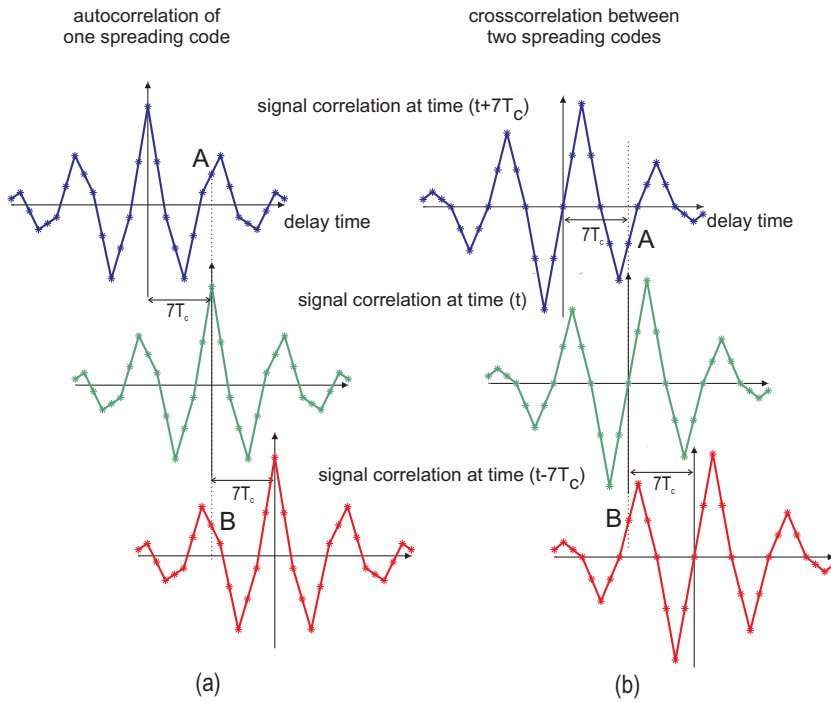


**Figure 2.4** The ISI and MAI illustrated with the (a) autocorrelation and (b) crosscorrelation function of the spreading codes

### 2.2.2 Multiuser Detector

The multiuser detector uses the information of all users jointly to better detect each individual user. It aims to find the most likely vector of all users, instead of only to extract a single user's data out of the composite received signal. The optimal multiuser detector (MLSE) is non-linear in nature, it compares the received data vector with all possible received vectors. Thus the complexity of this detector increases exponentially with the number of users. This implies a huge computational processing, which is not practical.

An important group of suboptimal multiuser detectors are the linear multiuser detectors. These detectors apply a linear mapping on the received signal to reduce the MAI seen by each user [6]. The Zero-Forcing (ZF) multiuser detector (MUD) inverts the  $\mathbf{A}$  matrix in order to extract the data vector  $\mathbf{d}$ . The detected data vector from the MUD-ZF can be written in matrix-vector notation as:

$$\begin{aligned}\hat{\mathbf{d}}_{\text{MUD-ZF}} &= (\mathbf{A}^H \mathbf{A})^{-1} \mathbf{A}^H \mathbf{r} \\ &= \mathbf{d} + (\mathbf{A}^H \mathbf{A})^{-1} \mathbf{A}^H \mathbf{n}.\end{aligned}\tag{2.8}$$

Here, the pseudo-inverse is applied because  $\mathbf{A}$  is not square. It can be seen that the MUD-ZF alleviates the MAI completely. By inverting  $\mathbf{A}$ , the MAI which is hidden in the term  $\mathbf{A}^H \mathbf{A}$  (c.f. 2.7) is avoided.

The MUD-ZF exhibits however one disadvantage. It causes a noise enhancement through the term  $(\mathbf{A}^H \mathbf{A})^{-1} \mathbf{A}^H \mathbf{n}$  in (2.8). This is similar to the noise enhancement experienced by a zero-forcing equalizer. A better linear MUD that takes the background noise into account is the minimum mean squared error (MMSE) MUD. The MUD-MMSE performs MAI suppression as far as it does not enhance the noise. Because of this compromise between noise enhancement and MAI suppression, the MUD-MMSE shows better

bit error rate than the MUD-ZF. The detected data vector from MUD-MMSE can be written as [12]:

$$\hat{\mathbf{d}}_{\text{MUD-MMSE}} = (\mathbf{A}^H \mathbf{A} + \sigma^2 \mathbf{I})^{-1} \mathbf{A}^H \mathbf{r}, \quad (2.9)$$

where  $\sigma^2$  denotes the variance of the additive noise.

### 2.2.3 Equalization

Papers published in the last couple of years have shown a realization that the choice for CDMA receivers is not only between the RAKE receiver and the MUD. Several authors began to see that a simple equalization can solve the MAI problem in CDMA systems effectively. Equalization was shown to outperform the RAKE receiver and it is especially suited for the downlink of CDMA systems [13], [14], [15].

On the outset, the equalizer seems quite similar to a RAKE receiver. We consider the multipath coefficients and use them to process the received signals. That is why sometimes people mistake the RAKE receiver for the equalizer, and are taken by surprise that the equalizer outperforms the RAKE receiver considerably.

The RAKE receiver attempts to exploit the diversity (cf. Section 2.2.1), whereas the equalizer simply turns back the multipath channel into a perfect delta impulse. In the matrix-vector notation, the output of the equalizer can be written as [13]:

$$\begin{aligned} \mathbf{y}_{\text{TDE-ZF}} &= (\mathbf{H}^H \mathbf{H})^{-1} \mathbf{H}^H \mathbf{r} \\ &= \mathbf{C} \mathbf{d} + (\mathbf{H}^H \mathbf{H})^{-1} \mathbf{H}^H \mathbf{n} \end{aligned} \quad (2.10)$$

Unlike the MUD, the equalizer does not invert the whole  $\mathbf{A}$  matrix, but rather only the channel matrix  $\mathbf{H}$ . The equalizer is a singleuser detection strategy, since the  $\mathbf{H}$  matrix contains



only the channel coefficients. Thus for the detection with the equalizer, the information of the spreading codes of other users is not needed.

Equation (2.10) displays the output of a ZF equalizer, which has the disadvantage of enhancing the noise. An MMSE version of the equalizer which alleviates this problem can be expressed as [13]:

$$\mathbf{y}_{\text{TDE-MMSE}} = (\mathbf{H}^H \mathbf{H} + \frac{\sigma^2}{K} \mathbf{I})^{-1} \mathbf{H}^H \mathbf{r}. \quad (2.11)$$

The equalizer is particularly suited for the downlink of a CDMA system, because in downlink all the users' data are transmitted via the same channel. Hence, the  $\mathbf{A}$  matrix can be subdivided into the  $\mathbf{H}$  and  $\mathbf{C}$  matrix (cf. Equation (2.4)). The  $\mathbf{H}$  matrix can then be inverted (equalized) and separately handled from the  $\mathbf{C}$  matrix. The effect of spreading is reversed by a despreading on the output  $\mathbf{y}_{\text{EQ}}$  of the channel equalization as is shown in (2.12)<sup>4</sup>. In the CDMA uplink, the equalization can not be easily implemented, because the columns of the  $\mathbf{A}$  matrix contain data from different users with different channel coefficients.

$$\hat{\mathbf{d}} = \frac{1}{Q} (\mathbf{C}^H \mathbf{y}_{\text{EQ}}). \quad (2.12)$$

The reason why the equalizer outperforms the RAKE receiver can be deduced by comparing (2.7) and (2.10). In CDMA downlink, the MAI is mainly caused by the multipath channel that destroys the orthogonality of the signals. If the channel is equalized, then the orthogonality is restored. The correlation function indicated in Figure 2.4 (b) is brought together to the zero point,

---

<sup>4</sup>The despreading can be done for one user only. It is then given by  $\hat{\mathbf{d}} = \frac{1}{Q} (\mathbf{C}^{(k)H} \mathbf{y}_{\text{EQ}})$ .

and no side-lobe of the crosscorrelation function is experienced by the despreading process. Thereby the MAI is suppressed.

Note also that the MAI problem with the RAKE receiver is partly caused by the correlation properties of the spreading codes. If there were perfect codes with perfect autocorrelation and crosscorrelation properties, there would be no MAI even with the RAKE receiver. However, such *utopian* codes have been shown to be non-existent. There are mathematical bounds showing that we can not optimize the one correlation property without sacrificing the other [16].

The time domain equalizers, however, do not necessarily simplify the detection algorithm. According to its size, the matrix  $\mathbf{H} \in \mathbb{C}^{(NQ+L-1) \times (NQ)}$  demands roughly the same effort for inversion as the matrix  $\mathbf{A} \in \mathbb{C}^{(NQ+L-1) \times (NK)}$ . The number of users  $K$  is usually lower than the spreading code length  $Q$ , however the equalizer does not necessitate the calculation to form the  $\mathbf{A}$  matrix out of the  $\mathbf{C}$  matrix and the channel coefficients. So the complexity of the time domain equalizer is roughly similar to the MUD. A better detector in terms of simplicity, while maintaining the ability to suppress MAI is still lurking around the corner. That will be the topic of the next following chapters.

# [3]

## CDMA Versus OFDM

*Discovery and invention, it could be said, is nothing more than putting a couple of old things together in a new relation. [17]*

**F**REQUENCY domain equalization (FDE) is actually not a new idea. The earliest paper about it can be traced back to 1973 [18]. The time domain equalization (TDE), on the other hand, has been known for quite some time to outperform the RAKE detector in CDMA downlink systems. Nevertheless, the application of the FDE for CDMA signal detection has only begun to be proposed recently [19], [20], [21].

This fact might not be very surprising, if we are willing to acknowledge that the way to discoveries does not follow a linear smooth flow of thought. Sparks of ideas, risky conjectures, and curious questions shape the turns on the road to new insights. And the story about FDE for CDMA began with a naive curious question, “Which system is actually better: CDMA or OFDM?”.

### 3.1 Comparison Overview

Now which one is better, Code Division Multiple Access (CDMA) or Orthogonal Frequency Division Multiplexing (OFDM)? The answer to this simple question does not seem to be simple at all. First of all, it is very difficult to compare two entirely different systems fairly. Second, the advantages and the problems associated with these systems are very different to each other.

Despite these difficulties, such a performance comparison between CDMA and OFDM is curiously very interesting. Both CDMA and OFDM were proposed as the candidates for the 3rd generation mobile telecommunication system. CDMA turned out to be the favored air interface and has become an important component in the IMT-2000 standard family. OFDM, on the other hand, became popular in the wireless broadcasting applications. DVB-T (Digital Video Broadcasting Terrestrial) and DAB (Digital Audio Broadcasting) are standards based on OFDM technique. Recently, OFDM has also gained popularity in the wireless LAN applications. Standards such as IEEE 802.11a and HIPER-

LAN/2 are the results of this growing interest in OFDM.

The OFDM system has gained much attention due to different reasons from the CDMA system (cf. Section 1.1). OFDM facilitates a simple equalization method in combating frequency selective fading channels [22]. It can even be applied without equalization if differential modulation is used (as proposed for DAB). The downside of an OFDM system is its sensitivity to frequency offset and its high peak to average signal power ratio (PAPR).

OFDM avoids the detrimental effects of the intersymbol interference (ISI) by introducing guard intervals which must be longer than the delay spread of the channel. The fading effect manifests itself as a complex gain at each subcarrier, thus enabling a simple equalizing method using a multiplier array at the receiver. For multiuser communication, OFDM is usually implemented in conjunction with other multiple access procedures such as TDMA.

Beside the pure curiosity, a performance comparison between CDMA and OFDM can also be very useful. It can serve as a starting point in designing future mobile telecommunication systems. It can also assist the decision in choosing between the two air interface standards for certain applications. Thus, a comparison between the two systems is worth an attempt [23].

The performance comparison presented in this chapter proceeds in two steps. First, a simple structure of both systems without any channel coding and interleaving will be compared. To simplify matters, we will concentrate only on the downlink. Within a constrained bandwidth, a comparable bit rate will be delivered, and the BER performance of both systems in selective fading channels will be observed. The second step involves existing standards. Two different standards with different parameters (bandwidth, bit rate, frame structure, channel estimation methods, channel coding etc) will be consciously compared at a similar spectrum efficiency (bit/s/Hz). Additionally, we also stretch the

limit of these systems and compare their performance in a very high velocity (350 km/h). DVB-T and UTRA-FDD (UMTS Terrestrial Radio Access - Frequency Division Duplex) were chosen for the comparison. A perfect synchronized system is assumed in all simulations.

The common operation of CDMA and OFDM systems will be observed. No known OFDM standards, implement OFDMA (yet). Therefore, the number of users is not a good criterion for the comparison. Instead, the overall data that can be delivered by the two systems will be observed.

The RAKE detector is chosen as the receiving method for the CDMA system. We acknowledge that the RAKE is not the best detector for CDMA. However, it is still the most common receiver for CDMA systems. Moreover, better receiving techniques such as multiuser detector algorithms, still imply a relatively high computational effort. The RAKE reception will be compared with a differential and a coherent OFDM detector.

## 3.2 Simple CDMA versus OFDM

For the first comparison, we consider a constrained bandwidth of 5 MHz. The CDMA system uses orthogonal Walsh codes and has a chip rate of 4.096 Mcps. The total symbol rate that can be delivered through this system is 4.096 Msps. This happens if we transmit with the spreading factor  $SF = 1$ , or if we transmit the data with  $K$  codes of length  $Q = K$  simultaneously (multicode transmission).

The OFDM symbols have a duration of useful part  $T_U = 40 \mu s$  and a guard length  $\Delta = 8 \mu s$ . The symbol duration is  $T_S = T_U + \Delta = 48 \mu s$ , and the carrier spacing  $\Delta f = 1/T_U = 25$  kHz. The 5 MHz bandwidth will be occupied with 200 carriers of spacing  $\Delta f$ . The total symbol rate of this system is  $T_U/T_S \times 5.10^6$

= 4.166 Msps.

The CDMA system uses a RAKE receiver which combines all multipaths. A perfect channel estimation is assumed for the RAKE receiver as well as for the OFDM coherent detector. The channel estimation for the RAKE receiver is done once every burst (2560 chips). QPSK modulation is used for both systems, and a carrier frequency of 1 GHz is assumed.

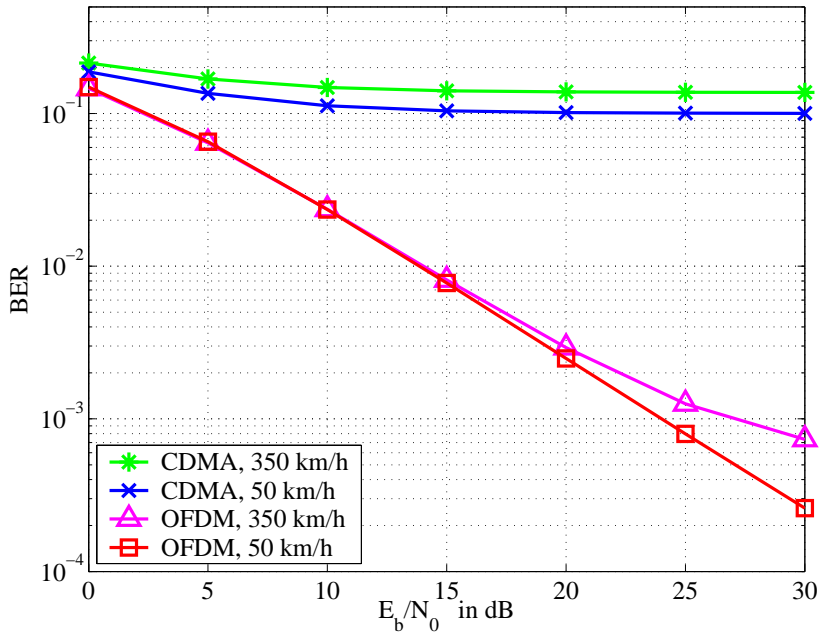


**Figure 3.1** CDMA (SF=16) and coherent OFDM in the typical urban channel

Figure 3.1 shows the performance of a CDMA and an OFDM system with mobile velocities of 50 km/h and 350 km/h in the typical urban channel. All codes in the CDMA system of the length 16 are used, therefore we obtain an overall symbol rate of 4.096 Msps. The OFDM system used for Figure 3.1 employs a coherent detection and has a symbol rate of 4.166 Msps.

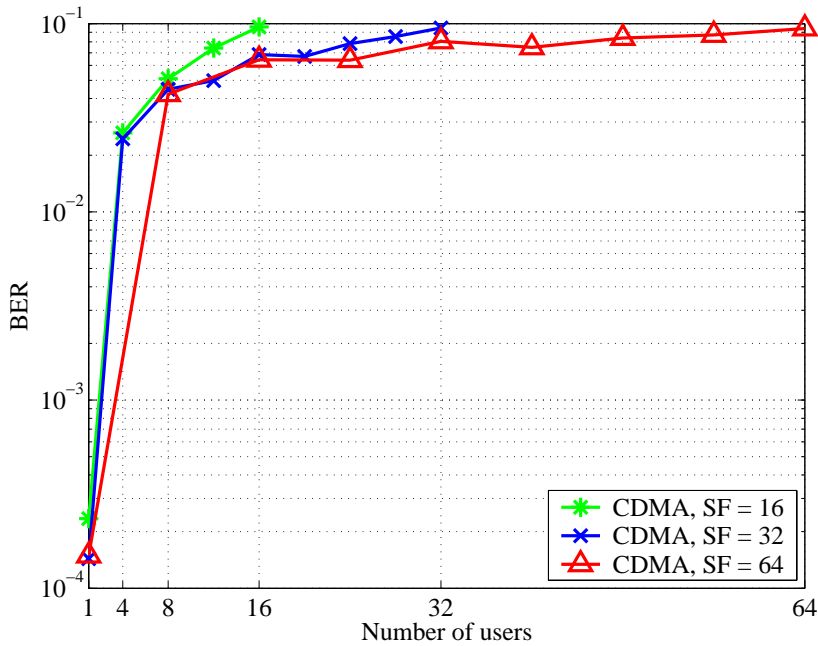


**Figure 3.2** RAKE in the typical urban channel (50 km/h,  $E_b/N_0 = 15$  dB)

In Figure 3.1, the OFDM system outperforms the CDMA system. It seems that the MAI in the CDMA system disturbs the detection substantially, hence a low BER is not attainable with the RAKE receiver. The disturbing effect of the MAI is shown in Figure 3.2, which displays the BER results of a RAKE reception in the typical urban channel with a mobile velocity of 50 km/h and an  $E_b/N_0 = 15$  dB. The MAI increases with the number of users, causing the BER of the RAKE receiver to get worse with increasing number of users.

If only one code is used in CDMA (one user), we will obtain an MAI-free reception with the RAKE receiver. This configuration achieves better BER results and now outperforms the OFDM



reception (Figure 3.3). However, this CDMA system delivers only 1/16 of the maximal symbol rate of the system. To increase the symbol rate, more codes should be used, thus increasing the MAI. Figure 3.3 includes the BER result for the same CDMA system with 3 users. It can be seen that the addition of only 2 users causes noticeable MAI in the system.

Using a higher spreading factor can not improve the BER, if the CDMA cell is saturated. This fact is demonstrated in Figure 3.2: A CDMA system with the spreading factor  $SF=64$  does not achieve better BER compared to  $SF=16$  if all codes are used. In Figure 3.2 all three CDMA systems reach  $BER = 10^{-1}$  at full load.

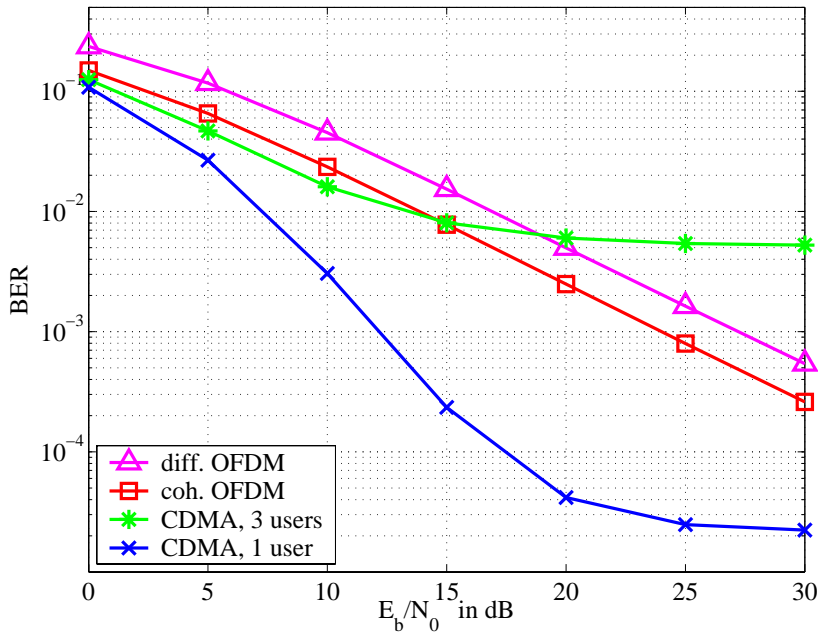


**Figure 3.3** CDMA ( $SF=16$ ) and OFDM in the typical urban channel (50 km/h)

It is also interesting to see the influence of a very high mobile

velocity (up to 350 km/h) on the system performance. The simulation results with  $E_b/N_0 = 20$  dB are shown in Figure 3.4. The coherent OFDM displays only a minimal performance degradation up to 350 km/h. CDMA A denotes a CDMA system using codes with the spreading factor 16, where all codes are used. CDMA A shows a poor performance over all mobile velocities. CDMA B denotes the same CDMA system as CDMA A, but has only one user, thus is free from MAI. We see, that it can perform well for low mobile velocities. The BER results from CDMA B becomes worse than the coherent OFDM system at velocities exceeding 200 km/h.

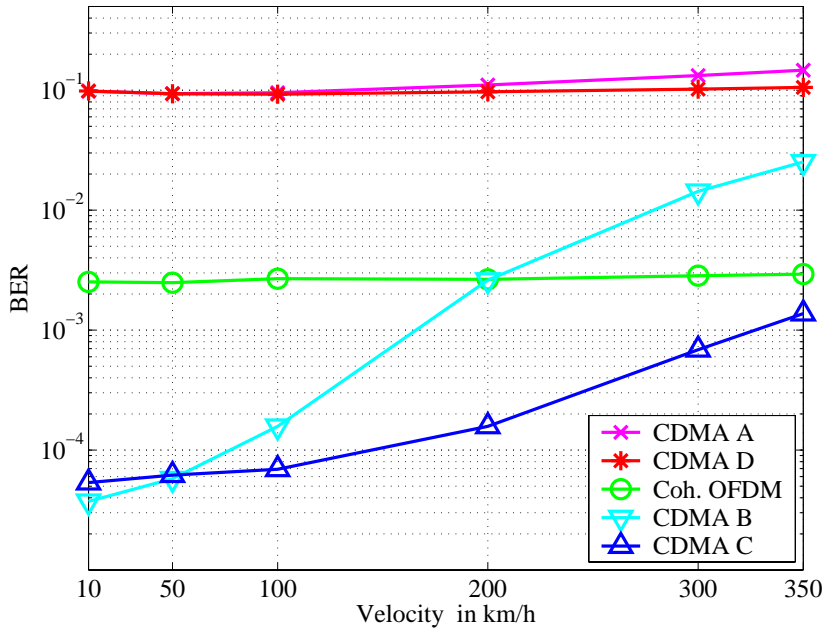


**Figure 3.4** Mobile velocity influence on CDMA and OFDM systems

CDMA C has also only one user (like CDMA B), but CDMA C performs its channel estimation once every 1280 chips, instead

of once every 2560 chips. By doing the channel estimation more often, the CDMA system can now better cope with the channel variation caused by the high velocity. CDMA C performs even better than OFDM up to 350 km/h. We have to note however, that CDMA B and CDMA C deliver only 1/16 of the maximal available data rate. Performing the channel estimation more often also implies more overhead for the midamble or pilot sequences.

Figure 3.4 also shows CDMA D, a saturated CDMA system with the channel estimation performed every 1280 chips. As can be seen, the channel estimation which is now performed more often, cannot improve the BER in a saturated CDMA system. CDMA D shows poor BER results just as CDMA A.

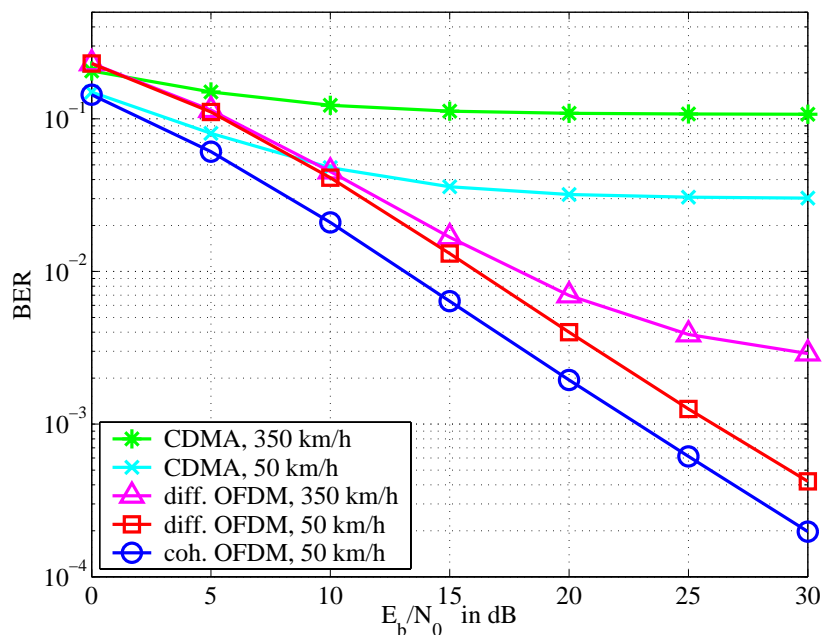


**Figure 3.5** CDMA (SF=16) and OFDM in the rural channel

Figure 3.5 displays the performance of CDMA and OFDM

systems in the rural channel. Additionally, simulations for a very high velocity (350 km/h) are also included. It can be seen that in a rural channel, the OFDM system outperforms the CDMA as well. Even the differential OFDM system can still function well at 350 km/h, whereas the CDMA system shows a poor BER. We also note however, that the saturated CDMA system performs better in the rural channel (Figure 3.5) as in the typical urban channel (Figure 3.1).

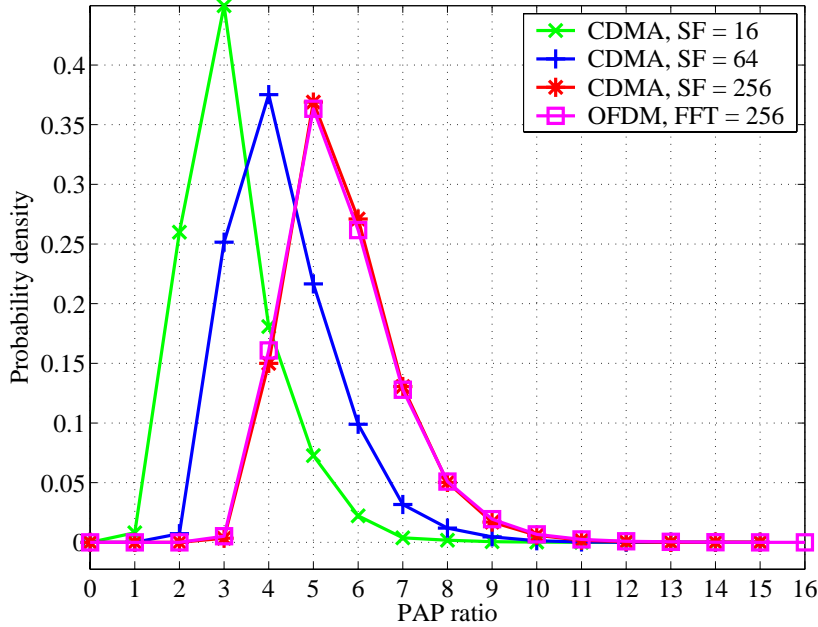


**Figure 3.6** PAPR of CDMA and OFDM signals

One of the well known problems of OFDM systems are the peak to average signal power ratio (PAPR) of OFDM signals. Because of the high PAPR, the power amplifier must operate at a higher back off. Figure 3.6 displays the PAPR of an OFDM signal obtained from an FFT of length 256. Along with it, several PAPR curves of CDMA downlink signals with different spreading

factors are shown. We see that the PAPR of the CDMA signal with the spreading factor 256 resembles the PAPR of the OFDM signal with the FFT length 256. Note that CDMA systems do not have a PAPR problem in uplink, where each user transmits only his data. In downlink however, CDMA signals may exhibit a PAPR problem similar to an OFDM system.

### 3.3 DVB-T versus UTRA-FDD

We simulate the DVB-T system with the 2K mode [24]. This mode uses 1705 carriers, of which 1512 are used for data. Each OFDM symbol has a useful symbol duration of  $T_U = 224 \mu\text{s}$ , thus the carrier spacing is  $\Delta f = 1/T_U = 4.464 \text{ kHz}$ . A guard interval of 1/8 of the symbol duration is used ( $\Delta = 28 \mu\text{s}$ ). This system uses 4 QAM modulation and delivers 11.44 Mbps in a bandwidth of 8 MHz, giving a bandwidth efficiency of 1.5 bit/s/Hz (only data, without pilots). To receive the DVB-T signals, a channel estimation algorithm based on Wiener filters as described in [25] is used. The carrier frequency of the DVB-T system is 800 MHz.

The UTRA-FDD mode according to [26] was chosen for the comparison. Six channels were transmitted during a Transmission Time Interval (TTI) of 80 ms with a spreading factor of 8. The channel estimation is done by correlating the pilot sequences. The RAKE receiver used, selects four paths with the greatest power for the maximal ratio combining. This system covers a bandwidth of 4.4 MHz and is able to deliver 5.485 Mbps, giving a bandwidth efficiency of 1.31 bit/s/Hz. The system is simulated at a carrier frequency of 2 GHz.

The following figures display the BERs of the coherent DVB-T system and the UTRA-FDD system. Figures 3.7 and 3.8 show the BER of an uncoded DVB-T and UTRA-FDD system in the typical urban and the rural channel, respectively. Because real communication systems always employ a certain channel coding

algorithm, the two systems are also simulated with channel coding, and the results are presented in Figures 3.9 and 3.10. DVB-T employs a concatenation of a convolutional code and a Reed Solomon code according to [24], UTRA-FDD uses turbo codes as specified in [27].

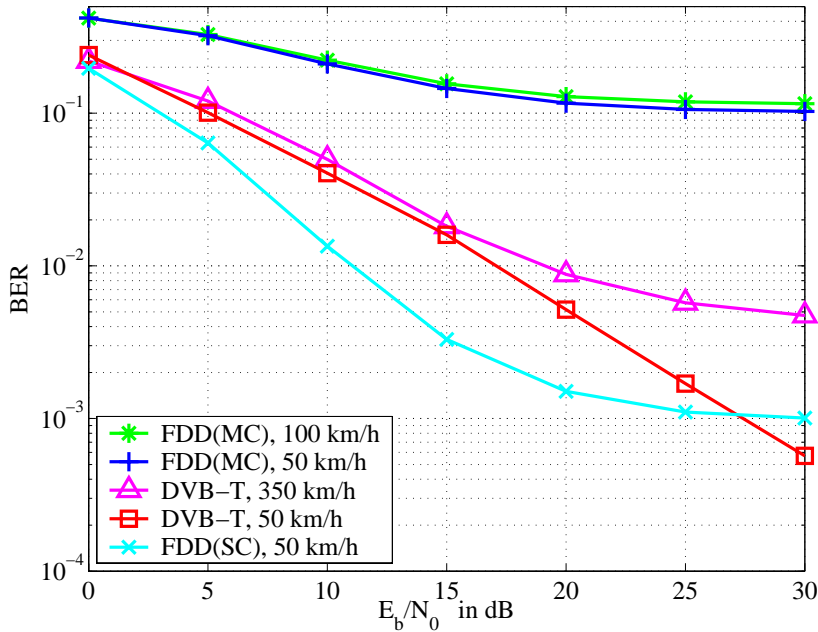


**Figure 3.7** Uncoded DVB-T and UTRA-FDD in the typical urban channel

The uncoded simulations (Figures 3.7 and 3.8) indicate that the DVB-T can achieve better BER results than the UTRA-FDD operating in the multi code (MC) mode. In the MC-mode, several codes are used by one user to increase the data rate. In the simulation, six codes are used in the FDD MC-mode. Figures 3.7 and 3.8 also display the single code FDD (SC), which demonstrates a good BER performance. However, the UTRA-FDD operating in single code delivers data only at 1/6 rate as the FDD MC.

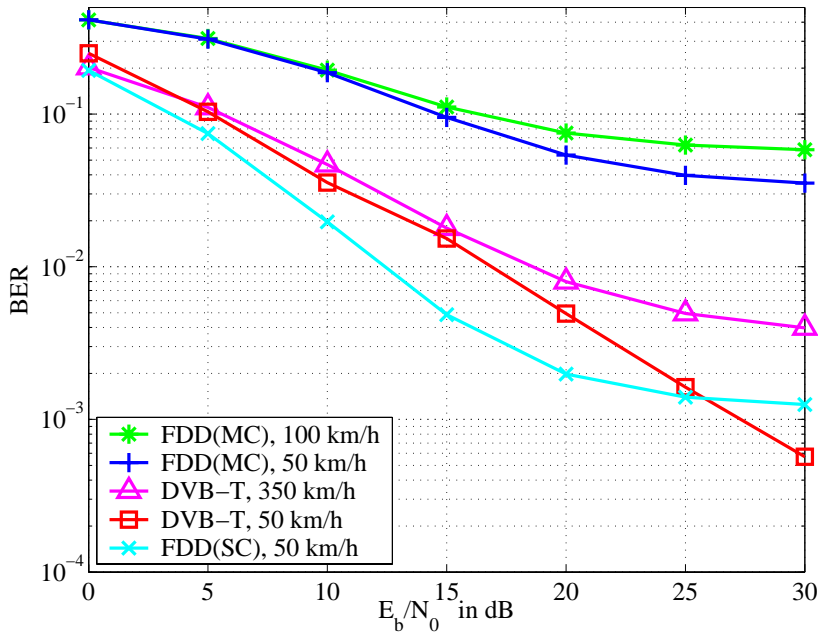


**Figure 3.8** Uncoded DVB and UTRA-FDD in the rural channel

Figures 3.9 and 3.10 show the coded simulation results. FDD BER results are obtained from turbo coding that performs four iterations and has a code rate of 0.356. We see that turbo codes start to improve the BER results after  $E_b/N_0 > 10$  dB.

Although the turbo code improves the FDD signal BER very much, the coded DVB-T still turns out to be superior in the typical urban channel (Figure 3.9). The concatenated convolutional and RS code used in DVB-T has a total code rate of 0.46, which means that the DVB-T delivers almost 30% more info bits than the UTRA-FDD. Even at 350 km/h, DVB-T still delivers a good BER.

In Figure 3.9, the FDD reception differs only a little at 100 km/h compared to 50 km/h. Nevertheless, at 250 km/h, the BER

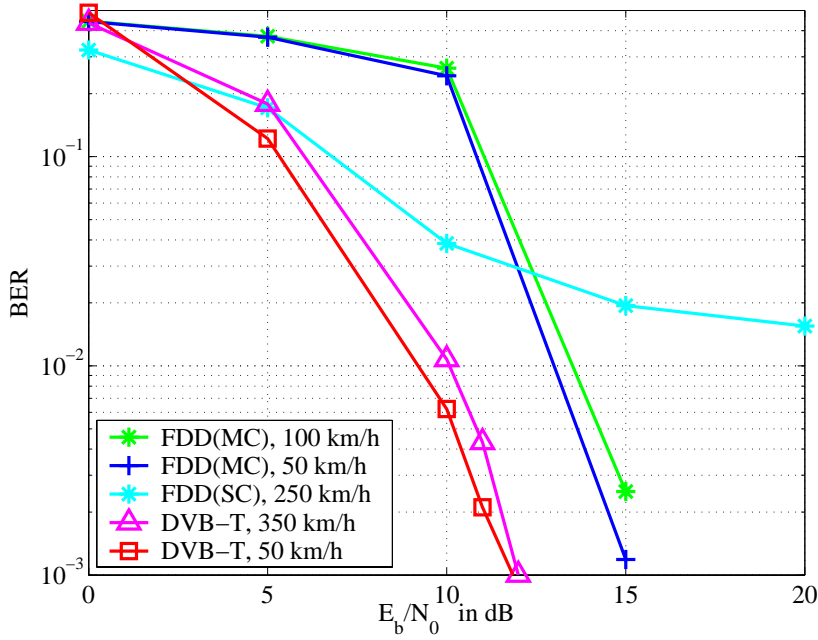


**Figure 3.9** Coded DVB-T and UTRA-FDD in the typical urban channel

result deteriorates. A channel coding algorithm cannot improve the BER of a signal in an environment full of noise. Improvements on the BER results can only be achieved by the channel coding at an  $E_b/N_0$ , at which the uncoded BER results have reached a certain good level. We observe from Figures 3.7 and 3.8 that the uncoded BER results of the FDD system does not vary too much for  $E_b/N_0$  below and over 10 dB. This means that a slight change caused by channel or mobile velocity variations can change the coded BER results of the saturated FDD system drastically.

Results of the coded simulations on the rural channel are shown in Figure 3.10. The rural channel has a shorter delay spread than the typical urban channel. For this reason, the UTRA-FDD shows a better BER result for the rural channel



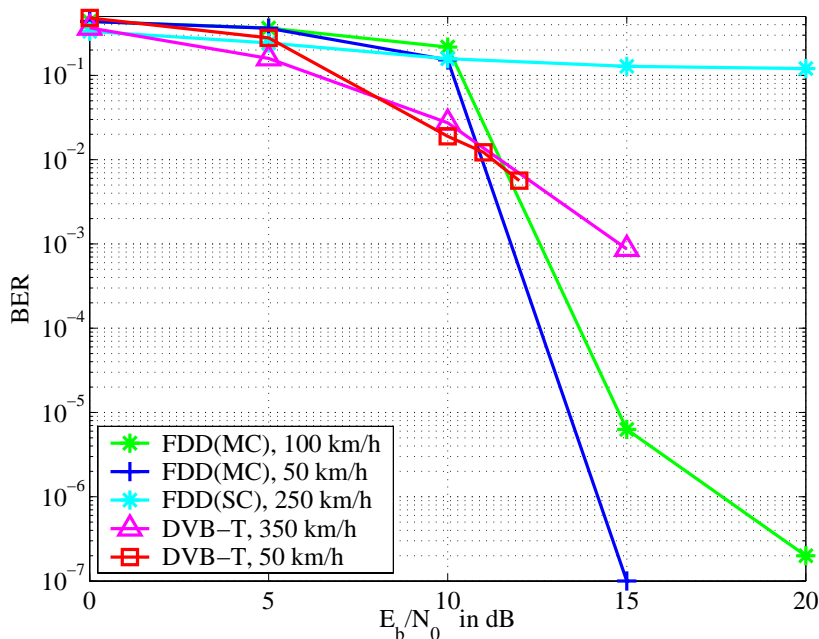


**Figure 3.10** Coded DVB-T and UTRA-FDD in the rural channel

than for the typical urban channel. In the rural channel, DVB-T still outperforms UTRA-FDD, although not as much as in the typical urban channel.

### 3.4 Is OFDM better than CDMA?

From the simulation results, we have seen that OFDM systems outperform CDMA systems with the RAKE receiver. Care has been taken to ensure - as far as possible - a fair comparison between the two systems. Furthermore, the two-step-comparison guards against the danger that the insight gained through the simulations is limited only to a particular situation or accidentally

acquired by an ill constructed simulation scenario. It seems that the OFDM systems outperform the CDMA systems consistently regardless of the channel characteristics, system parameters and channel codings.

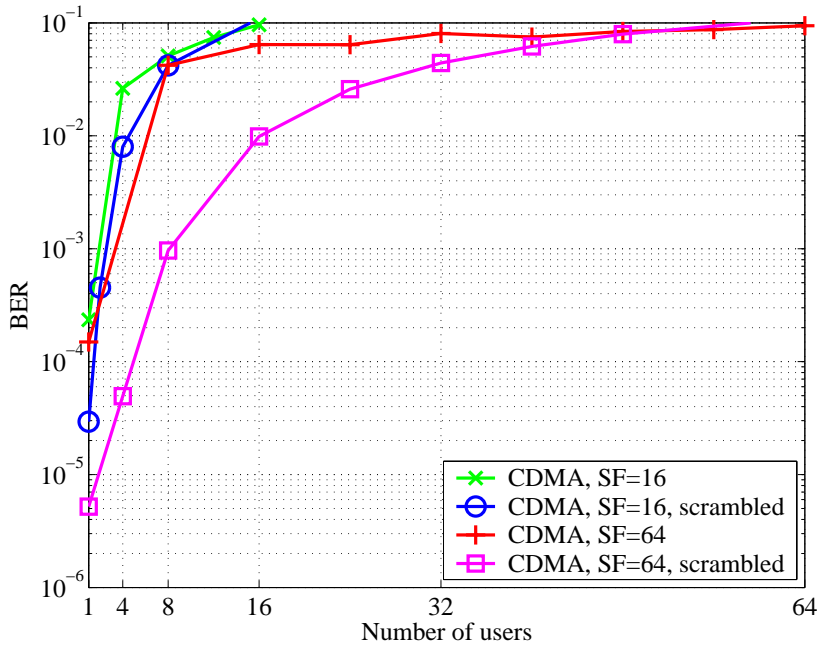


**Figure 3.11** RAKE detector with scrambled and unscrambled CDMA systems in the typical urban channel (50 km/h,  $E_b/N_0=15$  dB)

To be precise, we have not yet proven that OFDM systems are superior to CDMA systems in every respect. The OFDM systems which were investigated, do not include any multiple access procedure. We also have ignored the problem of frequency offset which is the weakness of OFDM systems. However, at the end of the day, the problem of CDMA systems has been clearly pinpointed, and that is the MAI which is caused by the RAKE

detector.

It is also known that the scrambling process can be beneficial for the correlation properties of orthogonal codes. The scrambling itself, for example in UTRA-FDD [26], is actually done to identify the mobile cells; but at the same time, it improves the correlation properties of the spreading codes [28]. The effect of scrambling is shown in Figure 3.11. It can be seen that the CDMA systems with scrambling show generally a better BER as the systems without scrambling. However, the scrambling process does not help any further if the number of users is equal to the number of available spreading codes (fully loaded cell). Thus the MAI remains a problem to be solved.



# 4

## Frequency Domain Equalization for CDMA Downlink

*Discovery consists of looking at the same thing as everyone else  
and thinking something different (Albert Szent-György)*

CHAPTER 3 indicates that OFDM systems outperform CDMA systems with the RAKE receiver which suffers from MAI. This insight leads to another more challenging question, “Can we transfer the OFDM system structure in such a way and implant it in a CDMA system to improve its performance?” Since the OFDM systems consistently outperform the CDMA systems with the RAKE receiver despite the channel characteristics and the system parameters, it seems to be logically feasible to improve the CDMA performance by *copying* the OFDM strategy into a CDMA system. Brooding on this, the author arrived on the idea of using frequency domain equalization (FDE) for CDMA detection [19],[21] <sup>1</sup>.

## 4.1 The FDE

The FDE has won the attention of researchers at around the same time as the OFDM system took its rise in popularity. Several authors even put the two systems side-by-side and observed a similar performance [22], [30]. Similarities between FDE and OFDM structure were also identified, and the coexistence between the two systems was explored [31].

The problem of equalization is actually a deconvolution problem, which reduces to a division (complex multiplication) operation when performed in the frequency domain. Figure 4.1 shows the structure of the frequency domain equalization (FDE). It consists of an FFT, a multiplier array and an IFFT block. The received discrete signal  $r(n)$  is first passed to an  $N$ -point FFT. Each

---

<sup>1</sup>As his paper [19] was presented, the author was not aware about the paper written by Baum et al. a few months earlier, proposing the same idea [20]. He found out later, interestingly enough, that Baum et al. have also conducted a similar performance comparison between CDMA and OFDM [29]. Looking at the problem from the same perspective, they naturally arrived at the same solution!

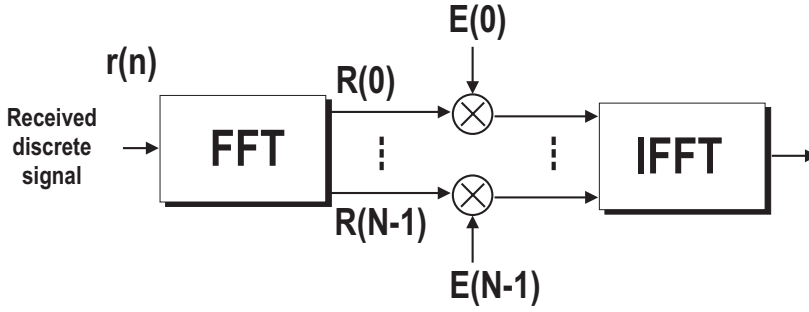


**Figure 4.1** Structure of FDE

output sample  $R(k) = \sum_{n=0}^{N-1} r(n)e^{-j2\pi kn/N}$ ,  $k = 0, 1, \dots, N-1$  is then multiplied by a complex coefficient  $E(k)$ , which is derived from the channel impulse response. Finally, the IFFT transforms the equalized signal back to the time domain.

The FDE complex coefficient  $E(k)$  can be derived according to the Zero-Forcing (ZF) criterion and it results in:

$$E(k) = \frac{1}{H(k)}, \quad (4.1)$$

or the Minimum Mean Square Error (MMSE) criterion, and we obtain [22], [30]:

$$E(k) = \frac{H^*(k)}{|H(k)|^2 + \sigma_n^2/\sigma_a^2} = \frac{H^*(k)}{|H(k)|^2 + 1/SNR}. \quad (4.2)$$

where  $H(k)$  is the  $k$ th discrete frequency element of the channel transfer function  $H(\omega)$ ,  $\sigma_n^2$  is the variance of the additive noise (AWGN), and  $\sigma_a^2$  is the variance of the transmitted data symbols.

The ZF equalizer shows several drawbacks. It enhances the noise for small  $H(k)$  and does not have a finite solution for  $H(k) = 0$ . The MMSE solution makes a trade-off between the ISI (gain and phase mismatch) and noise enhancement, thus it performs better than the ZF-FDE, especially for channels with spectral nulls or deep fading gains.

## 4.2 FDE for CDMA Downlink

The FDE belongs to the equalization approach. Hence in the matrix-vector notation, it follows the idea expressed in (2.10). The implementation of the equalizer in the frequency domain is based on the fact that every circulant matrix  $\mathbf{Z}$  can be written as [32], [33]:

$$\mathbf{Z} = \mathbf{F}^{-1}\mathbf{\Lambda}\mathbf{F}, \quad (4.3)$$

where  $\mathbf{\Lambda}$  is a diagonal matrix containing the eigenvalues of  $\mathbf{Z}$  in its diagonal. The vector multiplication with  $\mathbf{F}$  forms the Fourier transform of the vector. To compute the eigenvalue matrix  $\mathbf{\Lambda}$ , only the first column of  $\mathbf{Z}$  has to be transformed:

$$\mathbf{\Lambda} = \text{diag}(\mathbf{F}\mathbf{Z}(:, 1)) \quad (4.4)$$

"diag" corresponds to sorting the vector elements into the diagonal of a matrix and  $\mathbf{Z}(:, 1)$  is the MATLAB notation denoting the first column of  $\mathbf{Z}$ .

Substituting (4.3) in systems of equations like

$$\mathbf{Z}\mathbf{x} = \mathbf{b}, \quad (4.5)$$

we obtain:

$$\mathbf{\Lambda}\mathbf{F}\mathbf{x} = \mathbf{F}\mathbf{b}. \quad (4.6)$$

(4.5) can then be solved as follows:

$$\mathbf{x} = \mathbf{Z}^{-1}\mathbf{b} = \mathbf{F}^{-1}\mathbf{\Lambda}^{-1}\mathbf{F}\mathbf{b} \quad (4.7)$$

Implementing (4.7) for the inversion of the channel matrix  $\mathbf{H}$ , we arrive at the description of FDE. The output  $\mathbf{y}_{\text{FDE}}$  of the FDE can be expressed (using MATLAB notation) as:

$$\mathbf{y}_{\text{FDE-ZF}} = \text{IFFT} [\text{FFT}(\mathbf{r}) ./ \text{FFT}(\mathbf{H}(:, 1))] \quad (4.8)$$



The FDE description for CDMA in (4.8) corresponds exactly to the process shown in Figure 4.1. First, the received vector  $\mathbf{r}$  is Fourier transformed into the frequency domain. The output is then point-by-point divided (complex multiplication) with the Fourier transform of the channel impulse response  $\text{FFT}(\mathbf{H}(:, 1))$ . The results will finally be transformed back into the time domain with the IFFT. The estimate of the data symbols can then be obtained by despreading on the output of the FDE as in (2.12).

The implementation of the FDE with the MMSE criterion differs to (4.8) only in the complex values, which are used for the point-by-point division. In this case the complex coefficients are not obtained simply by FFT on the first column of  $\mathbf{H}$  (i.e. the FFT of the discrete channel impulse response), but they are derived according to (4.2)

### 4.3 Cyclic Prefix, Zero-Padding, Overlap-Cut

The circularity assumption of  $\mathbf{H}$  in (4.3) implies the circular (de-)convolution with the Fourier transform. It means, that the equalization in the frequency domain will be done based on the circulant matrix  $\tilde{\mathbf{H}}$ . An example of a circulant matrix  $\tilde{\mathbf{H}}$  of a channel with 4 taps ( $h_0, h_1, h_2, h_3$ ) is shown in (4.9) (with the number of symbols  $N = 2$ , and a spreading factor of  $Q = 4$ ).

$$\tilde{\mathbf{H}} = \begin{bmatrix} h_0 & 0 & 0 & 0 & 0 & h_3 & h_2 & h_1 \\ h_1 & h_0 & 0 & 0 & 0 & 0 & h_3 & h_2 \\ h_2 & h_1 & h_0 & 0 & 0 & 0 & 0 & h_3 \\ h_3 & h_2 & h_1 & h_0 & 0 & 0 & 0 & 0 \\ 0 & h_3 & h_2 & h_1 & h_0 & 0 & 0 & 0 \\ 0 & 0 & h_3 & h_2 & h_1 & h_0 & 0 & 0 \\ 0 & 0 & 0 & h_3 & h_2 & h_1 & h_0 & 0 \\ 0 & 0 & 0 & 0 & h_3 & h_2 & h_1 & h_0 \end{bmatrix} \quad (4.9)$$

Three data processing methods have been proposed to take this circularity into account: cyclic prefix, zero-padding and overlap-cut method. FDE for CDMA with cyclic prefix was proposed in [19],[20]<sup>2</sup>.

In the cyclic prefix method, the last  $n$  symbols in the group of  $N$  observed symbols will be copied to the front of the data group before sending. This cyclic extension will be removed at the receiver and the FFT will be done on the original  $N$  symbols. Figure 4.2 depicts the CDMA downlink system using FDE with cyclic prefix.

The effect of the cyclic prefix on the convolution and the equalization process is illustrated in Figure 4.3. The cyclic prefix extends the  $N \times Q$  chips of spread data  $\mathbf{Cd}$ , in which the shaded area of the data part  $X$  is copied to the front of the data block. The non-circular convolution with the channel will now appear circular because of the cyclic prefix. The hatched area below the cyclic prefix CP displays the area, which is influenced by the convolution spilling over out of the CP area; and because the CP area is a copy of the last sequences of the data block, the non-circular convolution appears as if it was obtained by a multiplication with the circulant matrix  $\tilde{\mathbf{H}}$  shown on the left of Figure 4.3. After removal of the cyclic prefix (Figure 4.2), the received data can then be processed with the circulant matrix  $\tilde{\mathbf{H}}$  implied by the FDE algorithm.

In the zero-padding method,  $n$  zeros will be added to the end of  $N - n$  symbols to build a group of  $N$  symbols before sending. At the receiver, the FFT will be done on the padded data block, the detected zeros at the end of this data block will then be discarded. Figure 4.4 illustrates this process. An example of one data slot containing 2560 chips is shown, which is divided into

---

<sup>2</sup>Note that early proposals of the FDE for CDMA take over the cyclic-prefix implementation, which is a feature of an OFDM system. This is very natural, considering how one arrives at the idea of FDE for CDMA.

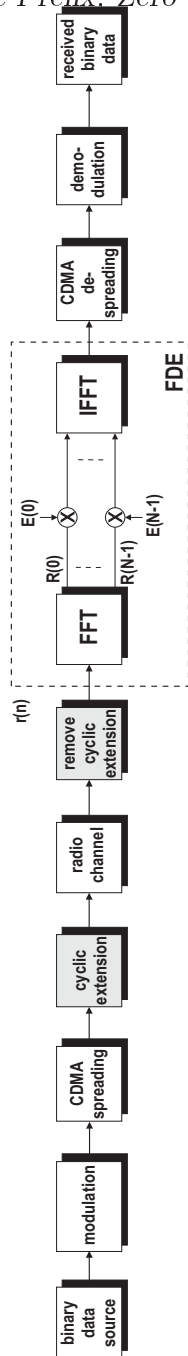
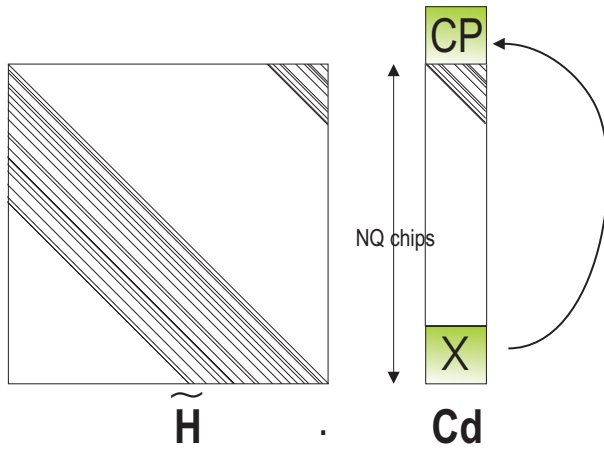
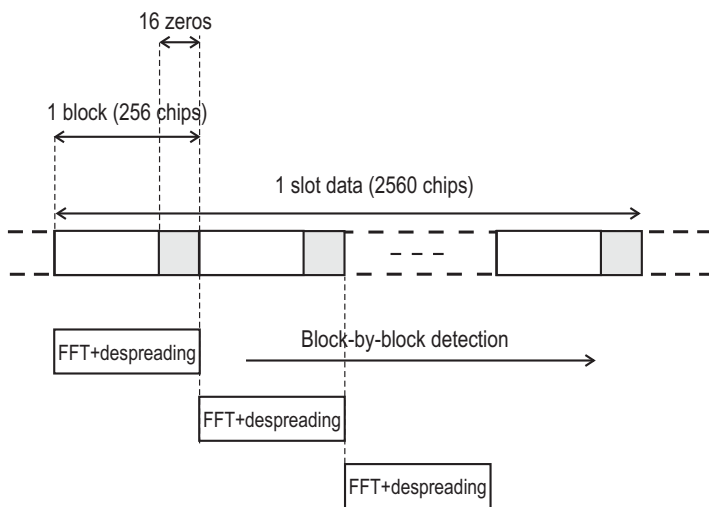


Figure 4.2 FDE detector for CDMA downlink with cyclic prefix



**Figure 4.3** The effect of cyclic prefix on the convolution between the spread data  $\mathbf{Cd}$  and the channel  $\mathbf{H}$



**Figure 4.4** CDMA transmission with the FDE detector using zero-padding

smaller blocks of 256 chips. The last 16 chips of each block consist of zeros. At the receiver, the FFT is performed on each data block of 256 chips. The detected zero symbols at the end of each block are discarded after the despreading. The cyclic prefix and the zero-padding method solve the problem that arises through the discrepancy between the *non-circular* channel convolution and the *circular* channel equalization. With these two methods, the length of the cyclic prefix or the trailing zeros should always be larger than the length of the channel impulse response.

Both the cyclic prefix and the zero padding method divide the data stream into small blocks of data by adding redundancies. There is however another way to implement FDE without redundancy, which here will be referred as the *overlap-cut* method. Vollmer et al. applied this method in implementing the linear multiuser detector in the frequency domain [34]. Machauer [35] took this method for the multiuser detector in time domain, and showed that the performance of the overlap-cut method can approximate the reference multiuser detector, which detects the whole data burst in one step.

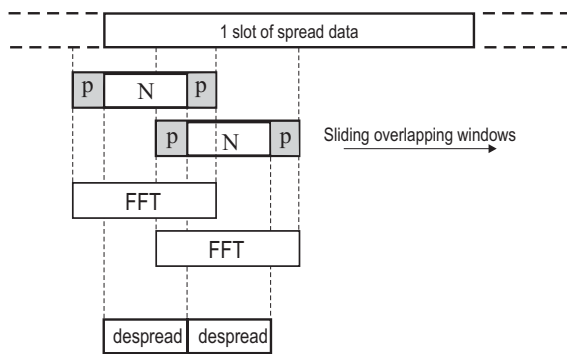


**Figure 4.5** CDMA transmission with the FDE detector using overlap-cut

The overlap-cut method is displayed in Figure 4.5. Here, the FFT is done on overlapping sliding windows of  $N + 2p$  symbols,  $p$  denotes the length of the pre- and postlap of the detection windows. The detected  $2p$  symbols at the edges of each window are discarded before despreading.

The overlap-cut method is similar to the overlap-save method, which can be used to perform a fast convolution on a data stream with an infinite length [36]. The difference is that the overlap-cut method works with a deconvolution. It is applied on the inverse of the circulant matrix  $\tilde{\mathbf{H}}$ . The overlap-save method gives exact convolution results, if it is used to perform a convolution in the frequency domain. On the other hand, the overlap-cut method is an approximation, because the inverse of the Toeplitz matrix  $\mathbf{H}$  is different from the inverse of its circulant matrix counterpart  $\tilde{\mathbf{H}}$ .

The feasibility of the overlap-cut method can be illustrated by looking at Figure 4.6, where the error profile of the detection using the overlap-cut method is shown<sup>3</sup>. For each curve in Figure 4.6, random data (+1 and -1) are generated for 3 overlapping windows in the overlap-cut method (Figure 4.5). These data were then convolved with a randomly generated channel with 4 taps, and then processed with the FDE using the overlap-cut method. Finally, the average error between the received data and the original data in the second data block (the data block in the middle) is calculated and displayed in Figure 4.6. For each curve, 10000 channel realizations were used.

It can be observed, that most of the detection-errors take place at the edges of the block. This means, these errors can be minimized by cutting away the edges of the data block after the FFT. Three block lengths are shown in Figure 4.6: 64, 128 and 256. The average error of the overlap-cut method decreases with

---

<sup>3</sup>The word *error* here does not refer to the bit error rate. Rather it is the Euclidean distance between the obtained data and the original data.

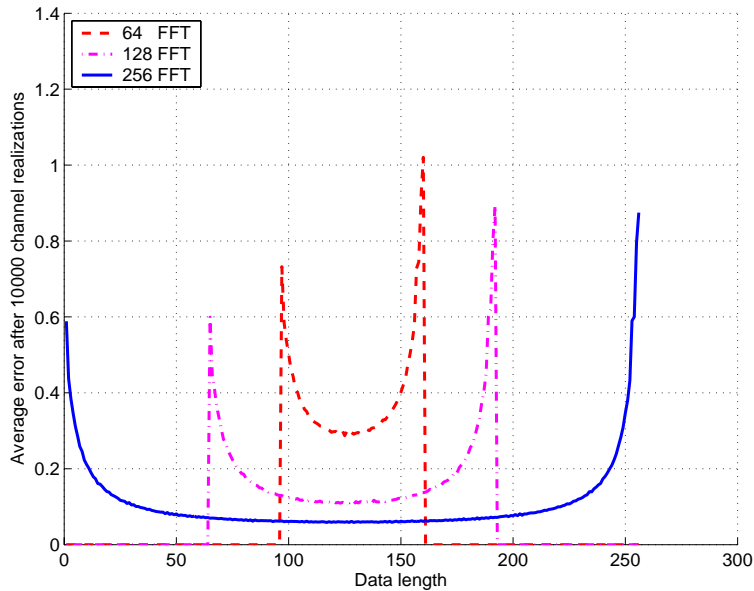


**Figure 4.6** Error profile of the overlap-cut method with the FFT block-length of 64, 128 and 256

increasing FFT length.

## 4.4 Performance of the FDE for CDMA Downlink

This section presents the simulation results of the FDE detector for a TD-CDMA downlink system with parameters taken from the UTRA-TDD standard [26], [37]. A normalized 4-tap time-invariant channel and the time-variant VehicularA channel [38] are used for the simulations. The 4-tap time-invariant channel is randomly generated for every UTRA-TDD slot (2560 chips). A perfect channel knowledge is assumed in the receiver, and the channel coefficients are updated every data slot.

The uncoded BER curves for the FDE-ZF with the 4-tap invariant channel are displayed in Figure 4.7. All variants of the FDE-ZF (cyclic prefix, zero-padding and overlap-cut) outperform the RAKE receiver. The performance of the time domain equalizer (TDE) according to zero-forcing (ZF) criterion is also shown. In a time-invariant channel, the performance of TDE and FDE is hardly distinguishable.

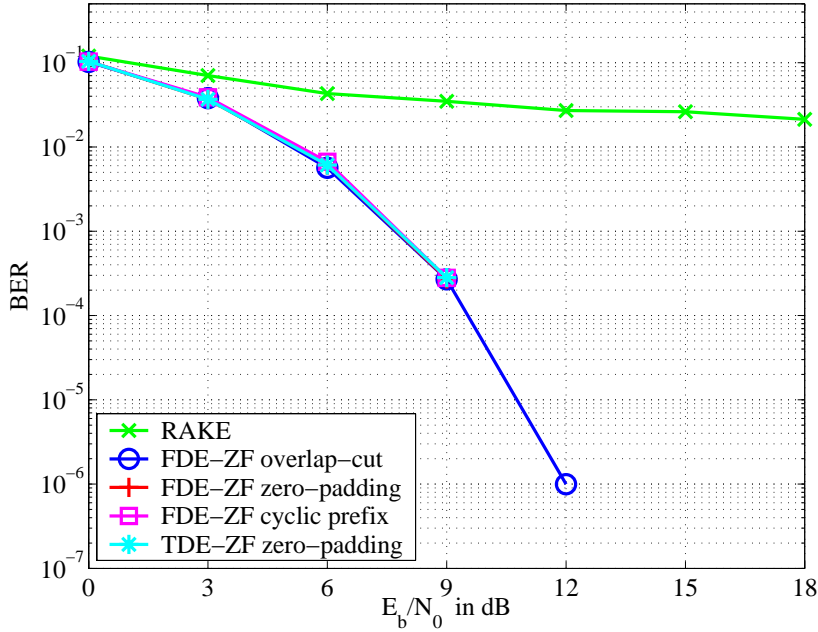


**Figure 4.7** Uncoded BER of the FDE-ZF detector in the UTRA-TDD system with a 4-tap time-invariant channel, spreading factor 16, 16 users

Figure 4.8 shows the corresponding BER results for the FDE-MMSE. The results show the same tendencies as the FDE-ZF. Moreover, comparing Figure 4.7 and Figure 4.8, we see an almost identical performance between FDE-ZF and FDE-MMSE in time-invariant channel.



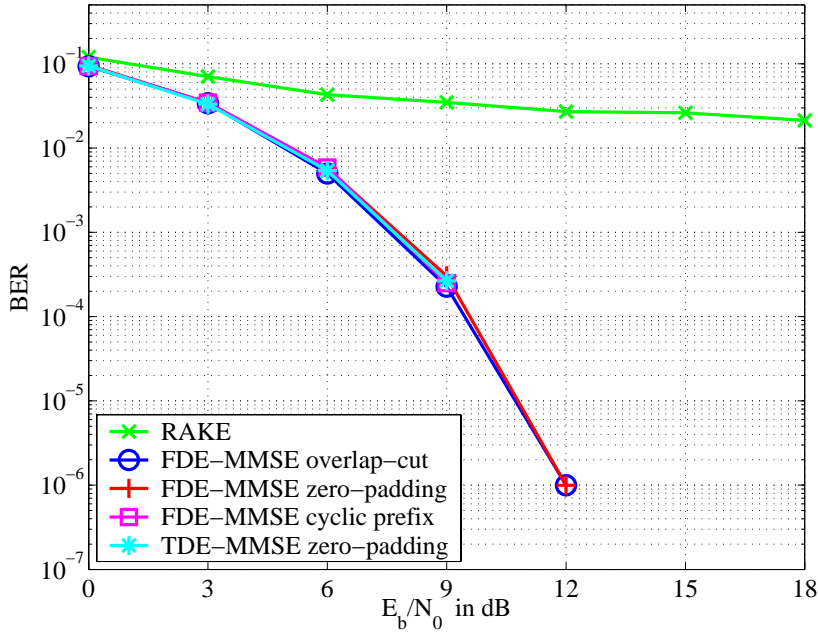


**Figure 4.8** Uncoded BER of the FDE-MMSE detector in the UTRA-TDD system with a 4-tap time-invariant channel, spreading factor 16, 16 users

Simulations with the VehicularA channel brought out behavior that is unobservable in the time-invariant channel. This is shown in Figure 4.9. Here, we can see differences in the performance between the various types of equalization detectors. The best BER is displayed by the TDE-ZF, followed by the FDE-ZF zero-padding and cyclic prefix, which show roughly the same performance, and lastly the FDE-ZF overlap-cut. These differences accentuate the effect of approximation in each variant of the equalizers.

The FDE approach is actually an approximation of the TDE. The Toeplitz channel matrix  $\mathbf{H}$ , which is inverted in the TDE, is replaced with the circulant approximation matrix  $\tilde{\mathbf{H}}$  in the

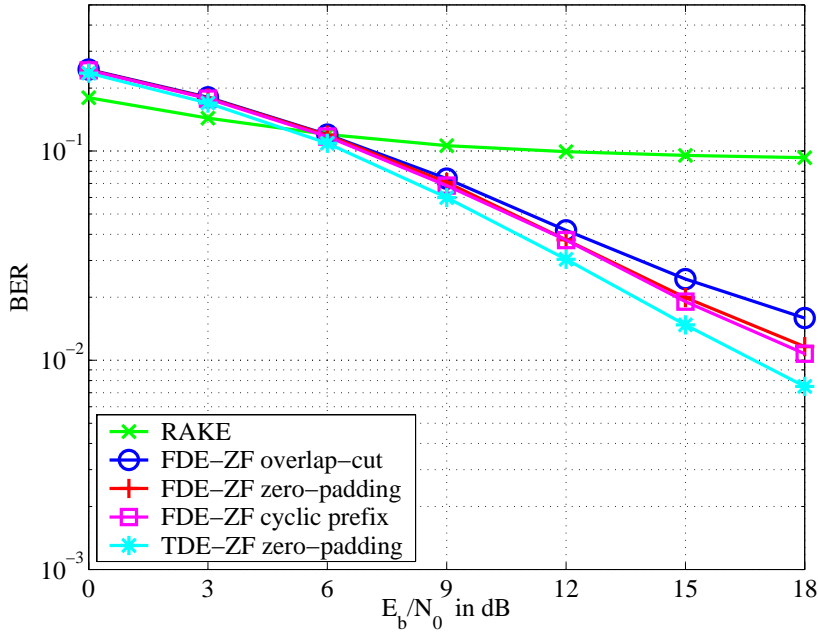


**Figure 4.9** Uncoded BER of the FDE-ZF detector in the UTRA-TDD system with the VehicularA channel (50km/h), spreading factor 16, 16 users

FDE. The inverse of the circulant matrix  $\tilde{\mathbf{H}}$  is not equal to the inverse of the Toeplitz matrix  $\mathbf{H}$ . However, it can be shown that the inverse of the circulant matrix converges to its approximated Toeplitz matrix with the rate of  $\mathcal{O}(1/N)$ , where  $N$  is the size of the matrix [39]. Even when the cyclic prefix and the zero-padding method solve the intersymbol interference completely by dividing the data stream into independent blocks, the effect of the approximation by the circulant matrix can still be observed in the BER of the FDE-ZF detectors in a time-variant channel.

The overlap-cut method adds another approximation level to the FDE approach. There is no strict division between the data blocks in the overlap-cut method, thus the influence of one block

continues to the next block. The cutting away of the edges of the detected data (cf. Figure 4.5) reduces the distortion. However, as can be expected, the overlap-cut method performs slightly worse compared to the cyclic prefix and the zero-padding method.

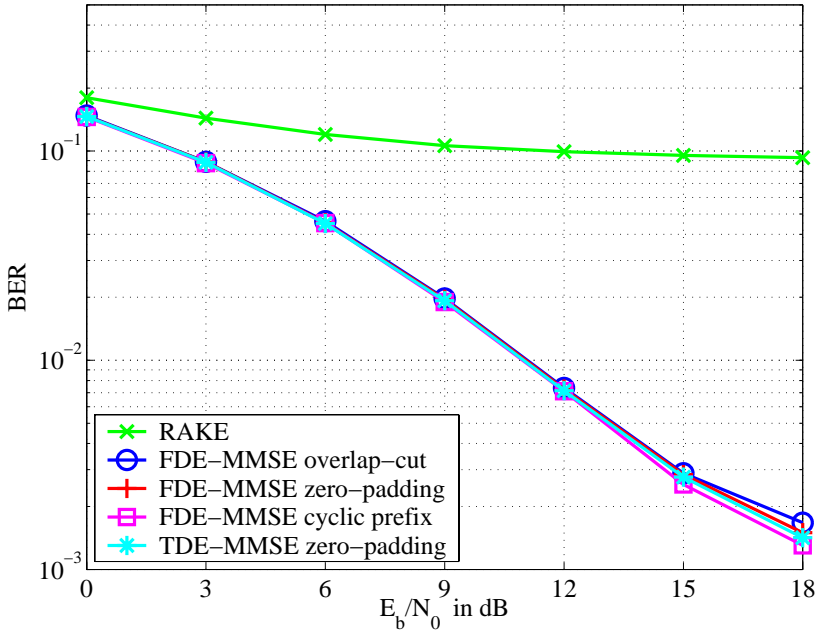
Despite the fact that the FDE detector is only an approximation to the TDE, it has been demonstrated to be a very good approximation. No BER difference can be seen in the time-invariant channel (Figure 4.7 and 4.8). Only after its effect is amplified by the noise enhancement in the FDE-ZF triggered by the time-variant nature of the channel, does the difference in BER come to front.

Figure 4.10 displays the FDE-MMSE detectors in VehicularA channel. The MMSE criterion damps down the noise enhancement and thus reduces the BER difference between the FDE variants. The FDE-MMSE shows even an almost identical BER to the TDE-MMSE. Comparing Figure 4.9 and Figure 4.10, it is clear that the MMSE equalizers outperform the ZF equalizers in the time-variant channel.

## 4.5 Complexity Considerations

The complexity of an  $M$ -point FFT is  $M \log_2 M$ . The FDE requires 3 Fourier transform operations, two for the equalization and one for transforming the channel impulse response estimate from the time domain to the frequency domain. We then obtain the complexity of the FDE in terms of the total complex multiplications:  $3M \log_2 M + M$ . The last  $M$  comes from the  $M$  complex multiplications conducted on the multiplier array between the FFT and the IFFT (Figure 4.1).

If only the most dominant factor is considered - i.e. the factor that increases fastest as the size of data increases - the complexity of an algorithm can be expressed with the  $\mathcal{O}(\cdot)$  notation. In this



**Figure 4.10** Unencoded BER of the FDE-MMSE detector in the UTRA-TDD system with the VehicularA channel (50km/h), spreading factor 16, 16 users

case, the FDE displays a complexity of  $\mathcal{O}(M \log M)$ , which shows a significant reduction compared to the complexity of the direct matrix inversion of dimension  $M \times M$  that displays a complexity of  $\mathcal{O}(M^3)$ , or to the low complexity equalization techniques that give a complexity of  $\mathcal{O}(M^2)$  [15]. In terms of simplicity, the FDE outperforms many other CDMA detection methods<sup>4</sup>.

This reduction in complexity can be readily observed from

<sup>4</sup>The RAKE receiver is basically a matrix-vector multiplication with a complexity of  $\mathcal{O}(M^2)$ . Baum [20] confirms the fact that the FDE detector can be simpler than a RAKE receiver.

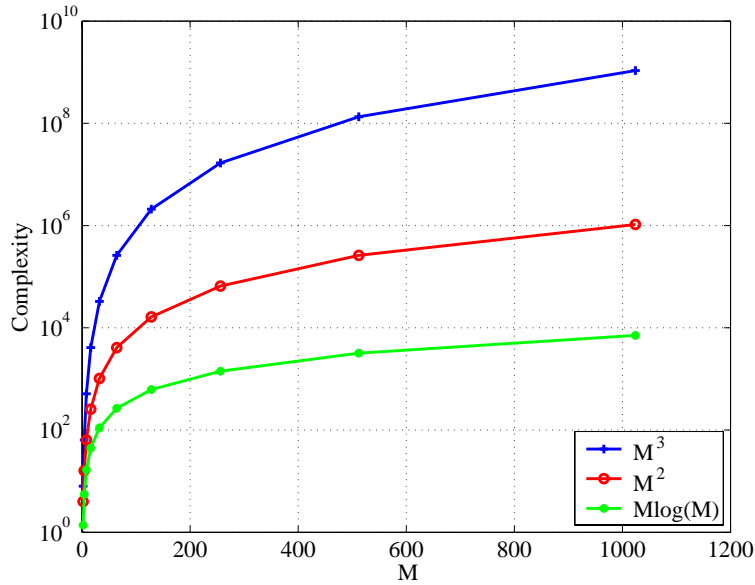


**Figure 4.11** Different complexity increase rates

the equation describing the FDE. Rewriting (4.8)

$$\mathbf{y}_{\text{FDE-ZF}} = \mathbf{F}^{-1} \mathbf{\Lambda}^{-1} \mathbf{F} \mathbf{r}, \quad (4.10)$$

it can be seen, that the matrix inverse  $\mathbf{\Lambda}^{-1}$  is trivial. Since  $\mathbf{\Lambda}$  is a diagonal matrix, its inverse is simply given by the reciprocal values of the diagonal elements. Hence no costly matrix inversion is needed by the FDE.

Figure 4.11 illustrates the complexity reduction that can be achieved by the FDE detection method ( $\mathcal{O}(M \log M)$ ) compared to other methods of complexity  $\mathcal{O}(M^2)$  and  $\mathcal{O}(M^3)$ . With  $M=256$ , the complexity reduction can be in the order of  $10^2$  to  $10^4$ .



## Equalizers Versus Multiuser Detectors

*It is usually possible to prove a property in more than one way. Such alternate proofs are always valuable in the engineering process, for they reaffirm the unity that knits together so many of the physical and mathematical properties which the engineer must master as part of his trade. [33]*

LOOKING long enough at a bunch of simulation results can trigger a hunch. Could it be that the achievable BER of the equalizer is similar to the BER of the linear multiuser detector (MUD)? Could they be even equal? Why shouldn't they? The orthogonality of the spread spectrum signals is after all restored as soon as the multipath channel is equalized in CDMA downlink. If the performance of the equalizer is different from the performance of the linear MUD, how much is the difference?

Loaded with questions, a master student was sent out to simulate and compare the two receivers. Old papers were dugged out to see if there are already hints for these particular questions. There are indeed such hints. Klein [13], for example, indicated that the performance of the singleuser equalizer is only slightly worse compared to the performance of the linear MUD. As the student finished his thesis, his simulation results also backed up the conjecture that equalizers are almost as good as linear MUDs in CDMA downlink, especially in a fully loaded cell. An e-mail discussion with a researcher who has worked with equalizers in CDMA, provided the final push in initiating the search for a mathematical demonstration of this phenomenon<sup>1</sup> [41].

## 5.1 Simulation Results

Before we discuss the formal demonstration of the performance comparison between equalizers and linear MUDs, let us first look at some simulation results. After having implemented the FDE and MUD in the UTRA-TDD downlink scenario, the following BER curves can be observed. Figure 5.1 shows the uncoded BER of FDE and MUD simulated with a time-invariant channel with the cell half loaded (spreading factor = 16 and number of users =

---

<sup>1</sup>The author appreciates the kind comments from Monisha Ghosh, Ph.D. at the Wireless Communications and Networking, Philips Research, USA [40].



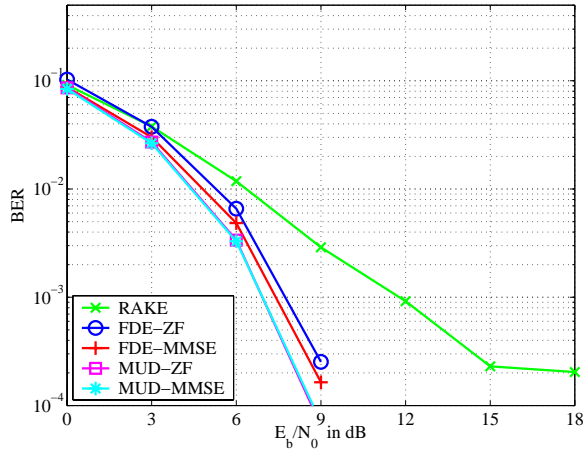


**Figure 5.1** Uncoded BER of the FDE and MUD in a time-invariant channel, spreading factor = 16 and number of users = 8

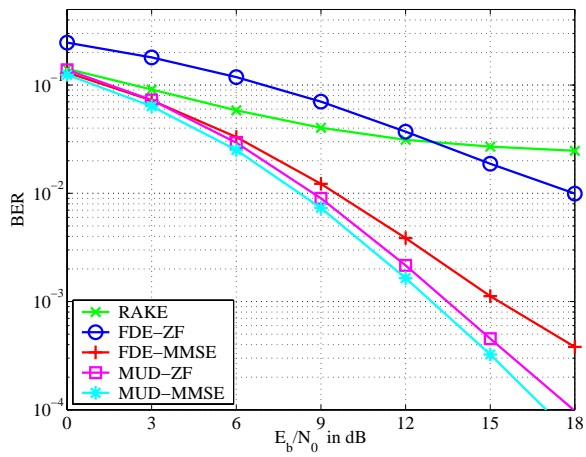


**Figure 5.2** Uncoded BER of the FDE and MUD in the VehicularA channel, spreading factor = 16 and number of users = 8, velocity = 50 km/h

8). As can be expected, the linear MUDs outperform the FDEs. The BER of a RAKE receiver is also included for comparison. Figure 5.2 shows similar results with the time-variant VehicularA channel. The best performance was displayed by the MUD, followed by the FDE and RAKE.

However, if we increase the number of users so that the cell is fully loaded, the BER curves of the FDE and the MUD approach each other. This is shown in Figure 5.3 and Figure 5.4. Figure 5.3 shows the BER of FDE and MUD in a fully loaded cell in time-invariant channel. Almost no difference can be observed here between the BER curves of FDE and MUD (they lie on top of each other). Figure 5.4 displays the BER for the VehicularA channel. Here, the advantage of the MMSE criterion over the ZF criterion can be seen. However, the underlying tendency is also apparent: the performance of the FDE becomes approximately equal to the linear MUD in a fully loaded cell. The FDE-ZF delivers a similar BER to the MUD-ZF, and the FDE-MMSE to the MUD-MMSE.

These observations lead to a conjecture, that the performance of the equalizers is indeed similar to the linear MUDs especially with a large number of users; and if the cell is fully loaded, the performance of the equalizers will become almost identical to the linear MUDs. Furthermore, since the simulations consistently show the same tendency regardless of the channel, it seems to be logical, if we can demonstrate this phenomenon mathematically regardless the channel.

## 5.2 FDE versus MUD

Considering the equalization in (2.10) and the despreading in (2.12) together, we can write the detected data vector by a ZF

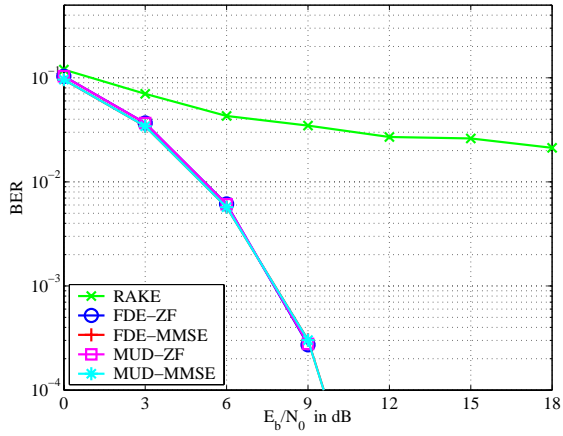


**Figure 5.3** Uncoded BER of the FDE and MUD in a time-invariant channel, spreading factor = 16 and number of users = 16

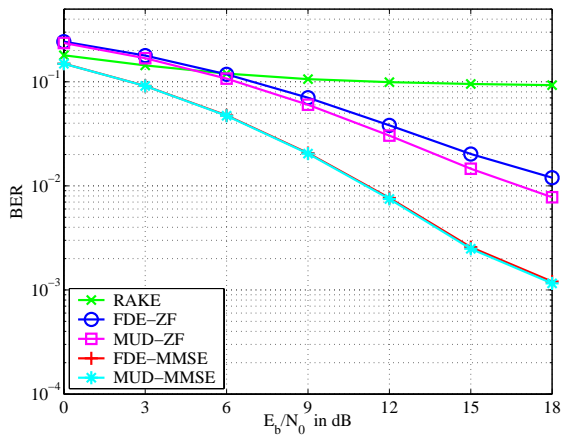


**Figure 5.4** Uncoded BER of the FDE and MUD in the VehicularA channel, spreading factor = 16 and number of users = 16, velocity = 50 km/h

equalizer (FDE-ZF) as<sup>2</sup>:

$$\begin{aligned}\hat{\mathbf{d}}_{\text{FDE-ZF}} &= \frac{1}{Q} \mathbf{C}^H (\mathbf{H}^H \mathbf{H})^{-1} \mathbf{H}^H \mathbf{r} \\ &= \frac{1}{Q} \mathbf{C}^H \mathbf{C} \mathbf{d} + \frac{1}{Q} \mathbf{C}^H (\mathbf{H}^H \mathbf{H})^{-1} \mathbf{H}^H \mathbf{n},\end{aligned}\tag{5.1}$$

and the data detected by a FDE-MMSE can be written as (cf. (2.11) and (2.12)):

$$\hat{\mathbf{d}}_{\text{FDE-MMSE}} = \frac{1}{Q} \mathbf{C}^H \left( \mathbf{H}^H \mathbf{H} + \frac{\sigma^2}{K} \mathbf{I} \right)^{-1} \mathbf{H}^H \mathbf{r}\tag{5.2}$$

This section will show mathematically that the BER of the FDE indeed approximates the BER of the corresponding linear MUD in a saturated CDMA downlink. The key to show this, is the fact that if  $K = Q$  (the number of users is equal to the spreading code length), then the matrix  $\mathbf{C}$ ,  $\mathbf{H}$  and thus  $\mathbf{A} = \mathbf{H}\mathbf{C}$  turn into square matrices. Of course, we acknowledge that  $\mathbf{H} \in \mathbb{C}^{(NQ+L-1) \times (NQ)}$  is not square because of the term  $L - 1$  in the dimension of the matrix; and since  $\mathbf{H}$  is not square,  $\mathbf{A}$  will not become a square matrix either even if  $\mathbf{C}$  is square when  $K = Q$ . However, it has been shown in Chapter 4 that  $\mathbf{H}$  can be closely approximated with the circulant matrix  $\tilde{\mathbf{H}}$  which is square. So the behavior of the linear multiuser detectors and equalizers when  $K = Q$  can be analyzed approximately with the assumption that  $\mathbf{H}$  and thus  $\mathbf{A}$  are square matrices with full rank.

If  $\mathbf{H}$  and  $\mathbf{A}$  are square, the following operation can be done

---

<sup>2</sup>Here the FDE equation is written similarly to the time domain equalizer, but in the analysis we take into account that the FDE assumes a circulant channel matrix  $\mathbf{H}$

to the equation of the MUD-ZF in (2.8):

$$\begin{aligned}
\hat{\mathbf{d}}_{\text{MUD-ZF}} &= (\mathbf{A}^H \mathbf{A})^{-1} \mathbf{A}^H \mathbf{r} \\
&= \left( (\mathbf{A}^H)^{-1} \mathbf{A}^H \mathbf{A} \right)^{-1} \mathbf{r} \\
&= \mathbf{A}^{-1} \mathbf{r} \\
&= (\mathbf{H}\mathbf{C})^{-1} \mathbf{r} \\
&= \mathbf{C}^{-1} \mathbf{H}^{-1} \mathbf{r}, \tag{5.3}
\end{aligned}$$

and the detected vector of the FDE-ZF in (5.1) can be expressed as:

$$\begin{aligned}
\hat{\mathbf{d}}_{\text{FDE-ZF}} &= \frac{1}{Q} \mathbf{C}^H (\mathbf{H}^H \mathbf{H})^{-1} \mathbf{H}^H \mathbf{r} \\
&= \frac{1}{Q} \mathbf{C}^H \mathbf{H}^{-1} (\mathbf{H}^H)^{-1} \mathbf{H}^H \mathbf{r} \\
&= \frac{1}{Q} \mathbf{C}^H \mathbf{H}^{-1} \mathbf{r}. \tag{5.4}
\end{aligned}$$

Note that the term  $\frac{1}{Q} \mathbf{C}^H$  describes the despreading process, which if multiplied with the spreading matrix  $\mathbf{C}$  (which contains orthogonal spreading codes), results in the identity matrix  $\mathbf{I}$ :

$$\frac{1}{Q} \mathbf{C}^H \mathbf{C} = \mathbf{I} \tag{5.5}$$

Comparing (5.3) with (5.4) and keeping (5.5) in mind, it can be seen that the data estimate obtained from (5.3) is equal to that obtained from (5.4) since  $\frac{1}{Q} \mathbf{C}^H = \mathbf{C}^{-1}$ . Thus the FDE-ZF is approximately equivalent to the MUD-ZF if the number of users is equal to the spreading factor ( $K = Q$ ).

Another way to see the effect of a square matrix  $\mathbf{H}$  and  $\mathbf{A}$  is as follows. If  $\mathbf{H}$  and  $\mathbf{A}$  are square and regular, then the *pseudo*-inverse is not needed to invert these matrices. The received signal  $\mathbf{r}$  can be directly multiplied by the inverse  $\mathbf{A}^{-1}$  and  $\mathbf{H}^{-1}$ , and we arrive immediately at (5.3) and (5.4).

The same argument can also be applied to FDE-MMSE and MUD-MMSE. The data detected by the MUD-MMSE in (2.9) can be written as:

$$\begin{aligned}\hat{\mathbf{d}}_{\text{MUD-MMSE}} &= (\mathbf{A}^H \mathbf{A} + \sigma^2 \mathbf{I})^{-1} \mathbf{A}^H \mathbf{r} \\ &= \left( (\mathbf{A}^H)^{-1} \mathbf{A}^H \mathbf{A} + (\mathbf{A}^H)^{-1} \sigma^2 \mathbf{I} \right)^{-1} \mathbf{r} \\ &= \left( \mathbf{H} \mathbf{C} + (\mathbf{H}^H)^{-1} (\mathbf{C}^H)^{-1} \sigma^2 \right)^{-1} \mathbf{r},\end{aligned}\quad (5.6)$$

and the FDE-MMSE:

$$\begin{aligned}\hat{\mathbf{d}}_{\text{FDE-MMSE}} &= \frac{1}{Q} \mathbf{C}^H \left( \mathbf{H}^H \mathbf{H} + \frac{\sigma^2}{K} \mathbf{I} \right)^{-1} \mathbf{H}^H \mathbf{r} \\ &= \frac{1}{Q} \left( (\mathbf{H}^H)^{-1} \mathbf{H}^H \mathbf{H} (\mathbf{C}^H)^{-1} + (\mathbf{H}^H)^{-1} \frac{\sigma^2}{K} \mathbf{I} (\mathbf{C}^H)^{-1} \right)^{-1} \mathbf{r} \\ &= \left( Q \mathbf{H} (\mathbf{C}^H)^{-1} + \frac{Q}{K} (\mathbf{H}^H)^{-1} (\mathbf{C}^H)^{-1} \sigma^2 \right)^{-1} \mathbf{r}.\end{aligned}\quad (5.7)$$

By taking (5.5) and substituting  $Q(\mathbf{C}^H)^{-1}$  with  $\mathbf{C}$ , it can be seen that (5.6) is equal to (5.7). Hence, the FDE-MMSE becomes approximately equal to the MUD-MMSE if the number of users is equal to the spreading factor ( $K = Q$ ).

We simulate the equalizer and multiuser detector again and display the BER against the number of CDMA users. Figure 5.5 shows the BER of equalizers (FDE-ZF and FDE-MMSE) and the

linear MUDs against the number of users in the time-invariant channel. It can be seen that the BER curves of all the equalizers and MUDs converge as the number of users increases. With 16 users, both equalizers show approximately the same performance as the MUDs. The BER of the RAKE receiver is also included for comparison. The performance of the RAKE deteriorates significantly as the number of users increases because of MAI.

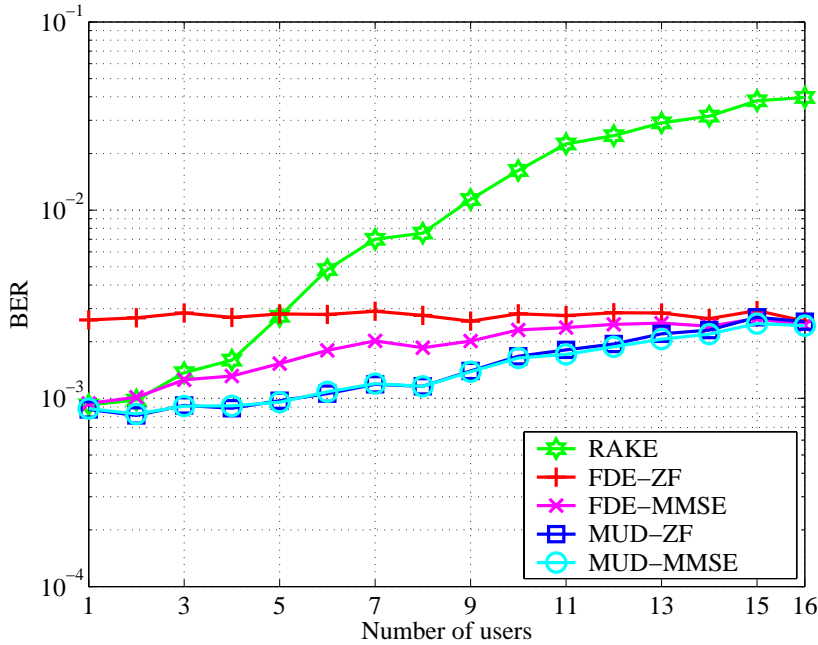


**Figure 5.5** Uncoded BER of the FDEs and the linear MUDs with an  $E_b/N_0$  of 7 dB, spreading factor  $Q$  of 16, and the 4-tap time-invariant channel

Figure 5.6 presents the uncoded BER in the time-variant VehicularA channel with an  $E_b/N_0$  of 10 dB. Here we can see the effects of the time-varying channel on the BER. The BER of the

MUD-ZF moves away from the BER of the MUD-MMSE as the number of users increases. However, the tendency that the BER of the equalizers (TDE-ZF and TDE-MMSE) approach the BER of the MUDs stays. We see that the BER curves of the MUDs are generally better than that of the equalizers; but as the number of users increases, the BER curves of the MUDs and the equalizers approach each other and eventually become equal for  $K = 16$ .

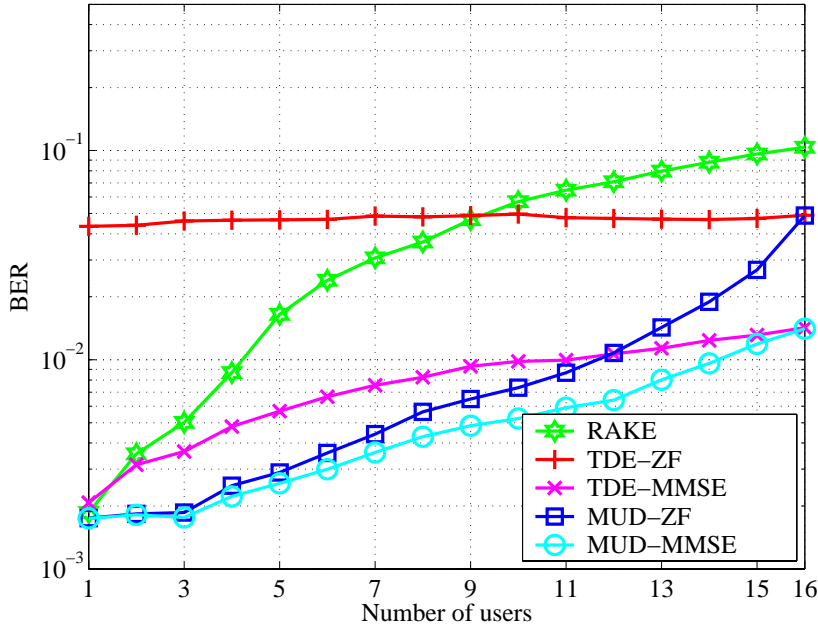


**Figure 5.6** Uncoded BER of the TDEs and the linear MUDs with an  $E_b/N_0$  of 10 dB, spreading factor  $Q$  of 16, and the VehicularA channel with a velocity of 50 km/h.

The time-variant channel also brings out the effect of the approximation with the circulant matrix  $\tilde{\mathbf{H}}$  in the FDE approach (cf. Chapter 4). This is shown in Figure 5.7. The time domain equalizer TDE-ZF shows a difference in BER compared to its



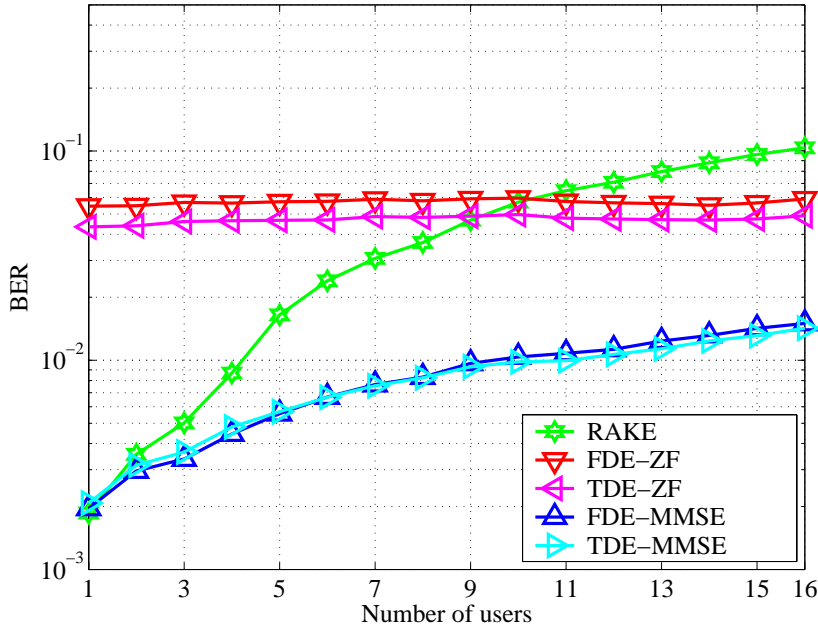


**Figure 5.7** Uncoded BER of the TDE and FDE with an  $E_b/N_0$  of 10 dB, spreading factor  $Q$  of 16, and the VehicularA channel with a velocity of 50 km/h.

frequency domain implementation FDE-ZF. This is because the inverse of  $\mathbf{H}$  and  $\tilde{\mathbf{H}}$  is in general not the same. But since the values at the upper right edge of  $\tilde{\mathbf{H}}$  - which contribute to the largest part of the difference between  $\mathbf{H}$  and  $\tilde{\mathbf{H}}$  - are taken care with the zero-padding method [21], the BER results of the TDE-ZF and the FDE-ZF are very close, and no difference can be observed between the two in the time-invariant channel. This difference is also so small that the addition of the SNR dependent term in the MMSE criterion, makes the BER difference between the TDE-MMSE and FDE-MMSE in the time-variant VehicularA channel disappear (Figure 5.7).

### 5.3 TDE versus MUD

Observing Figure 5.6 and Figure 5.7 triggers another intriguing question. Although the FDE becomes *approximately* equal to the MUD, the TDE seems to become *exactly* equal to the MUD in a fully loaded CDMA downlink system<sup>3</sup>.

It has been shown in Chapter 4 that the FDE is an approximation of the TDE, albeit a very close one. The approximation of the channel matrix  $\mathbf{H}$  with the circulant matrix  $\tilde{\mathbf{H}}$  shows its effect in the slightly different BER between the FDE-ZF and the TDE-ZF in Figure 5.7. Hence, the FDE is only *approximately* equal to the MUD in the fully loaded CDMA downlink with orthogonal codes (although again, the approximation of FDE is a very good one).

However, Figure 5.6 suggests that the TDE is *exactly* equal to the MUD in the fully loaded condition. It also means, that the mathematical demonstration of this behavior does not have to resort to the FDE approximation with circulant matrix  $\tilde{\mathbf{H}}$  as is done in the previous section. The fact that the spreading matrix  $\mathbf{C}$  alone turns into a square matrix if  $K = Q$  should be enough to allow the mathematical demonstration.

Revisiting (5.3), we see that if  $\mathbf{C}$  turns into a square matrix

---

<sup>3</sup>Because the author first dealt with FDE and its comparison to MUD [19], [21], [41], the realization of this fact came only after pondering on Figure 5.6 and Figure 5.7

when  $K = Q$ , then the following operations can be performed:

$$\begin{aligned}
\hat{\mathbf{d}}_{\text{MUD-ZF}} &= (\mathbf{A}^H \mathbf{A})^{-1} \mathbf{A}^H \mathbf{r} \\
&= \left( (\mathbf{HC})^H (\mathbf{HC}) \right)^{-1} (\mathbf{HC})^H \mathbf{r} \\
&= (\mathbf{C}^H \mathbf{H}^H \mathbf{HC})^{-1} \mathbf{C}^H \mathbf{H}^H \mathbf{r} \\
&= \mathbf{C}^{-1} \left( (\mathbf{C}^H)^{-1} \mathbf{C}^H \mathbf{H}^H \mathbf{H} \right)^{-1} \mathbf{H}^H \mathbf{r} \\
&= \mathbf{C}^{-1} (\mathbf{H}^H \mathbf{H})^{-1} \mathbf{H}^H \mathbf{r}, \tag{5.8}
\end{aligned}$$

Comparing (5.8) with the first line of (5.4) and remembering (5.5), we see that (5.8) is equal to (5.4). Notice, that to show the equality, we now do not move the non-square matrix  $\mathbf{H}$  across the matrix inverse sign. Thus the equality can be established without the assumption that  $\mathbf{H}$  is square.

Similar operations can be done to the MUD-MMSE:

$$\begin{aligned}
\hat{\mathbf{d}}_{\text{MUD-MMSE}} &= (\mathbf{A}^H \mathbf{A} + \sigma^2 \mathbf{I})^{-1} \mathbf{A}^H \mathbf{r} \\
&= \left( (\mathbf{HC})^H \mathbf{HC} + \sigma^2 \mathbf{I} \right)^{-1} (\mathbf{HC})^H \mathbf{r} \\
&= \left( \mathbf{H}^H \mathbf{HC} + (\mathbf{C}^H)^{-1} \sigma^2 \mathbf{I} \right)^{-1} \mathbf{H}^H \mathbf{r}, \tag{5.9}
\end{aligned}$$

Comparing (5.9) with the first line of (5.7) and taking (5.5) into account, we see that (5.9) is equal to (5.7).

## 5.4 Why MUD When an Equalizer is Good Enough?

In the preceding sections, it was shown that the performance of the equalizer is equal to the performance of the linear multiuser detector in a fully loaded CDMA downlink system using orthogonal spreading codes. The TDE shows exactly the same BER as the MUD at full load. The FDE, being an approximation of the TDE, shows an approximately identical performance as the MUD at full load.

Trivial it might seem, the analysis for a fully loaded system is interesting because it represents the worst case of MAI (excluding the overloaded case). These results would affect our choice for the CDMA receiving method. A legitimate question resulting from the comparison will be: Why use a multiuser detector in CDMA downlink when the equalizer is good enough? Considering the performance-to-complexity trade-off, which choice is wiser?

It is true that using the TDE instead of the linear MUD might not bring any gain in terms of simplicity. The inversion of the channel matrix  $\mathbf{H}$  implied by the TDE is not necessarily simpler than the inversion of the system matrix  $\mathbf{A}$  by the linear MUD, since the size of these two matrices is roughly the same. However, the frequency domain implementation reduces the complexity of the equalization algorithm significantly. The FDE can be implemented with a complexity of  $\mathcal{O}(N \log N)$ , which is much simpler compared to the MUD strategy which involves costly matrix inversion<sup>4</sup>.

Considering the BER-to-complexity trade-off, the equalizer is thus a better idea compared to the linear MUD for CDMA down-

---

<sup>4</sup>Vollmer et al. proposed a frequency domain variant of the linear MUD [34], which shows a tremendous simplification compared to the time domain linear MUD. However, the FDE still displays lower complexity than this FD-MUD.

link detection, since it delivers the same performance as the linear MUD in the worst case of MAI. This is particularly true for the FDE-MMSE, whose performance does not differ too much from the MUD-MMSE if  $K \neq Q$ . Furthermore, as a singleuser detector, the equalizer does not require any knowledge and signaling of the active spreading codes.

In a CDMA system with non-orthogonal codes, the effectiveness of the FDE compared to the MUD is slightly reduced. If non-orthogonal codes are used (e.g. Gold codes) the correlation in the received signal comes not only from the channel, but is also caused by the spreading codes itself. The MUD is capable to decorrelate this later distortion, whereas the FDE can only equalize the channel but cannot untangle the correlation inherent in the non-orthogonality of the spreading codes.

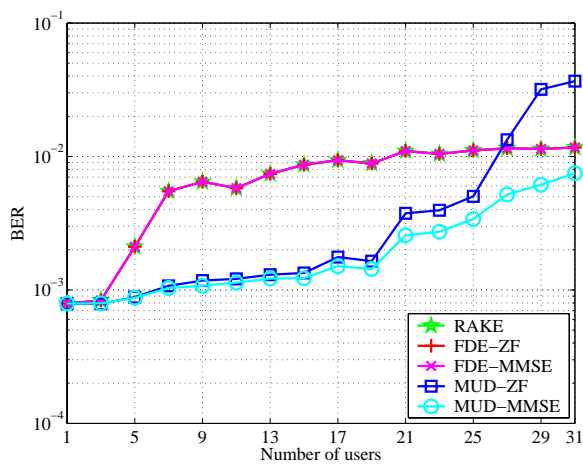


**Figure 5.8** Uncoded BER of the FDE and the linear MUD with an  $E_b/N_0$  of 7 dB, Gold codes with the spreading factor of 31, and AWGN channel

Figure 5.8 displays the performance of various detectors in a

CDMA system using Gold codes with the spreading factor of 31 (AWGN channel). The BER of the FDE detectors overlap exactly on the BER of the RAKE, because there is no multipath effect to be handled. The MUDs show a generally better performance as they decorrelate the received spread signals. Interesting phenomena can be observed by the MUD-ZF which show a rapidly increasing BER as the system approaches its full capacity. This is caused by the increased MAI due to the non-orthogonality of the codes. In contrast to Figure 5.8, the performance of the detector in a system using orthogonal codes in AWGN channel, is not influenced by the number of users (Figure 5.9)

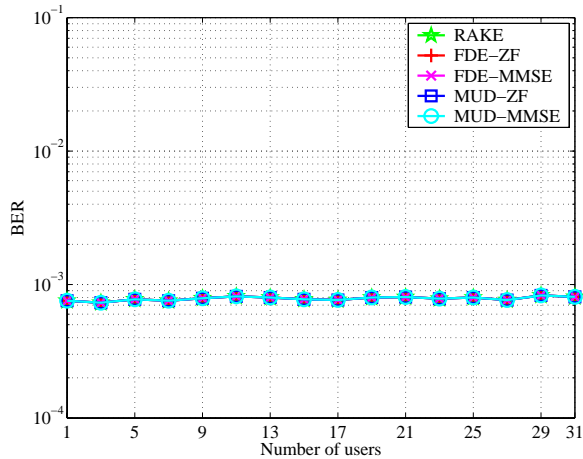


**Figure 5.9** Uncoded BER of the FDE and the linear MUD with an  $E_b/N_0$  of 7 dB, orthogonal Walsh codes with the spreading factor of 32, and AWGN channel

The more practice relevant case for CDMA systems in VehicularA channel with non-orthogonal codes is displayed in Figure 5.10. Again, Gold codes with spreading factor 31 are used. We see the same tendency as in the case of orthogonal spreading

codes: the BER of FDE becomes as good as MUD as the system approaches the full load. In Figure 5.10, the FDE-ZF is even better than MUD-ZF at full load, because of the MAI caused by the non-orthogonal codes that quickly overwhelms the MUD-ZF.

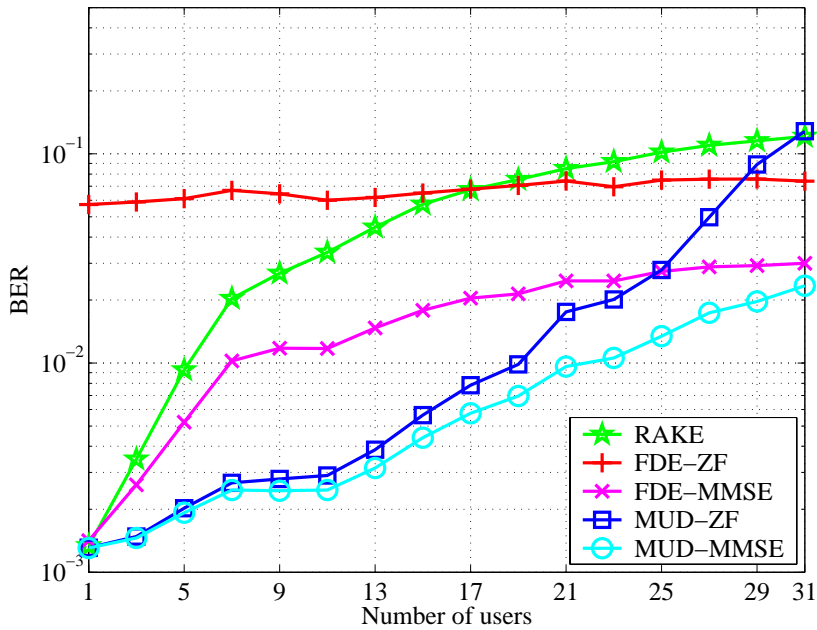


**Figure 5.10** Uncoded BER of the FDE and the linear MUD with an  $E_b/N_0$  of 10 dB, Gold codes with the spreading factor of 31, and the VehicularA channel with a velocity of 50 km/h





# 6

## Ideas Derived From FDE

*Nothing is more dangerous than an idea when it is the only one we have (Emile Chartier)*

*The best way to get a good idea is to get a lot of ideas (Linus Pauling)*

ONE answered question leads to two new questions. One gained insight leads to two new conjectures. This chapter presents - not two - but three more ideas derived from the FDE concept. The first is the FDE-RAKE: a parallel interference cancellation multiuser detector for CDMA downlink presented in Section 6.1 [42]. The second idea is the pre-FDE, a pre-equalization approach, which allows the application of FDE in CDMA uplink systems (Section 6.2), followed by a software-defined radio (SDR) baseband processing structure that can handle several air interface standards in Section 6.3.

## 6.1 FDE-RAKE

It has been shown that the FDE provides a good solution for the CDMA downlink detection with a low complexity. The FDE has been even demonstrated to be almost as good as a linear MUD. However, the linear MUD still offers a slight gain in BER over the equalizer as can be seen in Chapter 5. Now, the question is, can the FDE concept be expanded such that it can function as a multiuser detection and hence delivers the same BER as a linear MUD? The answer for that is the FDE-RAKE.

Contrary to most multiuser detection strategies, which perform their multiuser detection at the output of a conventional matched filter (RAKE detector), the detector proposed in this section conducts the multiuser processing after a chip level equalizer. A hard detection at the output of the equalizer yields temporary detected symbols, which will be used for a parallel interference cancellation (PIC). These detected symbols will be spread with the appropriate spreading codes, convolved with the estimated channel impulse response (CIR) and subtracted from the received CDMA signal, leaving the signal part of the wanted user. A conventional RAKE receiver will then be applied for the final data detection.

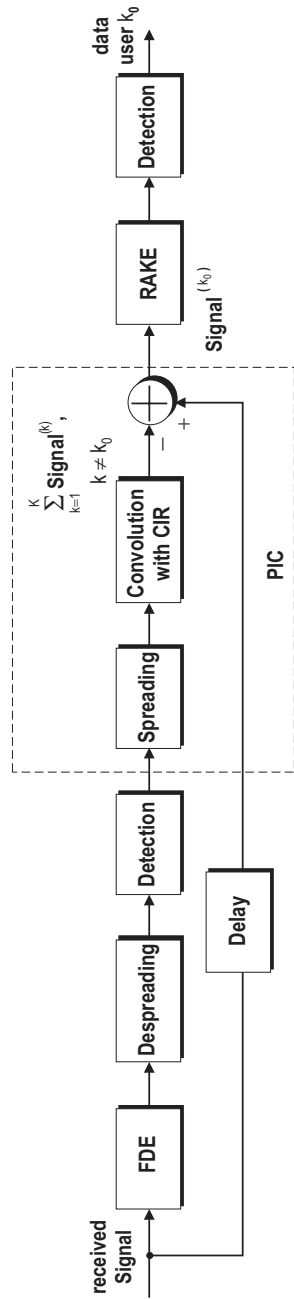


Figure 6.1 FDE-RAKE detector

The structure of the FDE-RAKE detector is displayed in Figure 6.1. After the equalization (FDE), despreading and a hard decision, the data will be spread and convolved with the estimated channel impulse response in order to calculate the contribution of each user's signal to the MAI. All signals except the signal from the considered user  $k_0$  will be subtracted from the total received signal (PIC), leaving the signal of user  $k_0$  free from MAI. A conventional RAKE detector is then applied on this signal to exploit the multipath diversity. Finally, a demodulation process will yield the data of user  $k_0$ .

The FDE-RAKE detector takes advantage of the fact that the RAKE detector can function very well in a MAI-free environment. Working on MAI-free signals provided by the PIC, the RAKE detector delivers additional gain due to multipath diversity, which was left unexploited by the FDE at the first stage. As a whole, the FDE-RAKE detector actually performs the same data processing as the linear multiuser detectors. The difference lies in the order of the algorithm. The linear multiuser detector processes the incoming signal first with the RAKE receiver to exploit the multipath diversity. It then applies a decorrelating strategy (by inverting the system matrix  $\mathbf{A}$ ) on the output of the first stage (cf. Chapter 2). The FDE-RAKE, on the other hand, first decorrelates the incoming signals by equalizing the channel, and then applies the RAKE detector. Because of this equivalence, the performance of the FDE-RAKE detector can be expected to be similar to the linear multiuser detector.

### 6.1.1 Simulation Results

The performance of the FDE-RAKE is evaluated by simulations in a CDMA system based on the UTRA-TDD [37] with the VehicularA channel [38]. Because of its simplicity, the zero padding method explained in Chapter 4 will be adopted for the simula-

tions.

The uncoded BER curves of the FDE based detectors and the RAKE receiver with 8 users are shown in Figure 6.2. The FDE detectors (FDE-ZF and FDE-MMSE) outperform the RAKE receiver at high SNR. The FDE-ZF shows, however, a bad performance because of noise enhancement at low SNR. If the SNR is lower than 12 dB, the FDE-ZF is even worse than the RAKE receiver. The best performance is displayed by the FDE-RAKE detector, which uses an FDE-MMSE as its first stage. This FDE-RAKE detector achieves about 2.5 dB gain compared to the FDE-MMSE at the BER of  $10^{-3}$ .

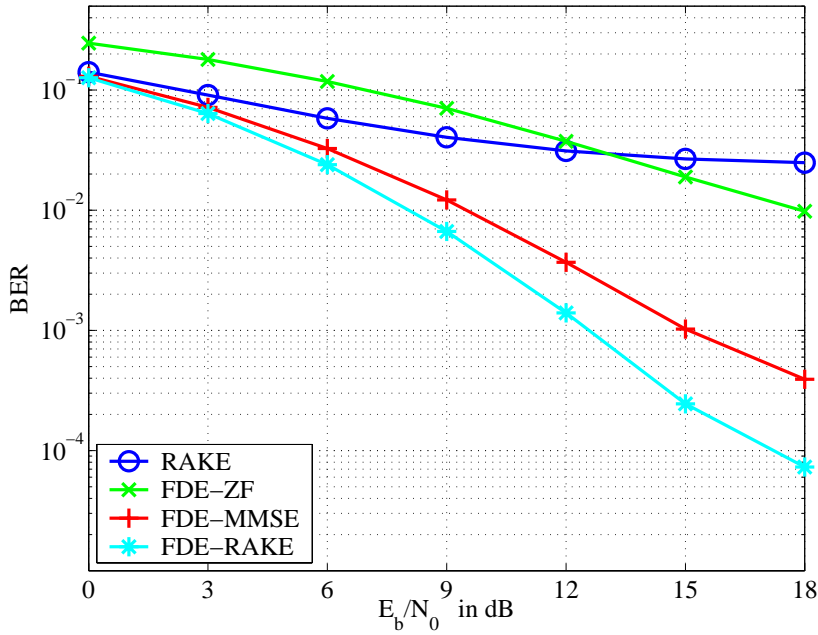


**Figure 6.2** Uncoded BER of the FDE based detectors and RAKE with  $K = 8$  users, spreading factor  $Q = 16$ , VehicularA channel with mobile velocity = 50 km/h.

The uncoded BER curves of the linear MUD are shown along with the RAKE receiver and the FDE-RAKE detector in Figure 6.3. Again, the RAKE receiver shows the worst performance. The best BER curves are displayed by the MUD-MMSE and the FDE-RAKE detector. This result confirms the conjecture that the performance of the FDE-RAKE will be similar to the performance of the linear MUD.

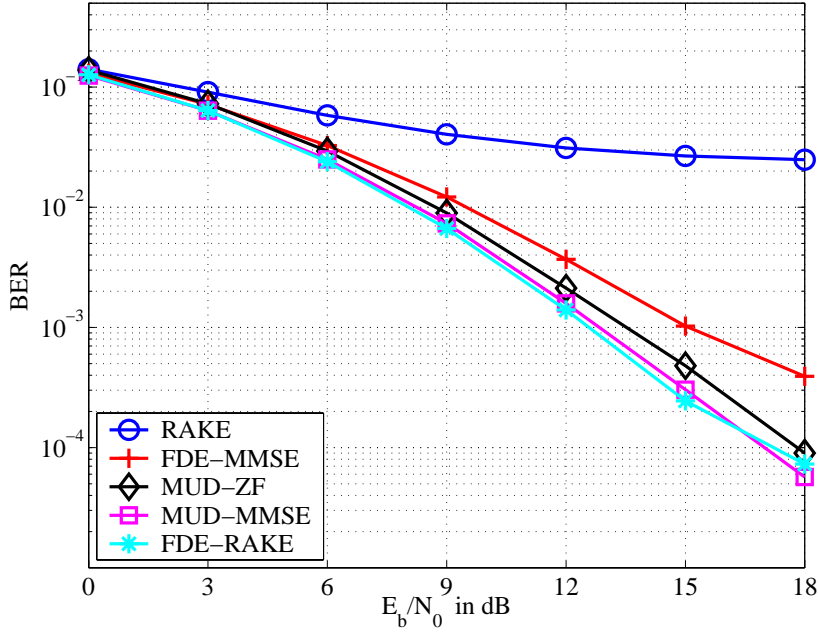


**Figure 6.3** Uncoded BER of the linear MUDs, RAKE, FDE-MMSE and FDE-RAKE detector with  $K = 8$  users, spreading factor  $Q = 16$ , VehicularA channel with mobile velocity=50km/h.

The BER curves plotted against the number of users are shown in Figure 6.4. All the curves are plotted at a constant SNR of 10 dB. The BER of the RAKE receiver deteriorates rapidly as

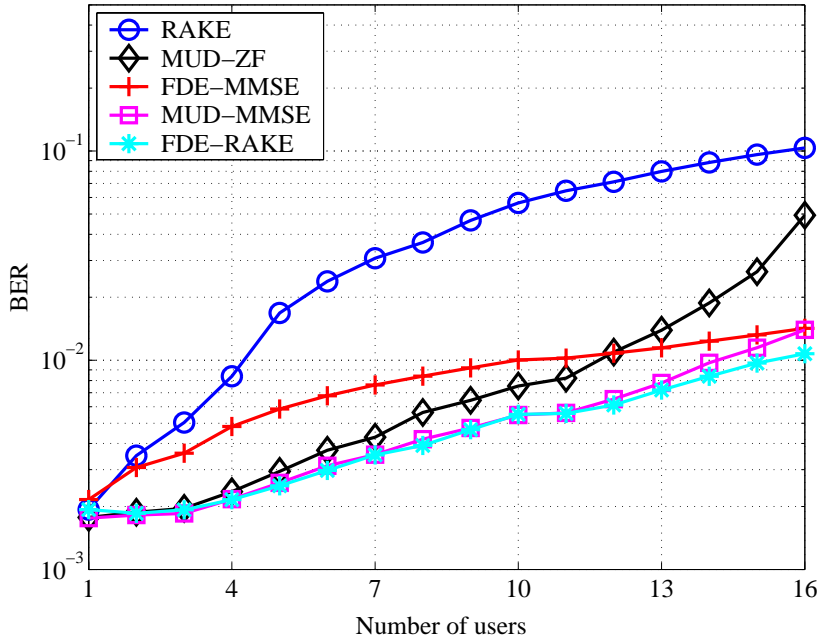


**Figure 6.4** Uncoded BER of the linear MUDs , RAKE, FDE-MMSE and FDE-RAKE detector with  $SNR = 10dB$ , spreading factor  $Q = 16$ , VehicularA channel with mobile velocity=50km/h.

the number of users increases. The BER of the MUD-ZF stays close with the MUD-MMSE at low load, but get worse fast if the cell is highly loaded. The BER of the FDE-MMSE coincides with the BER of MUD-MMSE at full load (16 users), as is demonstrated in the last chapter. The best performance is displayed by the FDE-RAKE, which is even slightly better than the MUD-MMSE at full load. This slightly better performance of the FDE-RAKE compared to the MUD-MMSE at full load can be better seen in Figure 6.5.

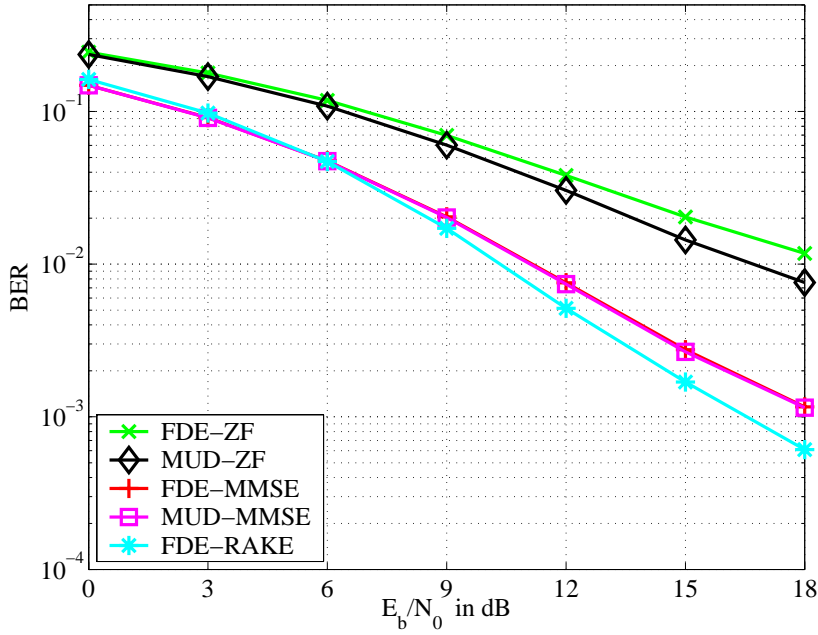


**Figure 6.5** Uncoded BER of the linear MUDs , RAKE, FDE-MMSE and FDE-RAKE detector with  $K = 16$  users, spreading factor  $Q = 16$ , VehicularA channel with mobile velocity=50km/h.

### 6.1.2 Complexity Consideration

A precise complexity comparison between the FDE-RAKE and the linear MUD is hard to provide, since it depends on a lot of implementation details, such as, the number of the RAKE fingers, matrix inversion method used by the linear MUD, etc. However a rough estimate of the complexity can be given.

As already mentioned, the linear MUD and the FDE-RAKE, each actually performs the same data processing but swap the order between the decorrelation and the RAKE receiver. If a



time domain equalizer is assumed for the first step of the PIC (i.e. TDE-RAKE), then a roughly equal complexity can be expected for the TDE-RAKE and for the linear MUD. However, the application of FDE at the first stage of the FDE-RAKE gives this PIC approach some gain in terms of simplicity compared to the linear MUD.

The important advantage of the FDE-RAKE lies in the good performance-to-complexity ratio of the first stage. The FDE outperforms the RAKE receiver, and at the same time is much simpler than the multiuser detector [21]. It has been even shown to display similar performance to a linear MUD in a fully loaded CDMA cell [41]. This means, the FDE alone already delivers a relatively good BER. The additional gain from the following PIC and RAKE receiver can then be applied optionally if it is needed. The gain of the two stage equalizer PIC detector compared to the plain equalizer can be further increased with the use of multiple antennas [43].

### 6.1.3 Comparison with Conventional PIC

The advantage of applying FDE as the first stage of the PIC becomes more apparent if the performance of the FDE-RAKE is compared to a conventional PIC detector. The conventional PIC detector uses a RAKE receiver as its first stage, and it performs the PIC on the output of this RAKE receiver.

Because its first stage (RAKE) still suffers from considerable MAI, the conventional PIC converges much slower than the FDE-RAKE. Figure 6.6 shows the BER of the conventional PIC compared to the FDE-RAKE. The PIC operation is iterated several times and the number of PIC stages is plotted on the x-axis. The other detectors are one-stage detectors (hence the straight-line curves), and are displayed for comparison. It can be seen that the FDE-RAKE only needs 2 stages (i.e. the FDE and the

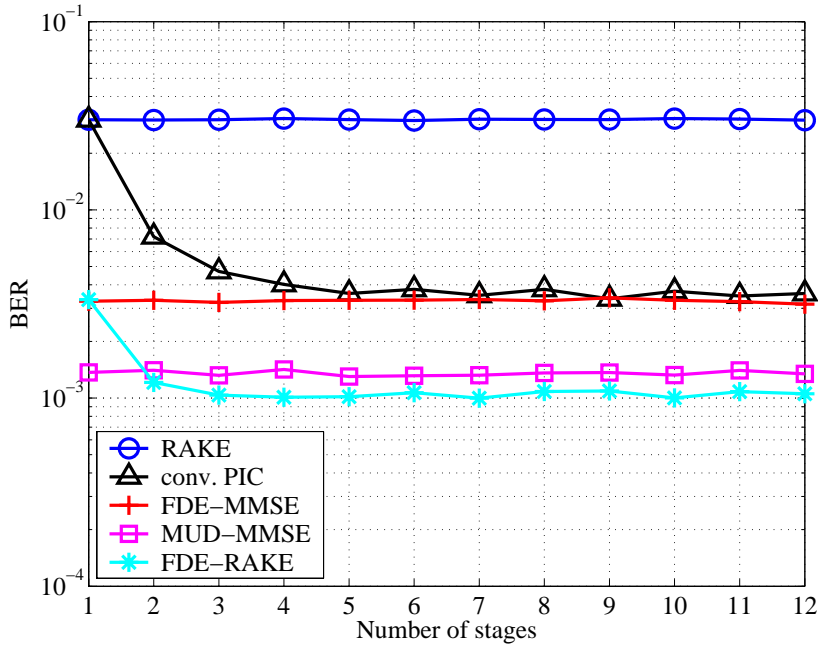


**Figure 6.6** Uncoded BER of the RAKE, FDE-MMSE, MUD-MMSE, conventional PIC and FDE-RAKE detector with  $K = 8$  users, spreading factor  $Q = 16$ , VehicularA channel with mobile velocity=50km/h, and  $E_b/N_0=12$ dB

RAKE) to reach the steady state BER, whereas the conventional PIC (RAKE-RAKE) needs 4 stages. Moreover, the steady state BER of the FDE-RAKE is better than the conventional PIC. The FDE-RAKE even outperforms the MUD-MMSE, whereas the conventional PIC only shows a comparable performance to the FDE-MMSE.

Figure 6.7 shows another problem that could happen to the conventional PIC. If the MAI is too high, it could happen that the conventional PIC does not converge at all. Figure 6.7 shows

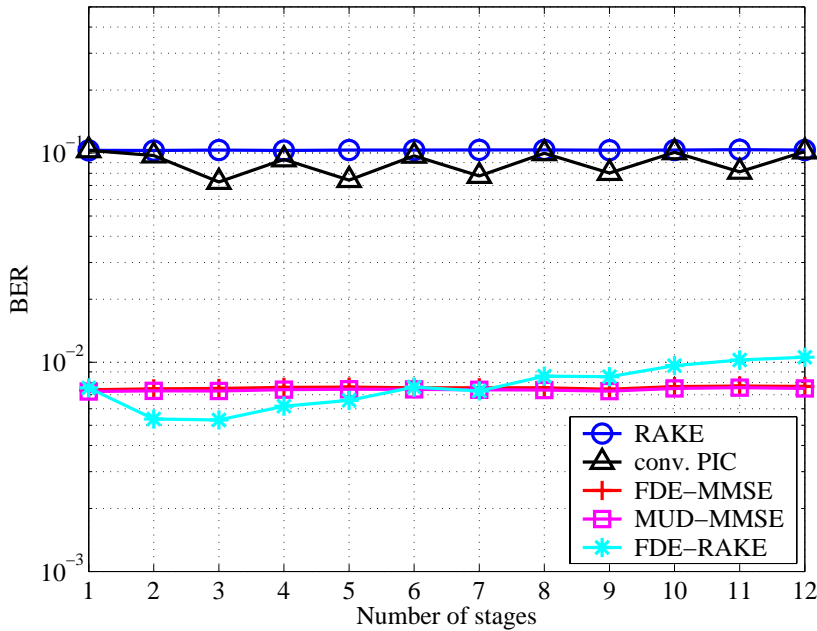


**Figure 6.7** Uncoded BER of the RAKE, FDE-MMSE, MUD-MMSE, conventional PIC and FDE-RAKE detector with  $K = 16$  users, spreading factor  $Q = 16$ , VehicularA channel with mobile velocity=50km/h, and  $E_b/N_0=12$ dB

the same detector curves as the previous figure, but with the number of users increased to 16. Here, the BER of the conventional PIC only oscillates and can not converge to a better BER with increasing number of PIC stages. The FDE-RAKE on the other hand, reaches the lowest BER again at the second stage (FDE+RAKE). The increase of BER with the increasing number of stages of the FDE-RAKE is caused by error propagation between the stages. However, this is quite uninteresting because we can always operate the FDE-RAKE only until the second stage where the FDE-RAKE already performs better than the

MUD-MMSE.

These phenomena of oscillating BER and of increasing BER with the increase of PIC stages are found in the time-variant VehicularA channel. In the 4-tap time-invariant channel environment, in which the MAI is not so disturbing, these phenomena can not be seen. The performance of the FDE-RAKE and the conventional PIC with the 4-tap time-invariant channel is shown in Figure 6.8.

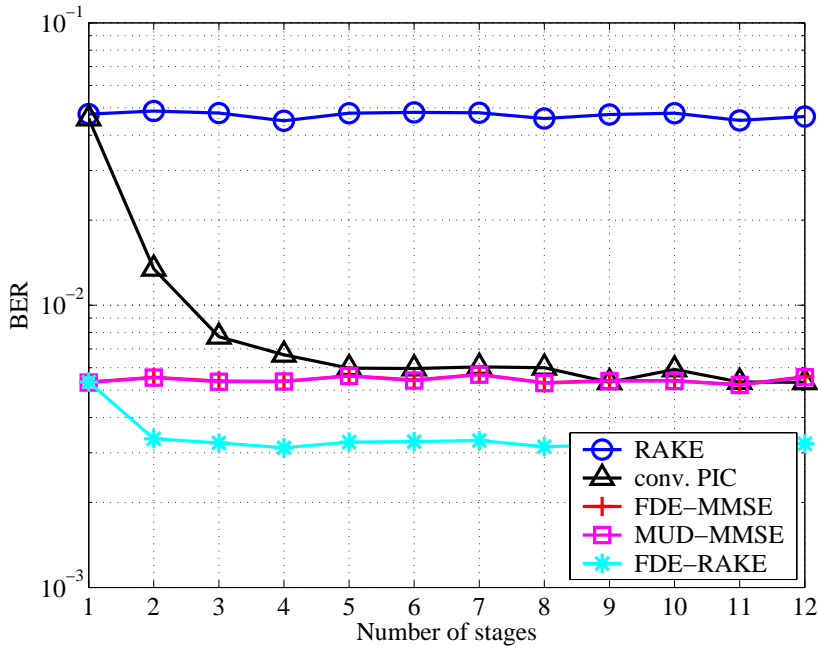


**Figure 6.8** Uncoded BER of the RAKE, FDE-MMSE, MUD-MMSE, conventional PIC and FDE-RAKE detector with  $K = 16$  users, spreading factor  $Q = 16$ , 4-tap time-invariant channel, and  $E_b/N_0=6\text{dB}$

## 6.2 Pre-FDE for CDMA Uplink

Frequency domain equalization has been shown in the previous chapters to be a good solution for the CDMA *downlink* detection. Exploiting the fact, that most of the MAI is caused by the multipath channel in CDMA downlink, the FDE solves the MAI problem by simply equalizing the channel. The undesired high complexity of long equalizers is circumvented by performing the equalization in the frequency domain.

The application of the FDE in CDMA *uplink*, on the other hand, is not that straightforward. Each user's signal, which arrives at the base station in CDMA uplink, went through different multipath channels. Equalizing these uplink channels simultaneously at the receiver is equivalent to performing a multiuser detection.

Equation (2.1) and (2.4) illustrate why the FDE is not readily applicable for CDMA uplink. Unlike in downlink, in CDMA uplink, the system matrix  $\mathbf{A}$  can not be subdivided into the channel matrix  $\mathbf{H}$  and the spreading matrix  $\mathbf{C}$  as in (2.4). The effects of spreading and transmission over several (uplink) multipath channels are thus not separable, and represented by the whole matrix  $\mathbf{A}$ .

If we equalize the received signals, according to only one of the uplink multipath channels, the orthogonality of the received signals will not be restored, because each user's signal arrived via different channels. Equalizing all the channels at once, i.e. inverting the  $\mathbf{A}$  matrix, is no difference than an MUD approach.

Of course, using a multiuser detector for the CDMA uplink at the base station is a possible alternative, since the computing power at the base station is not as limited as in the handhelds. However, there is a way to apply FDE in CDMA uplink and get the same advantages as in the downlink case, that is by using the *pre-FDE* concept.

With the pre-FDE, the equalization is done at each user's transmitter, before the channels mix up the signals of all users. The signal to be sent, is distorted (pre-equalized) at the transmitter in such a way, so that after the convolution with the channel we obtain the undistorted original data symbols. This approach is called *pre-equalization*. In a nutshell, with the pre-equalizer, the equalization algorithm is moved to the transmitter. The structure of a CDMA system utilizing pre-FDE is shown in Figure 6.9.

Figure 6.10 illustrates what happens in the uplink of a CDMA system using pre-FDE. Each transmitter pre-equalizes its own signal according to the mobile channel that it sees. The effects of *pre-FDE* and the *Channel* cancel each other out, so that only a simple despreading algorithm in the base station is needed to extract the transmitted data symbols.

To pre-equalize the uplink channel the transmitter uses the channel coefficients that were acquired by the channel estimation in the last downlink. This is possible provided that the channel is changing slowly enough and that the considered system is a TDD system, which uses the same frequency band for uplink and downlink.

According to the notation introduced in Chapter 2, the transmitted data by pre-TDE can be written as:

$$\mathbf{d}_{\text{pre-TDE}} = \mathbf{H}^H(\mathbf{H}\mathbf{H}^H)^{-1}\mathbf{C}\mathbf{d}, \quad (6.1)$$

where  $\mathbf{C}\mathbf{d}$  denotes the spread symbols. At the receiver, after the convolution with the channel we get:

$$\mathbf{r}_{\text{pre-TDE}} = \mathbf{H}\mathbf{H}^H(\mathbf{H}\mathbf{H}^H)^{-1}\mathbf{C}\mathbf{d} + \mathbf{n} = \mathbf{C}\mathbf{d} + \mathbf{n}, \quad (6.2)$$

and the data vector  $\mathbf{d}$  can be retrieved with a simple despreading. Notice that there is no noise enhancement caused by the equalization process (cf. (2.10) and (6.2)), because the equalization took place before noise is added by the channel.

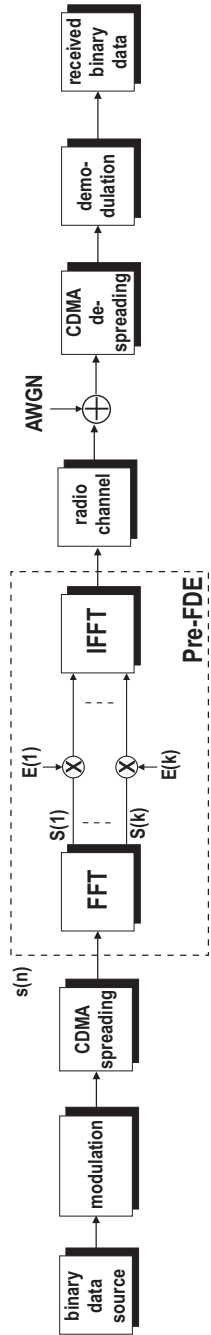
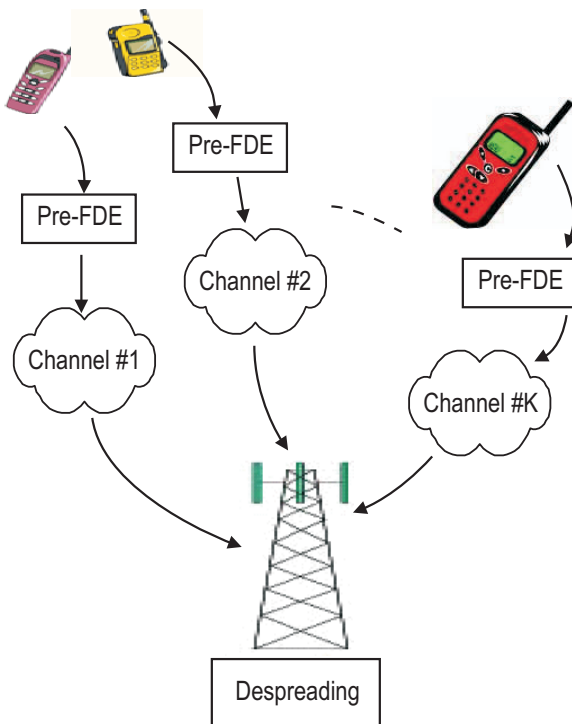


Figure 6.9 CDMA uplink with pre-FDE



**Figure 6.10** Uplink of a CDMA system with pre-FDE

The pre-FDE performs the equalization in the frequency domain. The pre-equalized data (at the transmitter) can be expressed as:

$$\mathbf{d}_{\text{pre-FDE}} = \mathbf{F}^{-1} \mathbf{\Lambda}^{-1} \mathbf{F} \mathbf{C} \mathbf{d} \quad (6.3)$$

$\mathbf{F}$  denotes the Fourier matrix and  $\mathbf{\Lambda}$  is a diagonal matrix derived from the channel coefficients, as described in Chapter 4.

### 6.2.1 Power Scaling and Zero Padding

The pre-equalization approach avoids the noise enhancement problem at the price of possibly having to transmit at higher power



[44]. A power scaling factor  $A$  can be introduced to ensure that the average pre-equalized transmit power is not higher than the transmit power without pre-equalization, i.e.  $E\|A\mathbf{d}_{\text{pre-FDE}}\|^2 = E\|\mathbf{d}\|^2$ .  $A$  is then given by:

$$A = \left[ \text{trace} \left( (\mathbf{F}^{-1} \mathbf{\Lambda}^{-1} \mathbf{F}) (\mathbf{F}^{-1} \mathbf{\Lambda}^{-1} \mathbf{F})^H \right) \right]^{\frac{1}{2}} \quad (6.4)$$

The zero-padding method (c.f. Chapter 4) is chosen to test the performance of the pre-FDE. Unlike the zero-padding for the FDE that has to be added at the end of each data block (c.f. Figure 4.4), for the pre-FDE these zeros should be put in front of each data block.

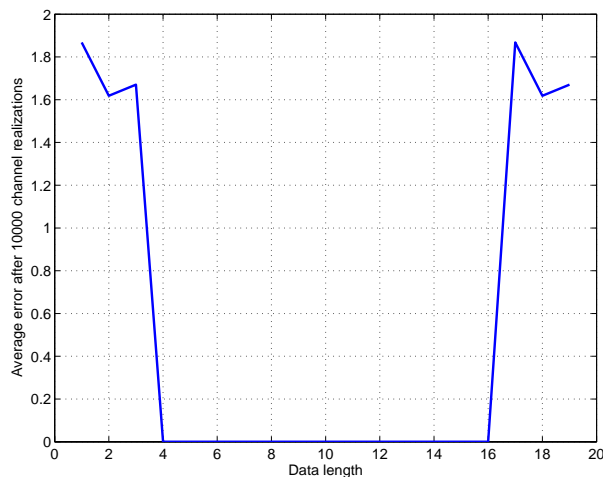


**Figure 6.11** Error profile of the pre-FDE method in a data block of length 16

The reason for this arrangement can be explained by referring to Figure 6.11. Here, the error profile of a pre-FDE method applied on a data block of length 16 is shown. The 16 randomly generated data will be processed by the pre-FDE filter for a randomly generated 4-taps channel. The output of this pre-FDE

filter was then convolved with the corresponding channel taps to regain the original 16 data. The average error (Euclidean distance) between the detected data and the randomly generated original data is then displayed in Figure 6.11. The averaging is done over 10000 channel realizations.

Note that the error takes place at the first 3 data, and at the next 3 data following the last (16th) value. With this in mind, it is appropriate if the zeros are added at the start of each block (the first 3 data in Figure 6.11), where the error is experienced. Furthermore the error following the last value (the 16th value) will spill over to the next data block (interblock interference). However, if the first values of the next block are also originally zeros, this interblock interference will spill over to the zero-padding part of the next block, which can be safely deleted after detection (Figure 6.12(b)).

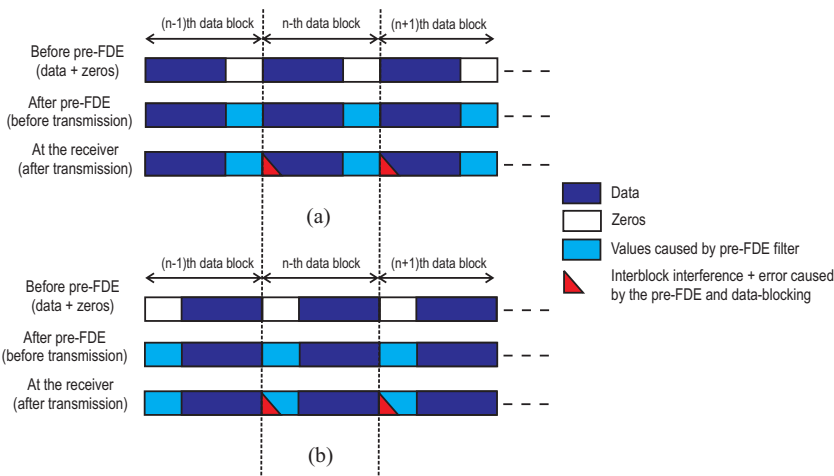


**Figure 6.12** Zero-padding arrangement for pre-FDE (a) trailing zeros at the end of a data block, (b) zeroes in front of a data block

At first glance, it seems impossible that a linear filtering followed by the convolution with the channel would necessitate dif-

ferent positioning of the zero-padding. However, the combined effect of the data-blocking and the circularity of the pre-FDE operation creates this difference. The data processing is performed block-by-block and this makes it necessary to place the zero-padding in front of each data block as is illustrated in Figure 6.12.

## 6.2.2 Simulation Results

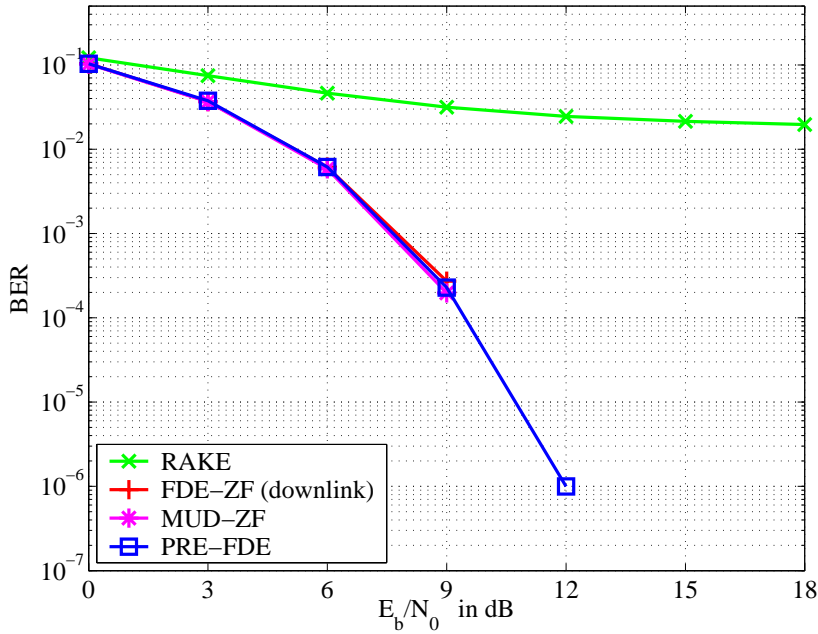


**Figure 6.13** Uncoded BER of the pre-FDE for UTRA-TDD uplink in a 4-tap time-invariant channel, spreading factor=16, 16 users

Figure 6.13 displays the performance of pre-FDE in a fully loaded cell (16 user with spreading factor 16) with a 4-tap time-invariant channel. Like the FDE, the pre-FDE outperforms the

RAKE receiver. Figure 6.13 also includes the BER of the MUD-ZF and the FDE-ZF (downlink case) for comparison<sup>1</sup>. MUD-ZF and FDE-ZF show almost identical performance to the pre-FDE.

Figure 6.14 shows the uncoded BER of the pre-FDE again along with several other receivers in VehicularA channel (50 km/h). Again, 16 users are simulated using codes with the spreading factor 16. The pre-FDE outperforms the RAKE receiver and even better than the MUD-ZF, which suffers from the noise enhancement. However, the (post) MUD-MMSE still outperforms the pre-FDE by about 3 dB.

### 6.2.3 Implementation Considerations

Most of the pre-coding proposals aimed to reduce the complexity of the receiving algorithm in the mobile station. Therefore, it was mostly proposed for the downlink of CDMA systems [45], [46], [47]. However, it is worth noting that most of these proposals concentrate on multiuser detector approaches<sup>2</sup>, which can not be reasonably implemented in the mobile station. Therefore, the downlink is mostly considered in these proposals.

The FDE (and pre-FDE) on the other hand, displays an elegant simplicity, that makes the implementation in base station as well as in mobile station possible. If the pre-FDE is used in downlink (implemented at the base station), it will enable a very simple receiver (a simple despreading) in the mobile station<sup>3</sup>. However, the FDE (implemented at the mobile station)

---

<sup>1</sup>The FDE in downlink can be regarded as a special case of uplink, in which the signal of all users arrived through the same channel. The power scaling of the pre-FDE allows us to draw and compare pre-FDE (uplink) and FDE (downlink) on the same graph, since the  $E_b/N_0$  of the two curves show the same average value on the x-axis.

<sup>2</sup>Several papers also proposed pre-equalizers (not MUD), but without the simple frequency domain processing [48], [49].

<sup>3</sup>The pre-RAKE approach is rather uninteresting because it also suffers

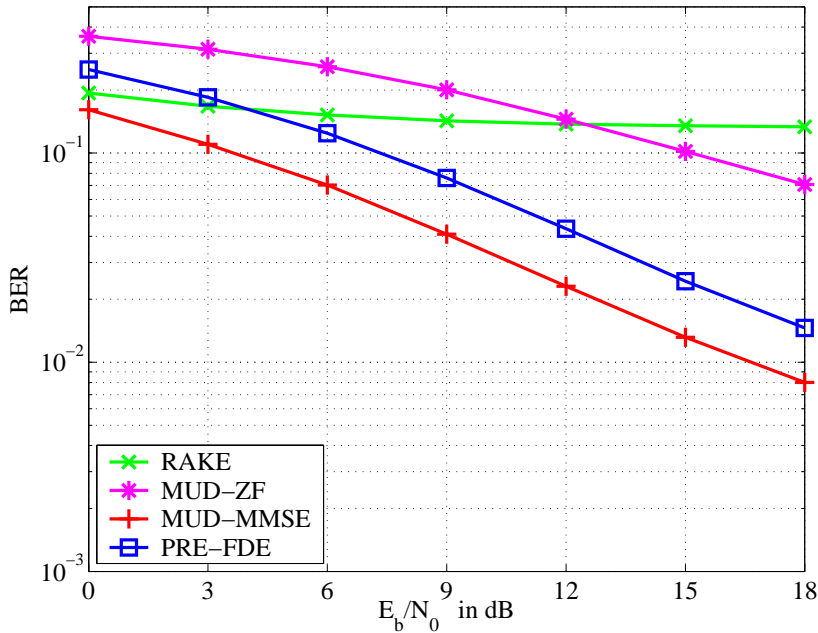


**Figure 6.14** Uncoded BER of the pre-FDE for UTRA-TDD uplink in the VehicularA channel (50km/h), spreading factor=16, 16 users

may deliver better BER because it does not have to scale down its transmitting power as the pre-FDE.

For uplink, the most natural receiver is actually the multiuser detector (at the base station), since the base station has to detect the data of all users anyway. So, if extreme simplicity of the mobile station is the main criterion, the combination of pre-FDE in downlink and multiuser detector in uplink can be chosen. If more resources are available at the mobile station, the FDE can be used instead of the pre-FDE in downlink. If simplicity of the basestation is also required, the pre-FDE can be applied in

---

heavily from MAI like the normal post-RAKE.

uplink.

One potential problem in the application of the pre-FDE should be mentioned here. The pre-FDE (in uplink) relies on the channel knowledge gained from the last downlink for its proper operation. If the channel changes rapidly, the channel taps acquired from the last downlink could have varied too much from the actual channel state. This could become worse, if two or more uplink slots using pre-FDE follows one downlink, which is possible in a system such as UTRA-TDD. In this case, some kind of channel state information should be transmitted to guarantee the proper operation of the pre-FDE.

Good performance and simplicity are not the only advantages provided by the FDE. The next section will introduce another useful advantage of using FDE based receiver in CDMA systems, namely the multimode baseband processing structure for various air access technologies.

### 6.3 Software-Defined Radio

The rapid development in the wireless and mobile communication technology offers a myriad of choices to get connected in the wireless world. CDMA technology in the 3G mobile communication systems, OFDM in the wireless LAN and broadcasting (e.g. DVB-T) systems, along with the existing 2G system are competing and complementing each other in offering wireless/mobile communication services. However, the users would not bother to ask the question, “What technology am I using now?” They just want to get connected, if possible, without changing the equipment they are using even as they switch to another system.

*Being wireless just for the sake of being wireless is not a valid goal. . . . subscribers care little about networks and technologies; they just want new stuff [50]*

The challenge in this situation is to come up with a single receiver structure that can work with all these systems. One idea that has rapidly gained popularity to enable multimode receivers is the *software radio* concept [51]. With the software radio, the software which is used to process the radio signal can be adjusted easily to adapt to the selected air access technology. However, a pure software radio approach that puts the A/D converter as close as possible to the antenna and lets all the following data processing be done by software, still poses difficulties to be overcome. A milder approach which is called the software-defined radio (SDR) offers a more feasible alternative. Examples of the SDR approach have been proposed in [52], [53]. The idea here is to exploit common structures between air access technologies and to design a software radio that can be reconfigured by a list of parameters.

### 6.3.1 SDR Based on FDE

One interesting aspect of the FDE is its similarity to an OFDM system structure [22], [30]. This is shown in Figure 6.15. The difference between the two systems lies in the order of the FFT/IFFT operation. The OFDM system uses the IFFT at the transmitter for the OFDM signal multiplexing, while the FDE puts the IFFT at the receiver side to transform the equalized data back into the time domain. This similarity between the structure and the performance of FDE and OFDM has the tendency to be rediscovered again and again [31],[54], [55].

In fact, the similarity between FDE and OFDM is the starting point for the idea of using FDE to improve CDMA detection performance (cf. Chapter 3). But the advantage of FDE does not stop there. Because a single carrier system using FDE and an OFDM system are very similar, it is then easy to see, that we can construct one single structure to handle OFDM and singlecarrier

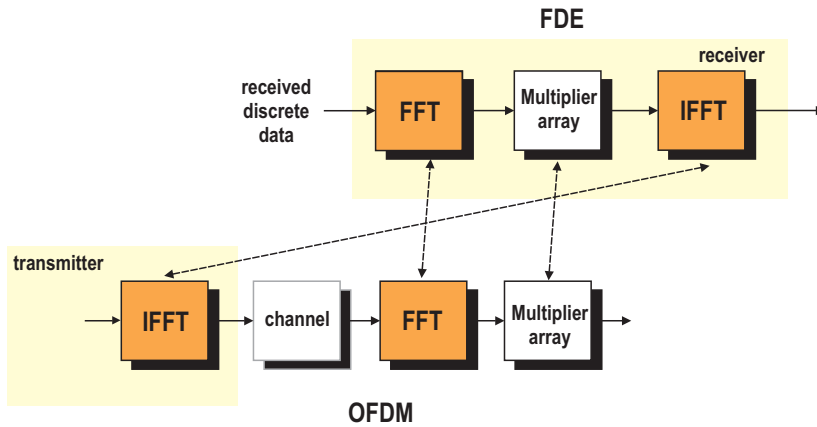


**Figure 6.15** Similarity between FDE and OFDM

systems simultaneously simply because we can *reuse* the parts of these systems, which are similar.

Falconer et al. [31] and Witschnig et al. [54], for example, mentioned the possibility to combine a single carrier system using FDE in uplink and an OFDM system in downlink of a mobile communication system. However, since the FDE has been shown to be also applicable in CDMA systems, we can then move even further. A unified baseband data processing structure can be constructed to handle several air interface standards including CDMA. Such a structure is shown in Figure 6.16.

The structure in Figure 6.16 can process a conventional TDMA (or FDMA signal), CDMA signal, and signals of a multicarrier system, such as OFDM and MC-CDMA. The TDMA/FDMA and the CDMA signals belong to the singlecarrier systems which require both the FFT and the IFFT operation as parts of the FDE detector. The CDMA signal needs a further despreading before the demodulation to complete the detection process. The multicarrier MC-CDMA and OFDM signals only need the FFT,



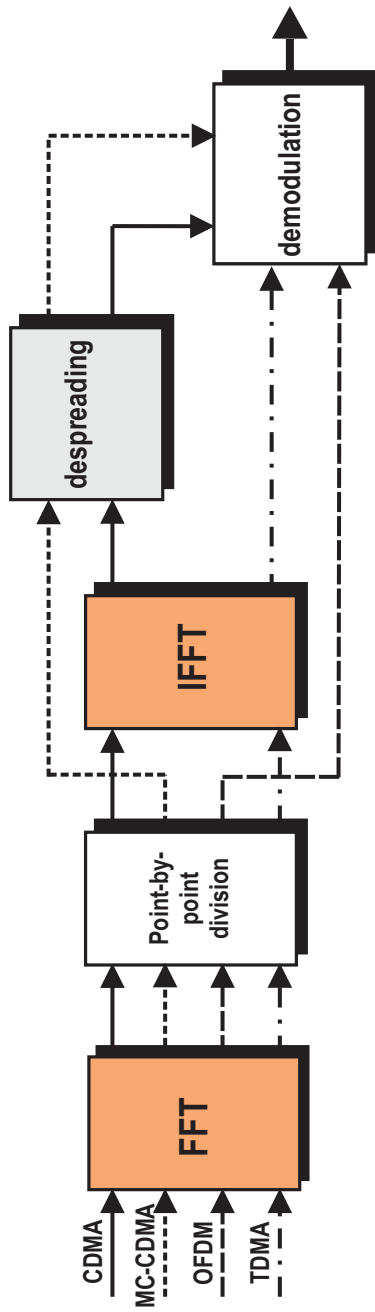


Figure 6.16 Structure of a multimode receiver based on FDE

as the equalization and detection are performed directly in the frequency domain. Like CDMA, the MC-CDMA signal also requires the despreading process before demodulation. The structure shown in Figure 6.16 provides a very elegant solution for a multimode receiver problem.

### 6.3.2 SDR for UTRA and WLAN

One interesting application of the structure in Figure 6.16 is the integration of 3G mobile communication and wireless LAN systems. The 3G standards family are all based on CDMA technology. On the other side, the dominating technology for WLAN is the OFDM system. Both IEEE 802.11a and the HIPERLAN/2 standards utilize the OFDM air interface technology.

Here we will consider a practical example in providing a multimode baseband processing structure for UTRA-TDD and WLAN system [56]. Since the use of FFT to detect an OFDM signal is widely known, we will concentrate here to show the feasibility of using the same detector structure to receive UTRA-TDD signal (the upper signal flow in Figure 6.17).

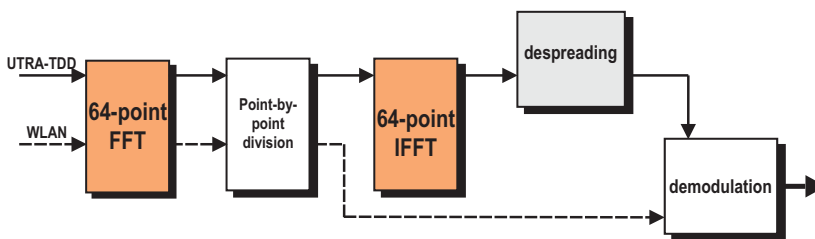


**Figure 6.17** SDR for UTRA-TDD and WLAN

Since both IEEE 802.11a and HIPERLAN/2 use 64-point FFT, this FFT length will also be used for the SDR. Note also that it is undesirable to modify the air interface standard of

UTRA-TDD, thus such algorithms that need a cyclic prefix insertion (as proposed in [20]) can not be used. Instead, we use the overlap-cut method (cf. Chapter 4) that makes it possible to use the FDE for CDMA downlink systems without cyclic prefix insertion.

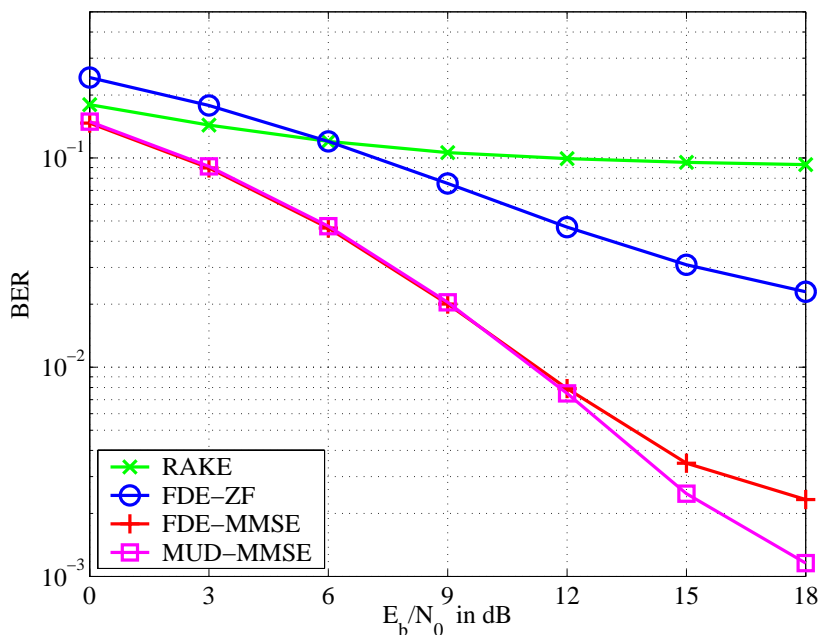


**Figure 6.18** Uncoded BER of the SDR with FDE for the UTRA-TDD system, spreading factor=16, number of users = 16, VehicularA channel 50 km/h

Figure 6.18 presents the uncoded BER of an FDE detector with the FFT length of 64 for the downlink of a UTRA-TDD system. There are 16 users in the cell accessing the system with OVSF codes of length 16. The overlap-cut method with pre- and post-lap of 16 chips is used. The simulation is done with the VehicularA channel [38], at a velocity of 50 km/h.

It can be seen that the FDE detector outperforms the RAKE receiver in the fully loaded cell. The FDE-MMSE detector offers a better BER than the FDE-ZF that suffers from noise enhancement. A BER curve of the MUD-MMSE is also given for comparison. The slight difference between the BER of the MUD-MMSE and the FDE-MMSE is caused by the approximation that comes from the overlap-cut method.

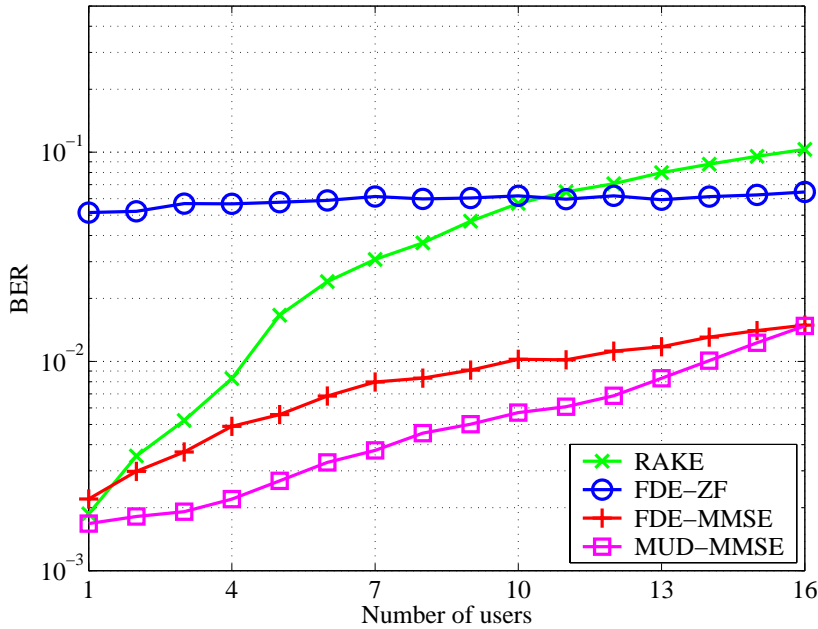


**Figure 6.19** Uncoded BER of the SDR with FDE for the UTRA-TDD system against the number of users,  $E_b/N_0 = 10dB$ , spreading factor=16, VehicularA channel 50 km/h

Figure 6.19 shows the simulation results plotted against the number of users. Here we see that the FDE detector performs very well in suppressing MAI compared to the RAKE receiver. The BER of the RAKE receiver deteriorates rapidly with increasing number of users.

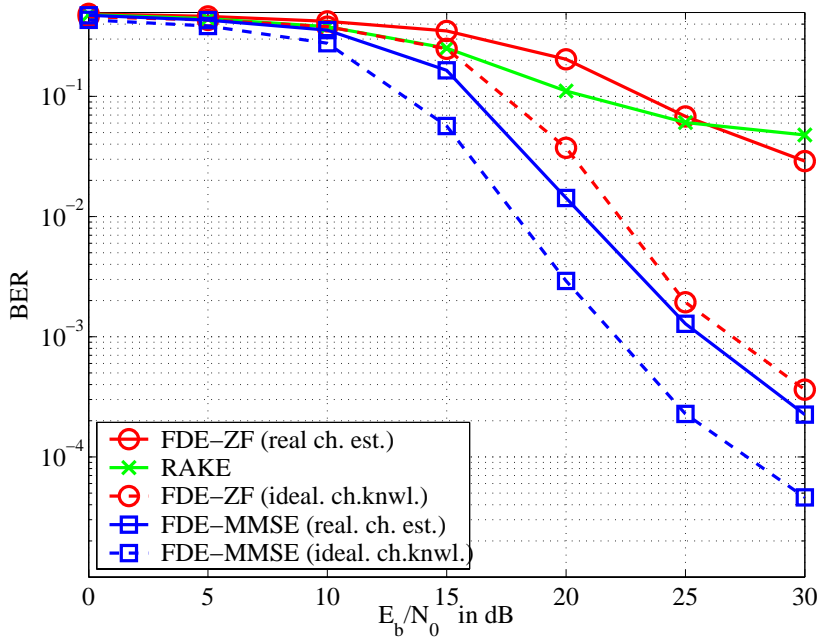


**Figure 6.20** Coded BER of the SDR with FDE for the UTRA-FDD system, spreading factor=32, number of users= 16, VehicularA channel 72 km/h, Viterbi decoder

The same basic principle was also tested with the UTRA-FDD and WLAN systems [57]. The feasibility of building a common baseband processing structure based on FDE is here confirmed once again. Figure 6.20 displays the BER of coded UTRA-FDD system using the FDE detector with 64-point FFT. 16 users utilizing spreading codes with spreading factor 32 are simulated in the VehicularA channel with a velocity of 20 m/s (72 km/h). Downlink data channels along with the synchronization and pilot channels according to UTRA-FDD standard were simulated.

Additionally, the BER with a real channel estimation is compared to the BER with an ideal channel knowledge in Figure

6.20. The FDE detector generally outperforms the RAKE receiver. However, if the effect of the imprecise channel estimation is also considered, the performance of the FDE-ZF deteriorates rapidly because of the noise enhancement inherent in the receiving algorithm.

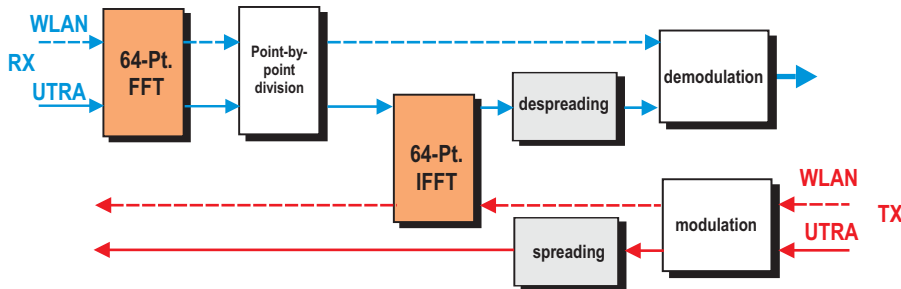


**Figure 6.21** Multimode transceiver for UTRA and WLAN

These simulation results demonstrate the capability of the FDE based detector in providing a common structure for two different systems, in this case CDMA and OFDM. The multimode transceiver for the case of WLAN and UTRA systems is shown in Figure 6.21. The FFT and IFFT operation are the core of the structure that are reused, thus providing a very compact transceiver algorithm for the two systems.

### 6.3.3 Advance Spectrum Allocation with SDR

#### Illusive Spectrum Scarcity

One problem that can be potentially solved by the multimode SDR is the spectrum scarcity problem. The spectrum auctions for the 3G mobile communication systems in Europe, which have brought in hundred billions of US dollars, calls our attention to the problem of spectrum scarcity. However, what seems to be expensive is not necessarily scarce. The spectrum is nothing than

an empty space through which our electromagnetic waves travel. Is the spectrum really scarce? Don't we have enough *empty space* for everyone out there?

We believe, that the limit of our spectrum capacity is still far from reached. Spectrum measurement samples showed that there are enough unused frequencies waiting to be exploited [58]. The Spectrum Policy Task Force, organized by the FCC found out, that even within the premium frequencies below 3 GHz in dense, revenue-rich urban areas, the most bands are quiet all the time [59].

The real problem lies rather on how we regulate the use of our spectrum. The spectrum licensing policy, which aims at reducing interferences from different systems, sets artificial limits on technology. This leaves large spectrum blocks being used inefficiently while other spectrum areas become very crowded, eventually causing an illusive spectrum shortage. Consequently, the extent to which there appears to be a spectrum shortage largely depends not on how many frequencies are available but on the technologies that can be deployed [59]. By changing our paradigm in using the spectrum, the scarcity problem can be alleviated.

### **Open Spectrum Access, Spectrum Pooling and SDR**

Having identified the cause of the spectrum scarcity, the ideal remedy is, of course, if we can abandon the practice of spectrum licensing completely. In the so called *open spectrum access* environment, all can access the spectrum freely and pay an access fee that is continuously and automatically determined by the demand and supply conditions at the time [60]. No licensing and auctioning is necessary. The technology to control the spectrum access seems to be within reach in this digital communication era.

*But all this technology is theory, not practice. In practice, the spectrum is full of legacy devices, blasting energy in the old ways over spectrum bought and owned by watchful tenants. After paying billions for the right to use a small slice of spectrum, owners are unlikely to embrace new invaders having nonstandard formats... So is wireless capacity limited and expensive, or is it infinite and free? And how do we get from here to there? [61]*

This quote from Lucky depicts perfectly our situation. Even if it is technologically possible to equip devices with the appropriate radio access etiquette that can support an open spectrum access, it is impossible to abolish the spectrum licensing practice in a short time. So, how do we move from the limited and expensive wireless capacity to the infinite and free resources? One idea that has been proposed to solve the problem is *spectrum pooling* [62].

The term *spectrum pool* was first mentioned by Mitola [63]. The word refers to the practice of pooling spectrum areas that can be used by devices equipped with certain radio access etiquette. Users can then choose the free frequencies from these pooled spectra.

In [62] the spectrum pooling idea is further expanded in several ways. First, it is assumed that this spectrum pooling system should be able to function on top of our traditional licensing (blocked) allocation system. Thus the spectrum pooling users must be able to access the unused spectra from the pool, and also release the frequencies as soon as the owner of the frequency block needs them. Furthermore, this *access-release* behavior should be implemented without any change in the spectrum owner's system.

With this spectrum pooling concept, the spectrum owners can offer their unused (or sporadically used) frequencies for rental. This is particularly beneficial, if there are indeed only minimal activities in the considered spectrum block. This results in a win-win situation: The spectrum owner can have a revenue source



while putting his idle frequencies into use, and the rental users get the valuable resources that they need. Hence, the overall spectrum usage efficiency is increased, and most importantly, we need not wait until we can get rid of the spectrum licensing practice. The increase in spectrum utilization that can be achieved by a spectrum pooling system is demonstrated in [64].

In [62], OFDM is assumed as the air access technology to enable spectrum pooling. In [65] the physical layer issues of the spectrum pooling are further discussed. However, the idea of spectrum pooling or adaptive resource allocation need not be attached to any air access technology. If an SDR structure that can handle several air access techniques is available, then an adaptive resource allocation can be practiced independent of the air access techniques. These *smart* SDR devices can listen to the resource signaling in their environment, tune their air access technology accordingly, and access the spectrum if they sense free resources. The free resources that can be exploited are thus not limited to spectrum, but can also be time-slots or free spreading codes.

The spectrum pooling concept can be an important concept to bridge the gap between the present blocked resource allocation and the future fully adaptive resource allocation. In any case, the SDR will play an important role in ushering the new era of wireless resource management, and the FDE based multimode detector could be one key technology in this context.



## Conclusions & The Continuing Work

*Whether in science or in art, then, the ability to judge that a work is finished is more an act of commitment to the continuousness of the creative process than it is a sign of having expressed the last word [66]*

*I realize now that knowledge itself is transitory and often of questionable validity. . . Knowledge won't sit still, and it isn't just the forging of new frontiers but the continual rewriting of the old frontiers as well [67]*

CDMA (spread spectrum) systems have been and are still providing a fertile ground for research. Reading the earliest until the most recently papers on CDMA systems, various moods ranging from over-optimism to realistic-expectation about this technique can be observed. Some things found in the earlier papers turned out curiously to be inaccurate or even incorrect. Thus, in the face of ever changing knowledge, an author will always run the danger to state faulty conclusions as he summarizes up his work. Despite this danger, this last chapter intends to do just that, to summarize the work.

The work centers around the idea of using frequency domain equalization (FDE) for CDMA data detection. Triggered by the observation that the OFDM system consistently outperforms CDMA system using a RAKE receiver (Chapter 3), the idea of FDE detector for CDMA was developed (Chapter 4). Unlike a time domain equalization (TDE), which does not really simplify the receiving algorithm due to large matrix inversion, the FDE provides both simplicity and good MAI suppression for CDMA detection.

The FDE was also found almost as good as the linear multiuser detectors, especially in fully loaded cells (Chapter 5). Furthermore, the overlap-cut method was introduced which renders the addition of cyclic prefix or zero-padding unnecessary for the implementation of FDE.

Several other ideas derived from the FDE approach are presented in Chapter 6. The FDE-RAKE extends the FDE detector into a parallel interference cancellation detector. This detector shows a slightly better performance than the linear multiuser detector for a roughly equal complexity. Another idea is the pre-FDE detector which moves the equalization to the transmitter and leaves a simple despreading to be done in the receiver to detect the CDMA signals. The pre-FDE enables the application of FDE in CDMA uplink.

However, the most interesting idea derived from the FDE concept is the multimode baseband processing structure, which can handle several air interface standards. The key to this structure is the striking similarity between the FDE and the OFDM system structure. Since the FDE has been shown to work also for CDMA systems, a common structure for CDMA (including other singlecarrier systems) and the multicarrier systems - which naturally perform their detection in the frequency domain - can be easily constructed.

Table 7.1 summarizes all the CDMA detectors discussed in this work.

## 7.1 Why CDMA? (revisited)

As mentioned in Chapter 1, initially, it was thought that the CDMA system can enable a wideband mobile communication without the use of long equalizers, which are needed in wideband non-spread spectrum systems [7]. However, the RAKE receiver turned out to be heavily influenced by MAI, and ironically, the FDE, which is an equalizer, provides a low complexity solution for suppressing the MAI in CDMA systems. A legitimate question is then, “why do we need CDMA after all?” Since the FDE can be applied equally well to non-spread spectrum systems.

Figure 7.1 presents an attempt to answer this question. The BER curves of an FDE-MMSE detector for CDMA systems with various spreading factors are displayed. The curve with spreading factor 1 represents a non-CDMA system, i.e. a conventional TDMA/FDMA transmission, in which the symbol rate is fixed at the same rate as the chip rate of a CDMA system to maintain the same capacity.

Since the simulations are done with the time-variant VehicularA channel, a residual MAI can still be observed, even if the

CDMA Detectors	
Name	Characteristics
RAKE	suffers from MAI, fairly simple
MUD	eliminates MAI, high complexity, requires information of other users
TDE	suppresses MAI, high complexity, applicable in CDMA downlink, no information of other users required
FDE	suppresses MAI, low complexity, applicable in CDMA downlink, no information of other users required, facilitate multimode detector
pre-FDE	suppresses MAI, low complexity, applicable in CDMA uplink and downlink, transmit power constraint needed, no information of other users required
FDE-RAKE	slightly better than MUD, fairly complex, applicable in CDMA downlink, information of other users required

**Table 7.1** Summary of CDMA detectors

channel is equalized by the FDE. Figure 7.1 shows that the non-CDMA system offers a better BER than the CDMA systems with the same capacity, because the non-CDMA system does not experience MAI due to spreading/despreading.

However, a non-CDMA system can not display a *graceful degradation* behavior. If the system load is low (a small number of users are accessing the system) the BER does not get better. A CDMA system, on the other hand degrades gracefully according to the system load. Figure 7.1 also displays CDMA systems with  $\frac{1}{2}$  and  $\frac{1}{4}$  capacity ( $SF = 16$ , 8 users and  $SF = 4$ , 1 user),

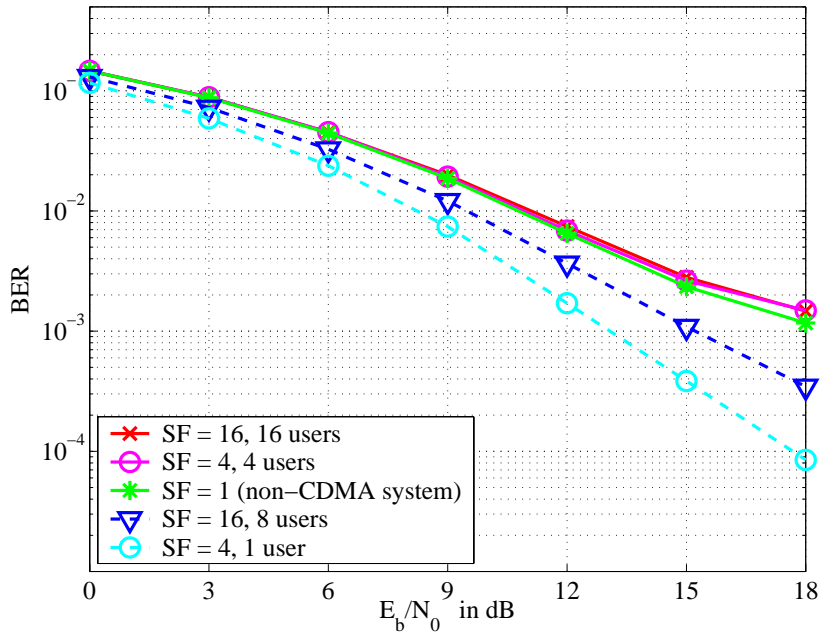


**Figure 7.1** BER of FDE-MMSE in a CDMA system with various spreading factors, UTRA-TDD system parameters, VehicularA channel (50 km/h)

which illustrate the graceful degradation. As Shannon put it, “It seemed like a very democratic way to use up the coordinates that you have, and to distribute the ‘cost of living’, the noise, evenly among everyone” [1]. That could be one important advantage of CDMA systems over a conventional TDMA/FDMA system<sup>1</sup>.

<sup>1</sup>The simulation includes scrambling according to UTRA-TDD standard. Systems without scrambling may show other behavior due to the bad correlation properties of the Walsh codes.

## 7.2 Further Research

Research activities on the frequency domain processing for CDMA systems can be expected to continue. It has been shown that the frequency domain processing also simplifies the implementation of diversity combining and MIMO systems for CDMA [68], [69], [70], [71]. These could be fruitful research topics for the next future.



# A

## UTRA

Universal Mobile Telecommunication System (UMTS) is the European proposal for the 3rd generation mobile communication systems. An overview on UMTS is presented in [72]. The UMTS Terrestrial Radio Access (UTRA) scheme consists of two modes: frequency-division duplex (FDD) [73] and time-division duplex (TDD) [37], which time-multiplexes the uplink and downlink in the same frequency band.

The UTRA-FDD and UTRA-TDD were harmonized to facilitate interoperability. The basic system parameters of UTRA are given in Table A.1.

Both systems use the orthogonal variable spreading factor (OVSF) codes as the channelization (user's signature) codes, however with different available spreading factors. The OVSF codes allow the mix of different spreading factors while preserving orthogonality. The OVSF codes can be defined using the code tree in Figure A.1. To maintain orthogonality, a code can only be used if and only if no other code on the path from the specific code to the root of the tree is used.

System Parameters		
Duplex scheme	FDD	TDD
Multiple access scheme	WCDMA	TD-CDMA
Spreading factor (uplink)	4,8,...,256	1,2,4,8,16
Spreading factor (downlink)	4,8,...,512	1 or 16
Chip rate	3.84 Mchip/s	
Modulation	QPSK	
Bandwidth	5 MHz	
Pulse shaping	Root raised cosine, $r = 0.22$	
Frame length	10 ms	
Number of time slots per frame	15	

**Table A.1** Basic system parameters of UTRA

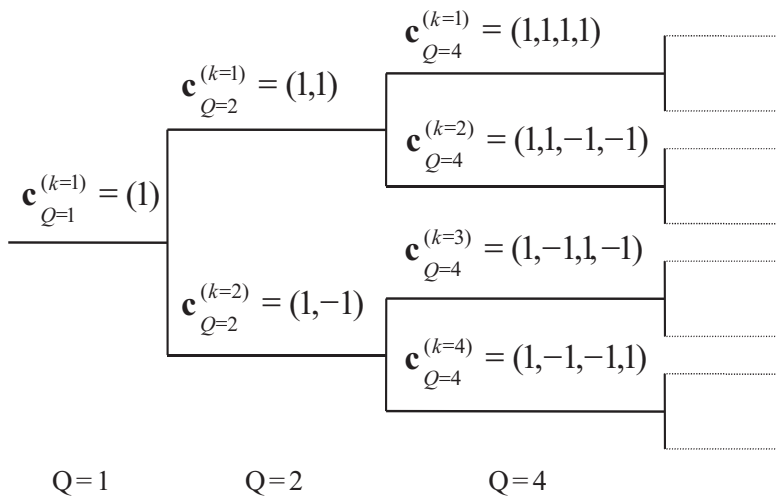


**Figure A.1** Code-tree for the generation of OVSF codes

## A.1 UTRA-TDD

The UTRA-TDD divides the radio frames into time slots, as can be seen in Figure A.2. Each time slot can be assigned flexibly either for downlink or uplink. This is illustrated in Figure A.3. This flexible assignment enables asymmetric UL/DL allocations.

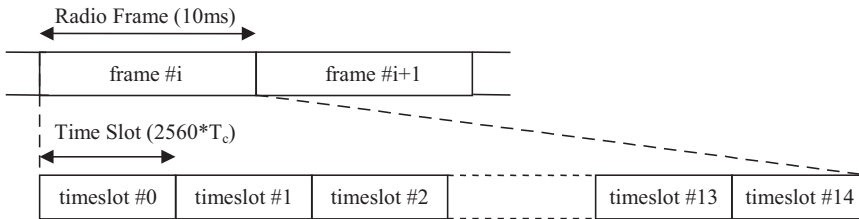


**Figure A.2** UTRA-TDD radio frame and time slots

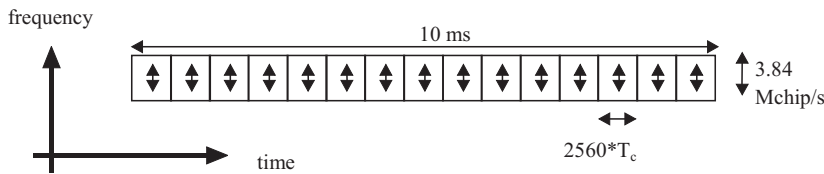


**Figure A.3** UTRA-TDD time slots flexible assignment

Each UTRA-TDD time slot consists of two data fields, a midamble and a guard period. Several burst types are available, and the details can be seen in [26]. For the simulations in this work, a simplified structure is assumed. The whole 2560 chips in a time slot are assumed to be data chips. The simulation with the time variant VehicularA channel assumed the knowledge of the channel taps at the middle of the time slot, where the midamble stands. If not otherwise stated, a perfect channel knowledge is

assumed (no channel estimation algorithm is performed in the simulations).

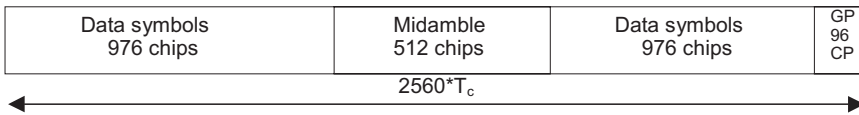


**Figure A.4** UTRA-TDD time slot structure

UTRA-TDD uses a chip-by-chip scrambling with the length 16 to identify the cells. Available scrambling sequences are listed in [26]. The scrambling sequence used in the simulations with UTRA-TDD in the preceding chapters is given by:

$$-j, -1, +j, -1, -j, -1, +j, -1, +j, +1, -j, +1, -j, -1, +j, -1.$$

This work focus on UTRA-TDD while showing several simulation results with the UTRA-FDD to show the extensibility of the presented ideas. Details on UTRA-FDD can be found in [26].

# B

## Channel Models

There are several channel models used by the simulations in this work. The typical urban and the rural channel is taken from COST 207 [74]. Table B.1 and Table B.2 display the mean value of the received power on each delayed path of the typical urban and the rural channel respectively.

Typical Urban Channel	
Delay in $\mu s$	Power in dB
0	-3
0.2	0
0.5	-2
1.6	-6
2.3	-8
5.0	-10

**Table B.1** Profile of the typical urban channel

The VehicularA channel is described in [38], and its profile can be seen in Table B.3. Its path intervals correspond to the

Rural Channel	
Delay in $\mu s$	Power in dB
0	0
0.1	-4
0.2	-8
0.3	-12
0.4	-16
0.5	-20

**Table B.2** Profile of the rural channel

VehicularA Channel	
Delay in $ns$	Power in dB
0	0
260.4	-2.5
520.8	-6.6
781.3	-9.5
1041.7	-13
1302.1	-13.6
1822.9	-15.5
2083.3	-25.5
2604.2	-21.5
2864.6	-25.5

**Table B.3** Profile of the VehicularA channel

chip duration of UMTS:  $T_c = 1/(3.84 \times 10^6)s = 2.6 \times 10^{-7}s$ .

The 4-tap time-invariant channel used in the simulations is simply 4 complex coefficients which are randomly generated. These 4 taps are normalized to give the power of 1 and are generated for every transmission in each time slot of the UTRA-TDD.

## Acronyms, Notation and Symbols

3G	Third Generation
CDMA	Code Division Multiple Access
DS	Direct Sequence
FDD	Frequency Division Duplex
FDE	Frequency Domain Equalization
FDMA	Frequency Division Multiple Access
FFT	Fast Fourier Transform
IMT-2000	International Mobile Telecommunication at 2000
ISI	Intersymbol Interference
ITU	International Telecommunication Union
MAI	Multiple Access Interference
MC-CDMA	Multicarrier CDMA
MLSE	Maximum Likelihood Sequence Estimator
MMSE	Minimum Mean Square Error
MUD	Multiuser Detector
OFDM	Orthogonal Frequency Division Multiplexing
OVSF	Orthogonal Variable Spreading Factor
PIC	Parallel Interference Cancellation
TD-SCDMA	Time Division – Synchronous CDMA
TDD	Time Division Duplex
TDMA	Time Division Multiple Access
UMTS	Universal Mobile Telecommunication System
UTRA	UMTS Terrestrial Radio Access
ZF	Zero Forcing

## Notation

$x$	index
$x$	variable
$\mathbf{x}_i$	i-th vector element
$X$	constant
$x(t)$	function
$X(f)$	Fourier transform of a function
$\mathbf{X}$	matrix
$\mathbf{X}(i, :)$	i-th row of the matrix $\mathbf{X}$
$\mathbf{X}(:, j)$	j-th column of the matrix $\mathbf{X}$
$(x_{i,j})$	Matrix coefficient of the i-th row and j-th column
$x ./ y$	element by element division
$\text{diag}(\mathbf{x}_i)$	arrange a vector into a diagonal matrix
$E\{X\}$	expected value
$\mathbf{X}^T$	matrix transpose
$\mathbf{X}^H$	matrix conjugate transpose
$\tilde{\mathbf{X}}$	circulant matrix

## Symbols

$\mathbf{A}$	system matrix
$A_i^{(k)}$	the i-th chip element of the $\mathbf{A}$ matrix of the k-th user
$\mathbf{c}_i^{(k)}$	the i-th chip of the spreading sequence of the k-th user
$\mathbf{C}$	channel matrix
$\mathbf{d}$	data vector
$\mathbf{d}^{(k)}$	data vector of the k-th user
$\mathbf{d}_n^{(k)}$	the n-th symbol of the data of the k-th user
$\hat{\mathbf{d}}$	detected data vector
$\mathbf{r}$	received vector
$E_b$	Energie per bit



<b>F</b>	Fourier matrix
<b>h</b>	channel impulse response vector
$h_i$	the $i$ -th channel tap
$\mathbf{h}^{(k)}$	channel impulse response of the $k$ -th user
<b>H</b>	channel matrix
$i$	Index
$k$	user index
$K$	number of users
$L$	channel impulse response length
$n$	discrete time variable
<b>n</b>	additive noise
$N$	number of considered symbols
$N_0$	noise power
$Q$	spread factor
$T_c$	chip duration
$T_b$	symbol duration
<b>y</b>	output vector
<b><math>\Lambda</math></b>	diagonal matrix derived from the channel impulse response



# References

- [1] F. Ellersick, "A conversation with Claude Shannon," *IEEE Communications Magazine*, vol. 22, no. 5, pp. 123–126, May 1984.
- [2] H.H. Chen, C.X. Fan, and W.W. Lu, "China's perspectives on 3G mobile communications and beyond: TD-SCDMA technology," *IEEE Wireless Communications*, vol. 9, no. 2, pp. 48–59, 2002.
- [3] T. Ojanperä and R. Prasad, *WCDMA: Towards IP Mobility and Mobile Internet*, Artech House Publishers, Boston - London, 2000.
- [4] R.A. Scholtz, "The evolution of spread-spectrum multiple-access communications," in *IEEE 3rd Int. Symp. on Spread Spectrum Techniques and Applications ISSSTA*, July 1994, vol. 1, pp. 4–13.
- [5] S. Verdu, *Multiuser Detection*, Cambridge University Press, Cambridge, UK, 1998.
- [6] S. Moshavi, "Multi-user detection for DS-CDMA communications," *IEEE Communications Magazine*, vol. 34, no. 10, pp. 124–136, Oct. 1996.
- [7] W.C.Y. Lee, "Overview of cellular CDMA," *IEEE Trans. on Vehicular Technology*, vol. 40, no. 2, pp. 291–302, May 1991.

- [8] D.L. Schilling, L.B. Milstein, R.L. Pickholtz, M. Kullback, and F. Miller, "Spread spectrum for commercial communications," *IEEE Communications Magazine*, vol. 29, no. 4, pp. 66–79, Apr. 1991.
- [9] D.L. Schilling, "Wireless communications going into the 21st century," *IEEE Trans. on Vehicular Technology*, vol. 43, no. 3, pp. 645–652, Aug. 1994.
- [10] S. Verdú, "Minimum probability of error for asynchronous gaussian multiple-access channels," *IEEE Trans. on Information Theory*, vol. 32, no. 1, pp. 85–96, Jan. 1986.
- [11] A. Klein and P.W. Baier, "Linear unbiased data estimation in mobile radio systems applying CDMA," *IEEE Jour. on Selected Areas in Communications*, vol. 11, no. 7, pp. 1058–1066, Sept. 1993.
- [12] A. Klein, G.W. Kaleh, and P.W. Baier, "Zero forcing and minimum mean-square-error equalization for multiuser detection in code-division multiple-access channels," *IEEE Trans. on Vehicular Technology*, vol. 45, no. 2, pp. 276–287, May 1996.
- [13] A. Klein, "Data detection algorithms specially designed for the downlink of CDMA mobile radio systems," in *IEEE 47th Vehicular Technology Conference*, Phoenix, Arizona USA, May 1997, vol. 1, pp. 203–207.
- [14] T.P. Krauss, M.D. Zoltowski, and G. Leus, "Simple MMSE equalizers for CDMA downlink to restore chip sequence: Comparison to zero-forcing and RAKE," in *IEEE Int. Conf. on Acoustics, Speech, and Signal Processing*, Istanbul, Turkey, June 2000, vol. 2, pp. 2865–2868.

- [15] L. Mailaender, “Low-complexity implementation of CDMA downlink equalization,” in *Int. Conf. on 3G Mobile Communications Technologies*, London, UK, Mar. 2001, pp. 396–400.
- [16] D. Sarwate, “Bounds on crosscorrelation and autocorrelation of sequences,” *IEEE Trans. on Information Theory*, vol. 25, no. 6, pp. 720–724, Nov. 1979.
- [17] M. Michalko, *Cracking Creativity: The Secrets of Creative Genius*, Ten Speed Press, Berkeley, California, 2001.
- [18] T. Walzman and M. Schwartz, “Automatic equalization using the discrete frequency domain,” *IEEE Trans. on Information Theory*, vol. 19, no. 1, pp. 59–68, Jan. 1973.
- [19] I. Martoyo and F. Jondral, “Frequency domain equalization for the downlink of CDMA mobile radio systems,” in *Summary of the International Symposium on Advances in Wireless Communications ISWC’02*, Victoria, Canada, Sept. 2002, pp. 97–98.
- [20] K.L. Baum, T.A. Thomas, F.W. Vook, and V. Nangia, “Cyclic-prefix CDMA: An improved transmission method for broadband DS-CDMA cellular systems,” in *Wireless Communications and Networking Conference WCNC’02*, Orlando, Florida, USA, Mar. 2002, vol. 1, pp. 183–188.
- [21] I. Martoyo, T. Weiss, F. Capar, and F. Jondral, “Low complexity CDMA downlink receiver based on frequency domain equalization,” in *IEEE 58th Vehicular Technology Conference, Fall*, Orlando, Florida, USA, Oct. 2003, pp. 987–991.
- [22] H. Sari, G. Karam, and I. Jeanclaude, “Transmission techniques for digital terrestrial TV broadcasting,” *IEEE Communications Magazine*, vol. 33, no. 2, pp. 100–109, Feb. 1995.

- [23] I. Martoyo, H. Schober, and F. Jondral, “CDMA versus OFDM, a performance comparison in selective fading channels,” in *IEEE 7th Int. Symp. on Spread Spectrum Techniques and Applications*, Prague, Czech Rep., Sept. 2002, vol. 1, pp. 139–143.
- [24] ETSI EN 300 744, “Digital video broadcasting DVB; framing structure, channel coding and modulation for digital terrestrial television,” Tech. Rep., ETSI, 2001.
- [25] H. Schober, F. Jondral, and R. Stirling-Gallacher, “Adaptive channel estimation for OFDM based high speed mobile communication systems,” in *Proceedings of the International Conference on Third Generation Wireless and Beyond*, San Fransisco, California, USA, May 30 - June 2, 2001, pp. 392–397.
- [26] ETSI TS 125 XXX, “Universal mobile telecommunications systems (UMTS),” Tech. Rep., ETSI, 2001.
- [27] ETSI TS 125 212, “Universal mobile telecommunications systems (UMTS) (multiplexing and channel coding (FDD)),” Tech. Rep., ETSI, 2001.
- [28] R. Machauer, *Multicode-Detektion im UMTS*, Dissertation: Forschungsberichte aus dem Institut für Nachrichtentechnik der Universität Karlsruhe (TH), Band 6, Karlsruhe, 2002.
- [29] K. Baum, V. Nangia, and K. Ramasubramanian, “A link performance study of DS-CDMA and OFDM for 4th generation cellular,” in *Int. Conf. on 3G Wireless and Beyond*, San Fransisco, California, USA, May 2001, pp. 472–477.
- [30] A. Czylik, “Comparison between adaptive OFDM and single carrier modulation with frequency domain equalization,”

in *IEEE 47th Vehicular Technology Conference*, Phoenix, Arizona USA, May 1997, vol. 2, pp. 865–869.

- [31] D. Falconer, S.L. Ariyavisitakul, A. Benyamin-Seeyar, and B. Eidson, “Frequency domain equalization for single-carrier broadband wireless systems,” *IEEE Communications Magazine*, vol. 40, no. 4, pp. 58–66, Apr. 2002.
- [32] Gene H. Golub and Charles F. van Loan, *Matrix Computations*, The Johns Hopkins University Press, Baltimore/London, 1996.
- [33] B.R. Hunt, “A matrix theory proof of the discrete convolution theorem,” *IEEE Trans. on Audio and Electroacoustics*, vol. 19, no. 4, pp. 285–288, Dec. 1971.
- [34] M. Vollmer, M. Haardt, and J. Götze, “Comparative study of joint-detection techniques for TD-CDMA based mobile radio systems,” *IEEE Jour. on Selected Areas in Communications*, vol. 19, no. 8, pp. 1461–1475, Aug. 2001.
- [35] R. Machauer and F. Jondral, “FFT-speed and windowed multiuser detector for UTRA-FDD high rate data mode,” in *IEEE 7th Int. Symp. on Spread Spectrum Techniques and Applications*, Prague, Czech Rep., Sept. 2002, vol. 3, pp. 712–716.
- [36] A.V. Oppenheim and R.W. Schaffer, *Digital Signal Processing*, Prentice-Hall, Inc., Englewood Cliffs, New Jersey, 1975.
- [37] M. Haardt, A. Klein, R. Koehn, S. Oestreich, M. Purat, V. Sommer, and T. Ulrich, “The TD-CDMA based UTRA-TDD mode,” *IEEE Jour. on Selected Areas in Communications*, vol. 18, no. 8, pp. 1375–1385, Aug. 2000.
- [38] ETSI, “Technical report 101 146: UMTS; UTRA concept evaluation,” Tech. Rep., ETSI, Dec. 1997.

- [39] P.J. Sherman, “Circulant approximations of the inverses of Toeplitz matrices and related quantities with applications to stationary random processes,” *IEEE Trans. on Acoustics, Speech and Signal Processing*, vol. 33, no. 6, pp. 1630–1632, Dec. 1985.
- [40] M. Ghosh, “Adaptive chip-equalizers for synchronous DS-CDMA systems with pilot sequences,” in *IEEE Global Telecommunications Conference (GLOBECOM)*, San Antonio, Texas, USA, Sept. 2001, vol. 6, pp. 3385–3389.
- [41] I. Martoyo, G.M.A. Sessler, J. Luber, and F. Jondral, “Comparing equalizers and multiuser detectors for CDMA downlink systems,” in *IEEE 59th Vehicular Technology Conference, Spring*, Milan, Italy, May 2004.
- [42] I. Martoyo and F. Jondral, “FDE-RAKE: A PIC multiuser detector for CDMA downlink,” in *IEEE 8th International Symp. on Spread Spectrum Techniques and Applications (ISSSTA)*, Sydney, Australia, 2004, pp. 47–50.
- [43] S. Chowdhury and M.D. Zoltowski, “Combined MMSE equalization and multiuser detection for high-speed CDMA forward link with sparse multipath channels,” in *35th Asilomar Conf. on Signals, Systems and Computers*, Pacific Grove, CA, USA, Nov. 2001, pp. 389–393.
- [44] Z. Wang and G.B. Giannakis, “Wireless multicarrier communications,” *IEEE Signal Processing Magazine*, vol. 17, no. 3, pp. 29–48, 2000.
- [45] B.R. Vojčić and M.J. Won, “Transmitter precoding in synchronous multiuser communications,” *IEEE Trans. on Communications*, vol. 46, no. 10, pp. 1346–1355, 1998.



- [46] S. Georgoulis and D.G.M. Cruickshank, "Pre-equalization, transmitter precoding and joint transmission techniques for time division duplex CDMA," in *3G Mobile Communication Technologies Conference*, London, UK, Mar. 2001, pp. 257–261.
- [47] D. Reynolds, A. Høst-Madsen, and X. Wang, "Transmitter precoding for CDMA in fading multipath channels: Strategy and analysis," in *IEEE Int. Conf. on Communications*, Anchorage, AK, USA, May 2003, pp. 3331–3335.
- [48] M. Joham and W. Utschick, "Downlink processing for mitigation of intracell interference in DS-CDMA systems," in *IEEE 6th Int. Symp. on Spread Spectrum Techniques and Applications*, Parsippany, NJ, USA, 2000, vol. 1, pp. 15–19.
- [49] S. Georgoulis and D.G.M. Cruickshank, "Transmitter-based inverse filters for reducing MAI and ISI in CDMA-TDD downlink," *IEEE Trans. on Wireless Communications*, vol. 3, no. 2, pp. 353–358, 2004.
- [50] M.W. Oliphant, "Third-generation wireless must wait for services to catch up," *IEEE Spectrum*, vol. 39, no. 6, pp. 14, 16, June 2002.
- [51] J. Mitola, "The software radio architecture," *IEEE Communications Magazine*, vol. 33, no. 5, pp. 26–38, May 1995.
- [52] A. Wiesler and F.K. Jondral, "A software radio for second- and third-generation mobile systems," *IEEE Trans. on Vehicular Technology*, vol. 51, no. 4, pp. 738–748, July 2002.
- [53] F.K. Jondral, "Parameter controlled software defined radio," in *Software Defined Radio Forum Technical Conference*, San Diego, California USA, Nov. 2002, vol. 2.

- [54] H. Witschnig, A. Koppler, A. Springer, R. Weigel, and M. Huemer, "A comparison of an OFDM system and a single carrier system using frequency domain equalization," *European Trans. on Telecommunications*, vol. 13, no. 5, pp. 519–530, 2002.
- [55] M. Huemer, A. Koppler, R. Weigel, and L. Reindl, "A review of cyclically extended single carrier transmission with frequency domain equalization for broadband wireless transmission," *European Trans. on Telecommunications*, vol. 14, no. 4, pp. 329–341, 2003.
- [56] I. Martoyo and F. Jondral, "Multimode receiver with frequency domain equalizer," in *4th International Workshop on ITS Telecommunications*, Singapore, July 2004, pp. 318–322.
- [57] P. Rykaczewski, I. Martoyo, Z. Liu, and F. Jondral, "Multimode detector and IQ imbalance compensator in a software defined radio," in *IEEE Radio and Wireless Conference (RAWCON)*, Atlanta, GA, USA, 2004.
- [58] F. Capar, I. Martoyo, T. Weiss, and F.K. Jondral, "Analysis of coexistence strategies for cellular and wireless local area networks," in *IEEE 58th Vehicular Technology Conference, Fall*, Orlando, Florida USA, Oct. 2003, pp. 1812–1816.
- [59] G. Staple and K. Werbach, "The end of spectrum scarcity," *IEEE Spectrum*, vol. 41, no. 3, pp. 48–52, Mar. 2004.
- [60] E.M. Noam, "Taking the next step beyond spectrum auctions: Open spectrum access," *IEEE Communications Magazine*, vol. 33, no. 12, pp. 66–73, Dec. 1995.
- [61] R.W. Lucky, "The precious radio spectrum," *IEEE Spectrum*, vol. 38, no. 9, pp. 90, Sept. 2001.

- [62] T. Weiss and F. Jondral, "Spectrum pooling - an innovative strategy for the enhancement of spectrum efficiency," *IEEE Communications Magazine*, vol. 42, no. 3, pp. S8–S14, 2004.
- [63] J. Mitola, "Cognitive radio for flexible mobile multimedia communications," in *IEEE International Workshop on Mobile Multimedia Communications*, Nov. 1999, pp. 3–10.
- [64] F. Capar, I. Martoyo, T. Weiss, and F.K. Jondral, "Comparison of bandwidth utilization for controlled and uncontrolled channel assignment in a spectrum pooling system," in *IEEE 55th Vehicular Technology Conference, Spring*, Birmingham, Alabama USA, May 2002, vol. 3, pp. 1069–1073.
- [65] I. Martoyo, F. Capar, T. Weiss, and F. Jondral, "Spectrum pooling : Physical layer issues," in *13th Mobile & Wireless Communications Summit (IST)*, Lyon, France, June 2004, pp. 1016–1019.
- [66] D. Shekerjian, *Uncommon Genius, How Great Ideas Are Born*, Penguin Books, USA, 1990.
- [67] R.W. Lucky, "The impermanence of knowledge," *IEEE Spectrum*, vol. 41, no. 3, pp. 80, Mar. 2004.
- [68] F.W. Vook, T.A. Thomas, and K.L. Baum, "Cyclic-prefix CDMA with antenna diversity," in *IEEE 55th Vehicular Technology Conference, Spring*, Birmingham, AL, USA, May 2002, vol. 2, pp. 1002–1006.
- [69] A. Gusmão, R. Dinis, and N. Esteves, "On frequency-domain equalization and diversity combining for broadband wireless communications," *IEEE Trans. on Communications*, vol. 51, no. 7, pp. 1029–1033, 2003.
- [70] R.L. Choi and R.D. Murch, "Frequency domain pre-equalization with transmit diversity for MISO broadband

- wireless communications,” in *IEEE 56th Vehicular Technology Conference, Fall*, Vancouver, BC, Canada, 2002, vol. 3, pp. 1787–1791.
- [71] A. Burg, M. Rupp, S. Haene, D. Perels, N. Felber, and W. Fichtner, “Low complexity frequency domain equalization of MIMO channels with applications to MIMO-CDMA systems,” in *IEEE 58th Vehicular Technology Conference, Fall*, Orlando, Florida, USA, Oct. 2003, pp. 468–472.
- [72] M. Haardt and W. Mohr, “The complete solution for third-generation wireless communications: Two modes on air, one winning strategy,” *IEEE Personal Communications*, vol. 7, no. 6, pp. 18–24, 2000.
- [73] E. Dahlman, B. Gudmundson, M. Nilsson, and J. Sköld, “UMTS/IMT-2000 based on wideband CDMA,” *IEEE Communications Magazine*, vol. 36, no. 9, pp. 70–80, Sept. 1998.
- [74] COST 207, “Digital land mobile radio communications,” Tech. Rep., Office for Official Publications of the European Communities, Luxemburg, 1989.

# Theses

- David Vicente Perez Garcia: *Complete Complementary Code für CDMA*
- Jaroslav Luber: *Frequenzbereichsentzerrung (FDE) vs. Multiuser Detektor (MUD) für CDMA-System*
- Zoltan Bartha: *Frequenzbereichsentzerrungs-Detektor für UTRA*
- Nikolaus Bissias: *OFDM-Praktikumsversuch*
- Diego Garcia Gallen: *Frequency Domain Equalization with Diversity in CDMA System*
- Pureza Galindo Latorre: *Software Radio and Near-Far Effect Aspects of Frequency Domain Equalization in CDMA*
- Liu Zhenhua: *I/Q Imbalance Compensation and Frequency Domain Equalization*
- Yin Wenxuan: *FDE-RAKE, ein Multiuserdetektor für CDMA*
- Sun Bo: *Pre-FDE mit Diversity für CDMA Uplink*
- Ignacio Izquierdo: *FDE-MIMO for CDMA*



# Index

- 3G, 2, 96, 100, 104
- cdma2000, 2
- circulant, 42–44, 48, 51, 52, 62, 66
- complexity, 4, 10, 110
  - FDE, 53–55
  - FDE-RAKE, 82–83
  - FFT, 53
  - TDE, 19
- correlation, 19, 37, 71
  - autocorrelation, 5, 15, 19
  - crosscorrelation, 6, 15, 19
- cyclic prefix, 43–48, 100, 110
- DAB, 22
- DVB-T, 22, 24, 31–35, 96
- FFT, 4, 40, 43, 44, 47, 48, 97, 98, 102, 104
  - length, 100
- Gold codes, 71, 72
- graceful degradation, 6, 112, 113
- HIPERLAN/2, 23, 100
- IEEE 802.11a, 22, 100
- IFFT, 40, 41, 43, 97, 98, 104
- IMT-2000, 3
- ISI, 15, 23
- multimode, 4, 8, 96, 98, 100, 104, 107, 111
- optimal multiuser detector, 10, 16
- overlap-cut, 43–48, 101, 110
- OVSF, 13, 101, 115
- PAPR, 23, 30
- parallel interference cancellation, 76, 110
- scrambling, 13, 37, 113
- software radio, 96, 97
- software-defined radio, 76, 97
- spectrum pooling, 106, 107
- Toeplitz, 48, 51, 52
- UMTS, 2, 13
- UTRA-FDD, 2, 24, 31–35, 102, 115–118
- UTRA-TDD, 2, 49, 58, 78, 100, 115–118
- WLAN, 100, 102
- zero-padding, 43–48, 67, 91, 110





# Curriculum Vitae

## Personal Data

Name	Ihan Martoyo
Date of birth	May 18,1973
Place of birth	Jakarta
Nationality	Indonesian

## Elementary Education

1980-1992	Elementary and intermediate school in Jakarta, Indonesia
-----------	--

## Studies and Occupational History

1992-1996	Bachelor in electrical engineering at Institut Teknologi Bandung, Indonesia
-----------	---

1996-1998	System Engineer at PT. Elektrindo Nusantara, Jakarta, Indonesia
-----------	---

1998-2000	Master in electrical engineering at Universität Karlsruhe
-----------	---

since 2001	Teaching/research assistant ( <i>wissenschaftlicher Angestellter</i> ) at the Institut für Nachrichtentechnik, Universität Karlsruhe.
------------	---